NASA TM-81375

NASA Technical Memorandum 81375

NASA-TM-81375 19830001839

PRELIMINARY ANALYSIS OF STS-4 ENTRY FLIGHT DATA

September 1982

NASA

National Aeronautics and
Space Administration

Ames Research Center
Dryden Flight Research Facility
P.O. Box 273
Edwards, California 93523

errata change
10-19-82

NASA

Reply to Attn of: AI

October 12, 1982

TO: Langley Research Center
Attn: Library

FROM: AI/Linda J. Quinby, Editor

SUBJECT: Technical Memorandum 81375, Preliminary Analysis of STS-4 Entry Flight Data

The report number on the cover and title page of the Technical Memorandum referenced above is incorrect. The COSATI page reflects the correct number, which is TM-81375.

Please make the appropriate corrections on your copy.

Linda J. Quinby

Linda J. Quinby

NASA TM-81375

NASA Technical Memorandum 81375

PRELIMINARY ANALYSIS OF STS-4 ENTRY FLIGHT DATA

Ames Research Center
Dryden Flight Research Facility
Edwards, California

NASA

1982

N83-10109 #

SUMMARY

Dryden has completed a preliminary analysis of the data obtained during entry of the STS-4 Flight. Planned maneuvers were flown during this flight to increase the quality of stability and control analysis, similar to the techniques used during STS-3. This approach will unquestionably decrease the number of flights needed to fully document the Orbiter's flying qualities.

Results of the derivative extraction and analysis process are presented for both the longitudinal and lateral-directional axes. Comparisons are made with pre-flight predictions as well as with the results obtained from Flights STS-1 through STS-3. Lift/Drag ratios, obtained from the analysis of the two planned push over-pull up maneuvers, are compared with predicted ratios.

Time histories of two areas of manual flying (CSS Mode) are presented. One is during flight around the heading alignment circle and the other is from pre-flare to landing. The PIO tendencies of the Orbiter are discussed but showed us no reason for concern during this flight.

Finally, the results of the Aero-Thermal data analysis will have to be provided at a later time. As with Flight STS-1, we failed to get any DFI data from the on-board recorder. Therefore, any Aero-Thermal data will be limited to what we could receive from real-time telemetry. This is, of course, later in the entry than the high heating regime.

NOMENCLATURE

Acronyms

ACIP	aerodynamic coefficient identification package
ADB	aero data book
AGL	above ground level
ASI	aero stick input
C.G.	center of gravity
CSS	control stick steering
DFI	Development Flight Instrumentation
DFRF	Dryden Flight Research Facility
EAFB	Edwards Air Force Base
FPS	feet per second
GPC	general purpose computer
GMT	Greenwich mean time
IMU	inertial measurement unit
JSC	Johnson Space Center
KSC	Kennedy Space Center
MMLE	modified maximum likelihood estimation
MSL	mean sea level
PCM	Pulse Code Modulation
PIO	pilot-induced ocillation
PKQ	suppression factor
PSF	pound per square foot
PTI	programmed test input
PUPO	pull-up, push-over

RCS	reaction control system
RHC	rotational hand controller
STS	space transportation system
VEAS	velocity equivalent airspeed, knots

Symbols

A	Axial force
a_n	normal acceleration, g
a_x, a_l	longitudinal acceleration, g
a_y	lateral acceleration, g
BF	body flap, deg
b	span, ft
C_A	$A/\bar{q}S$
CA_α	$\partial CA/\partial\alpha$
CA_{BF}	$\partial CA/\partial_{\delta BF}$
CA_{SB}	$\partial CA/\partial_{\delta SB}$
CA_{YJ}	$\partial CA/\partial_{\delta YJ}$
$CA_{\delta e}$	$\partial CA/\partial_{\delta e}$
C_l	rolling moment/$\bar{q}Sb$
$C_{l_{\delta a}}$	$= \frac{\partial C_l}{\partial_{\delta a}}$
C_{l_β}	$= \frac{\partial C_l}{\partial \beta}$
$C_{l_{\delta_r}}$	$= \frac{\partial C_l}{\partial \delta_r}$
C_m	pitching moment/$\bar{q}S\bar{c}$
C_{m_q}	$= \frac{\partial C_m}{\partial\ q}$
Cm_α	$\partial Cm/\partial\alpha$
$C_{m_{\delta e}}$	$= \frac{\partial C_m}{\partial \delta_e}$

$C_{m_{BF}}$	$= \frac{\partial C_m}{\partial BF}$
Cm_{SB}	$\partial Cm/\partial\delta_{SB}$
Cm_{YJ}	$\partial Cm/\partial\delta_{YJ}$
C_N	$N/\bar{q}S$
$C_{N\alpha}$	$\partial C_N/\partial\alpha$
CN_{BF}	$\partial C_N/\partial\delta_{BF}$
CN_{SB}	$\partial C_N/\partial_{\delta SB}$
$CN_{\delta e}$	$\partial C_N/\partial_{\delta e}$
C_{N_α}	$= \frac{\partial C_N}{\partial\alpha}$
C_n	yawing moment/$\bar{q}Sb$
$C_{n\beta}$	$= \frac{\partial CN}{\partial\beta}$
$Cn_{\delta a}$	$= \frac{\partial C_n}{\partial\delta a}$
$Cn_{\delta r}$	$= \frac{\partial C_n}{\partial\delta r}$
C_y	yawing moment/$\bar{q}S$
$C_{y\beta}$	$= \frac{\partial C_y}{\partial\beta}$
$C_{y\delta a}$	$\partial C_y/\partial_{\delta a}$
$C_{y\delta r}$	$= \frac{\partial C_y}{\partial\delta_r}$
$\bar{c}$	mean aerodynamic chord, ft
com	command
D	Drag Force
g	acceleration due to gravity

h	altitude
$\dot{h}$	altitude rate, ft/sec
I	moment of inertia, slug-ft^2
L	Lift force
L/D	Lift to Drag ratio
L_{RJ}	rolling moment due to roll jet
L_{YJ}	rolling moment due to yaw jet
M	Mach number
M_{D_J}	pitching moment due to down jet
M_{u_J}	pitching moment due to up jet
N	Normal force
N_{RJ}	yawing moment due to roll jet
N_{YJ}	yawing moment due to yaw jet
p	roll velocity, deg/sec
$\dot{p}$	roll acceleration, deg/sec^2
q	pitch velocity, deg/sec
$\bar{q}$	dynamic pressure, psf
r	yaw velocity, deg/sec
$\dot{r}$	yaw acceleration, deg/sec^2
S	wing area, ft^2
SB	speed brake
t_o	plot start time (Greenwich mean time)
V	velocity
$\dot{V}$	velocity rate, ft/sec^2
x	body axis longitudinal coordinate
Y_{RJ}	yawing force due to roll jet
Y_{YJ}	yawing force due to yaw jets
y	body axis spanwise coordinate

z	body axis vertical coordinate
α	angle of attack, deg
β	angle of sideslip, deg
δa	aileron deflection, deg
δ_e	elevator position, deg
$\delta_{\dot{e}}$	$= \frac{\partial \delta e}{\partial t}$
δ_r	rudder position
Δ	increment
θ	pitch angle
ϕ	roll angle
γ	flight path angle

Introduction

The fourth flight of the Space Shuttle ended on July 4, 1982 with a landing on Runway 22 at Edwards Air Force Base. The primary test objectives of the STS-4 entry were to obtain performance, stability, and control data from a series of planned maneuvers, to demonstrate Autoland capability down to preflare, and to land the orbiter on a limited length, hard surface runway for the first time.

A time history of the entire descent phase of the flight is shown in Figure 1. Table 1 lists the planned entry maneuvers used for data analysis, and Table 2 lists the weight, inertia, and C.G. characteristics used in the analysis.

Stability and Control Derivative Extraction Results

The STS-4 flight data includes intentional stability and control maneuvers in addition to the planned bank reversals similar to those on STS-1, 2, and 3. The intentional maneuvers included one longitudinal Aero Stick Input (ASI), five lateral-directional Programmed Test Inputs, and 2 pullup-push-over maneuvers. The intentional maneuvers resulted in the best stability and control

maneuvers for the flight. All of the intentional maneuvers as well as the bank reversals and other miscellaneous maneuvers were analyzed and stability and control derivatives were obtained.

The mathematical formulation of the estimation techniques (MMLE3) used in the following analysis is contained in reference 1. The preliminary results for STS-1, STS-2, and STS-3 are contained in references 2-4.

In general the analysis of STS-4 closely followed that of STS-1, STS-2, and STS-3 described in references 2-4. The ACIP data were biased and noisy similar to the way they were on STS-3 (Ref. 4) .

Longitudinal Stability and Control Derivatives

Analysis

Beginning with STS-4, the emphasis of the stability and control derivative analysis has changed somewhat. There were few good quality longitudinal maneuvers in the first three flights. As a result, we attempted analysis of numerous small incidental motions of marginal quality for derivative estimation. This analysis established the general trends of several of the derivatives along the nominal entry corridor. The scatter in the estimates tended to be fairly large due partly to the use of marginal quality data. Little useful information could be obtained about most of the normal and axial force derivatives.

Furthermore, between the large scatter and the lack of a good matrix of test conditions, it was not possible to attribute the trends to particular effects such as angle of attack or Mach number; the derivatives were simply presented along the entry timeline.

We have now reached the point where little more can be learned by additional marginal quality maneuvers at the same conditions. Therefore, we are being more selective in our choice of maneuvers to analyze. We analyzed about 20 longitudinal maneuvers on STS-4, half as many as on the previous flights. Our aims are now to get more accurate results along the nominal entry corridor and to investigate the effects of off-nominal conditions in order to help expand the entry flight envelope.

Figure 2 presents the longitudinal derivative estimates (except for pitching moment due to elevon) from STS-4 for Mach numbers above 1 and dynamic pressure above 20 psf. Some of the best data are the clumps near Mach 8 and Mach 13, which are results obtained during the two pushover/pullup maneuvers. We also had good data from the Mach 21.5 ASI and some maneuvering near Mach 2.5. There appears to be some information on the normal force derivatives due to angle-of-attack and elevon on this flight. There was too much scatter in our previous estimates of these derivatives for them to be useful.

It was obvious on several of the maneuvers from STS-4 that there was a significant non-linearity in the pitching

moment due to elevon. Evidence of this non-linearity had been noted previously, but we had not felt that there were enough data to quantify it. Figure 3 presents the estimates of pitching moment due to elevon from all 4 flights. The data from the first 3 flights were screened so that only the good quality maneuvers were used for this figure. The lines on the figure represent maneuvers that were analyzed with an elevon squared derivative. For these maneuvers, the pitching moment due to elevon is a linear function of the elevon position, rather than a single point. The data indicated by crosses lie in the 38-42 degree angle-of-attack range. There is a very clear trend of this data as a function of elevon position. There is also a strong angle-of-attack dependence. There is a sufficient matrix of body flap and Mach number points in these data to establish that there is no significant dependence of the elevon effectiveness on body flap position or Mach number (at least for the range of these data, which are all above Mach 2.5). These trends agree well with the predictions of this derivative (not shown on this figure). The flight results were analyzed completely independent of the predictions, thus ensuring an unbiased verification. We did not examine the data book for these trends until after the flight results were analyzed and this plot was made.

The pitch jet derivatives in the early entry regime are shown in figure 4. These data are similar to data obtained on previous flights and show no new results.

Data from Mach 4 to landing are shown in figure 5. These data generally agree with the predictions.

Summary of Longitudinal Derivatives

We have about exhausted the usefulness of the marginal quality small incidental motions for derivative estimation. Further efforts will require good quality maneuvers to improve the results along the nominal entry corridor and to expand the entry envelope. Expansion of the entry envelope will require more data of the type presented herein for the elevon effectiveness, where we examine the dependencies of the derivatives on the flight condition and configuration in a way that allows for extrapolations to other entry profiles. The pushover/pullup maneuvers of STS-4 provided the first good data of this type by giving us several different angles of attack at otherwise similar conditions.

Lateral-Directional Analysis

The rotary or rate derivatives were held fixed at the Aero Data Book (ADB) values for the results presented here. It is not believed that fixing the rotary derivatives has a major effect on the results presented. The yaw and roll jets are modeled the same way as described in reference 4.

STS-4 results showed that reliable information on the sideslip and differential elevon (aileron) derivatives could not be obtained below a dynamic pressure of 10 psf

which also had been indicated on previous flights. The sideslip and aileron derivatives for maneuvers performed below a dynamic pressure of 10 psf are fixed at the flight determined value that occured near a dynamic pressure of 10 psf.

In general, changes in estimates of the effect of the yaw jets below a Mach number of 3 were found to be small. Thus for most of the analysis of maneuvers in this region the yaw jets were fixed at the ADB values as they were on STS-2 and STS-3. The overall analysis of the data will be enhanced by a good air data system as previously discussed in reference 3.

Lateral-Directional Derivative Results

The lateral-directional derivative estimates are plotted in figures 6 through 10. The derivatives are plotted versus IMU V/1000 or M in figures 6, 7, 8, and 10, and versus GPC dynamic pressure, $\bar{q}$, in figure 9. The symbol is the derivative estimate and the vertical bar is the uncertainty bound. The poorer the estimate, the larger the uncertainty bound. The dashed line is fairing of the flight-determined derivative estimates; it is shown as a dotted line where less certainty in the fairing is indicated. The solid line is the ADB value for the derivatives. The solid ticked lines are the ± 1 variation applied to the ADB values. All data are referenced to 65% of the body length.

The lateral-directional stability and control derivatives are plotted as a function of M for all cases where $\bar{q}$ from GPC is greater than 10 psf in figures 6, 7, 8, and 10. The RSC jet derivatives are plotted against $\bar{q}$ in figure 9. For $\bar{q}$ between 0 and 20 psf, the jet derivatives are plotted versus $\bar{q}$ as the effect is due more to $\bar{q}$ than Mach number in this flight regime.

Figure 6 shows the lateral-directional stability and control derivatives plotted versus M and compared to the ADB derivatives based on STS-4 flight conditions. In general the flight derivatives are showing the same trends with respect to the ADB values as has been indicated in the analysis of the first three flights.

Figure 7 shows all of the estimates from STS-1, 2, 3, and 4 plotted with ADB values and variations of STS-2, because most high quality maneuvers were obtained on STS-2. Above a Mach number of 3 most of the estimates agreed fairly well with those obtained from the first three flights. Figure 7 shows that the fairings are almost the same as those given for STS-1, STS-2, and STS-3.

The aileron effectiveness continues to indicate a dependence on elevon position as was discussed for STS-3 in reference 4. This effect is clearly indicated for $C_{l_{\delta a}}$ and $C_{n_{\delta a}}$ in figure B. A similar effect is shown as a nonlinearity in elevon effectiveness (discussed in Longitudinal Stability and Control Derivatives Section) which would be expected if the aileron effectiveness was a function of elevon position.

Figure 8 shows the same data as figure 7 for Mach numbers below 4. The indication of a large $C_{l_{\delta r}}$ and $C_{Y_{\delta r}}$ for small rudder deflections is still present as was indicated on STS-3 (ref. 4). These large effects are probably not due to rudder position alone, but whatever the underlying cause they are due to something correlated with rudder deflection. Since the yaw and roll rate derivatives are fixed at the ADB values, the effect shown here as a rudder effect may well be due to the rate derivatives. It seems quite likely that this effect, which persists in the same region as the quarter hertz wing rock, may be due to shock interaction or movement or due to flow separation. For the flight conditions flown to date the wing rock has presented no major problems, however if separation is an underlying cause, the character of this minor wing rock may be exacerbated if the Shuttle were flown at a higher angle of attack below Mach 2.

Figure 9 shows the derivatives against dynamic pressure for $\bar{q}$ between 0 and 20 psf. The flight data show essentially the same trends as previously reported. The effect of aileron effectiveness due to elevon position can also be seen in figure 9.

Figure 10 shows the derivatives estimated from Programmed Test Input (PTI) maneuvers as a function of IMU Mach number. In general, the trends are very well defined and for the most part the fairings of all the estimates given in figure 7 would suffice here. The aileron effectiveness dependence on elevon position is very

evident. The main point deduced from this figure is that the PTI maneuvers give higher quality estimates with less scatter and smaller uncertainty bounds. Starting with STS-5 many more PTI's will be performed each flight resulting in higher quality estimates, which will be essential for the envelope expansion aimed at allowing greater variations in center of gravity position.

Although the best estimates are being obtained from the PTI maneuvers, there needs to be a continuing effort in analyzing the other maneuvers (bank reversals, etc.) to make sure the PTI estimates are representative of the Shuttle where it normally maneuvers.

In order to assess the previously mentioned dependence of aileron effectiveness on elevon position, $C_{l_{\delta a}}$ and $C_{n_{\delta a}}$ are shown against elevon position in figure 11. The figure shows all of the estimates from PTI maneuvers at Mach numbers above 5 for three different ranges of angle of attack. $C_{l_{\delta a}}$ appears to be a nearly linear function of elevon position from an elevon position of -3.5° to 6°. $C_{n_{\delta a}}$ seems nearly linear for positive elevon deflection but it is difficult to conclude anything for negative deflections. An effect of angle of attack on aileron effectiveness is also seen on this figure. The effect, very evident in $C_{l_{\delta a}}$, is presumed to be a function of angle of attack rather than Mach, because of the conclusion reached for the longitudinal analysis of $C_{m_{\delta e}}$.

Summary of Lateral-Directional Derivatives

The derivatives obtained from STS-4 agreed fairly well with the derivatives obtained on previous flights. The effects evident during the mild wing rock between Mach 1 and 2 are still present. If these effects are due to separation the wing rock may be worsened if a higher angle of attack is flown. The dependence of aileron effectiveness on elevon position above a Mach number of 10 seen on STS-3 was conclusively verified on STS-4. The greater desirability of the PTI maneuvers was shown using the results of the last 3 STS flights. The ACIP system still showed bias and noise problems and steps need to be implemented to alleviate these problems.

Lift/Drag Analysis

Push over-pull up maneuvers were performed during the entry of STS-4 for two Mach number ranges. Angle-of-attack varied from approximately 29° to 44° for Mach numbers from 11.8 to 14.0 and from approximately 24° to 35° for Mach numbers from 7.1 to 8.6. This variation in angle-of-attack for these two Mach number ranges permits comparing the flight and predicted ratios of lift-to-drag as a function of angle-of-attack, figures 12 and 13. The flight lift-to-drag ratio was calculated using 1 sps data from the equation:

$$L/D = \frac{a_n \cos\alpha + a_l \sin\alpha}{a_n \sin\alpha - a_l \cos\alpha}$$

where a_n and a_l are the normal and longitudinal accelerations in g's, respectively, α is the angle-of-attack, and L/D is the lift-to-drag ratio.

The speedbrakes were at a constant setting for each of the data sets. They were fully closed for Mach numbers from 11.8 to 14.0 and at 87° for Mach numbers from 7.1 to 8.6. The flight data are adjusted to a 5° elevon position. The vast majority of the data were within $\pm 2^\circ$ of the 5° elevon position for the Mach 11.8 to 14.0 data and within $\pm 1^\circ$ of the 5° elevon position for the Mach 7.1 to 8.6 data. The predicted values are also for a 5° elevon position and the same speedbrake position as the respective flight data.

The dominant trend for both sets of the flight data is higher lift-to-drag ratios for a given angle-of-attack than the predicted values. The lift-to-drag ratio for Mach numbers from 11.8 to 14.0, figure 12, is up to 3% higher for the lower angles-of-attack. It then decreases to 2% higher as angle-of-attack increases and agrees at the highest angle-of-attack. The lift-to-drag ratio for Mach numbers from 7.1 to 8.6, figure 13, is up to 2% higher for the lower angles-of-attack and decreases to 1% higher at the higher angles-of-attack. The maximum lift-to-drag ratio measured during wind-tunnel tests occurs at an angle-of-attack of 17.5°. The lift-to-drag ratio reaches .75 of this maximum value for the 11.8 to 14.0 Mach number maneuver and .88 of the maximum value for the 7.1 to 8.6 Mach number maneuver.

Terminal Area Maneuvering

Heading Alignment Circle

A time history of the CSS flying around the heading alignment circle is shown in figure 14. After engaging the CSS mode, several cycles of a low amplitude pilot induced oscillation (1-degree/second) at about Ø.3 hertz can be seen. Once stabilized on the desired trajectory around the heading alignment circle, only slight oscillations of very small amplitude can be seen. The potential PIO shown here should not present a significant problem. This flight condition does not require continuous, high-gain tracking of the guidance commands. As a result, any PIO tendency can easily be reduced by relaxing on the tracking task.

Approach and Landing

At the end of the heading alignment circle, the AUTO mode was selected. The alignment to the staight in portion of the approach and acquisition of the steep glide slope was done in AUTO. CSS was engaged prior to the flare and a time history from preflare to landing is shown in figure 15. The initial part of the flare maneuver was at 1.2g and this was increased to 1.5g during the last half of the flare. Near the end of the flare maneuver, nose-up stick command was decreased abruptly which gave rise to some PIO suppressor activity (PKQ, figure 15-b). The final approach

was accomplished with low gain control of flight path angle which was maintained between 0 and -1 degrees. Touchdown occurred at about 205 knots with essentially no flare. No PIO suppressor activity was seen between preflare and touchdown. This approach demonstrates the advantage of the shallow final glideslope approach. In this type of approach, the pilot is not required to make accurate altitude judgements since an acceptable landing can be made without performing the final flare.

TABLE 1 STS-4 ENTRY MANEUVERS

Event	GMT (Day 185) (HH:MM:SS)	Velocity (FPS)	Altitude (Ft MSL)	Maneuver Trim Conditions				
				Dynamic Pressure (psf)	Angle of Attack (Deg.)	Elevon (Deg.)	Body Flap (Deg)	Speed Brake (Deg)
First Turn	15:45:08	24340	251700	15.2	40.3	6.4	1.7	0
$\bar{q}$ = 24 Roll PTI-1	15:46:36	23730	241100	25.0	40.0	5.5	4.7	0
M = 21 Roll PTI-1	15:50:01	21480	228900	42.5	38.4	6.3	3.1	0
M = 21 Pitch ASI	15:50:21	21200	227300	43.4	38.5	6.1	3.1	0
M = 18 Roll PTI-1	15:53:27	17900	207100	62.6	40.1	5.6	3.1	0
M = 16 Roll PTI-1	15:54:32	16300	196700	77.0	40.0	5.3	3.1	0
M = 13 PUPO-1	15:55:56	13800	181600	97.0	39.4	4.8	1.5	0
First Bank Reversal	15:57:22	11200	174000	76.0	40.3	2.0	1.5	0
M = 8 PUPO-2	15:58:54	8350	144300	130.0	32.4	5.0	-0.2	87.2
Second Bank Reversal	16:00:11	6350	124400	190.0	24.4	3.9	5.1	87.2
Third Bank Reversal	16:02:28	3360	93250	231.0	17.3	2.8	6.3	74.0
M = 3 Yaw PTI-4	16:02:56	2860	89900	215.0	16.4	2.0	-0.3	63.0
Fourth Bank Reversal	16:03:19	2560	83200	230.0	14.1	1.0	-1.8	58.4

Table 2

STS-4

WEIGHT, CG, INERTIAS

Weight	2Ø9989.6	Lbs.
IX	94Ø274.6	Slug-Ft.^{2}
IY	6963845.9	Slug-Ft.^{2}
IZ	7271295.3	Slug-Ft.^{2}
IXZ	153Ø32.6	Slug-Ft.^{2}

XCG = 1Ø93.5 ZCG = 373.Ø YCG = -1.Ø inches

These were used as constants for the entire entry.

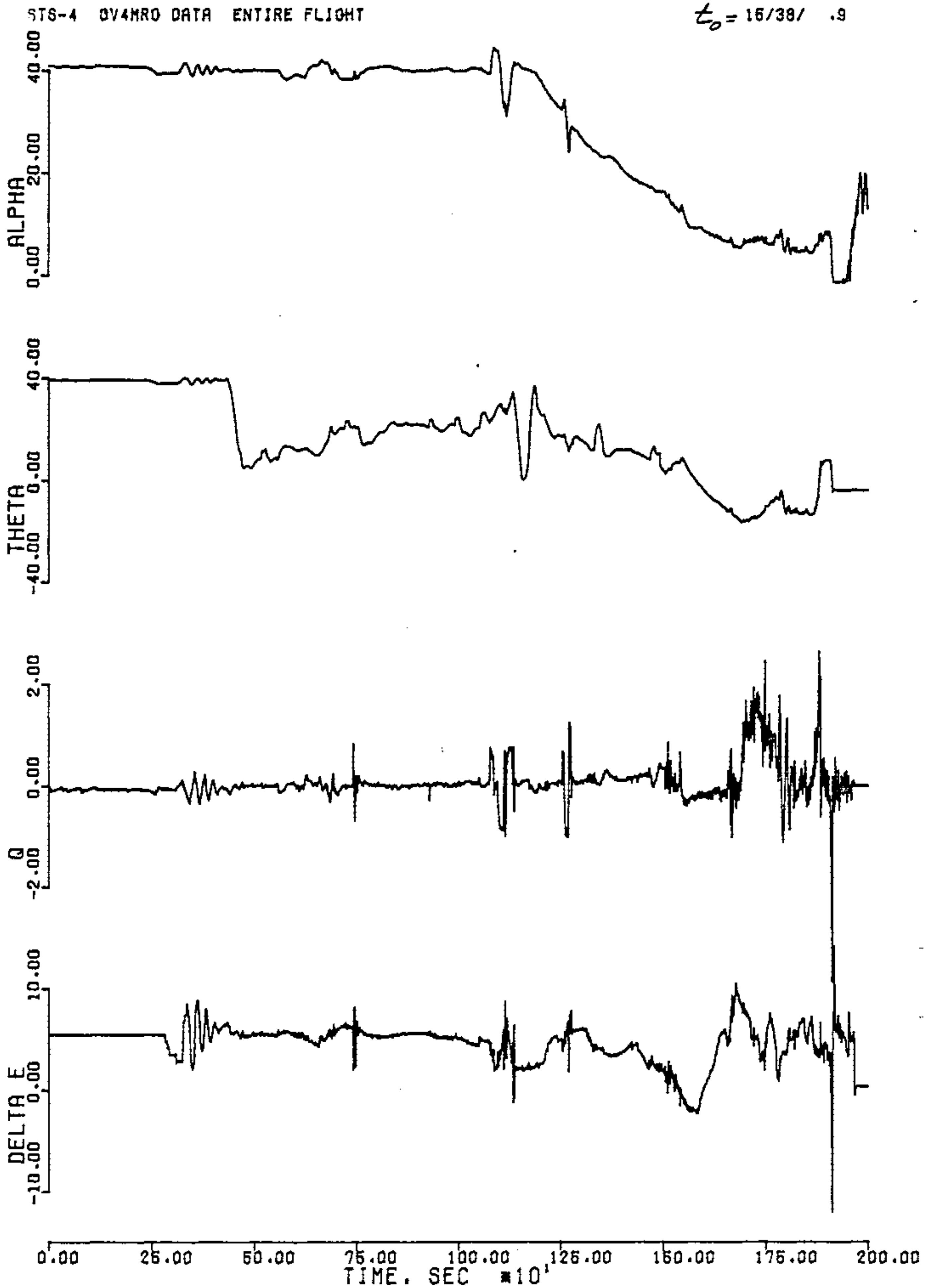

FIGURE 1a - ENTRY TIME HISTORY, 480,000 FT. TO LANDING

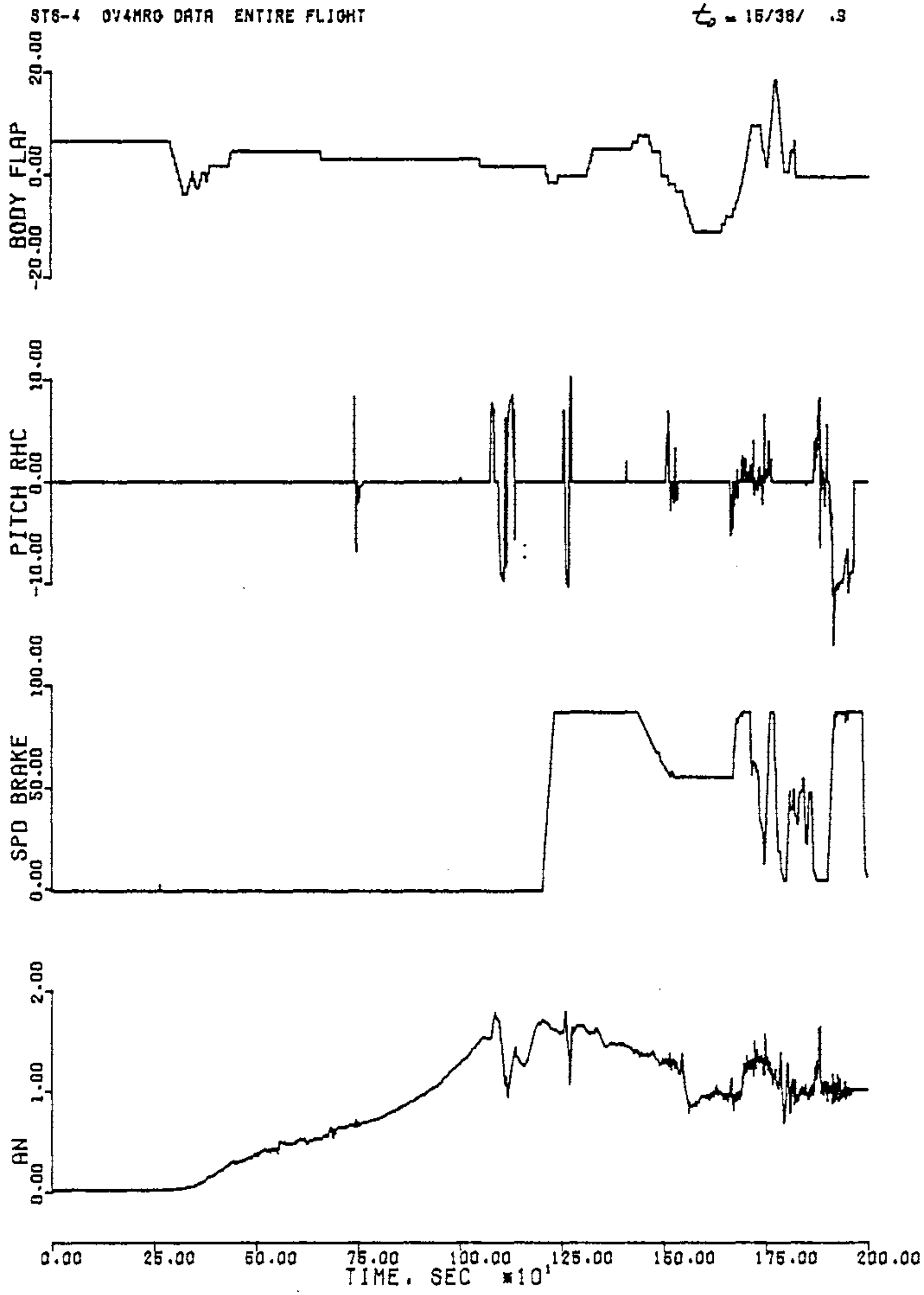

FIGURE 1b - (CONTINUED)

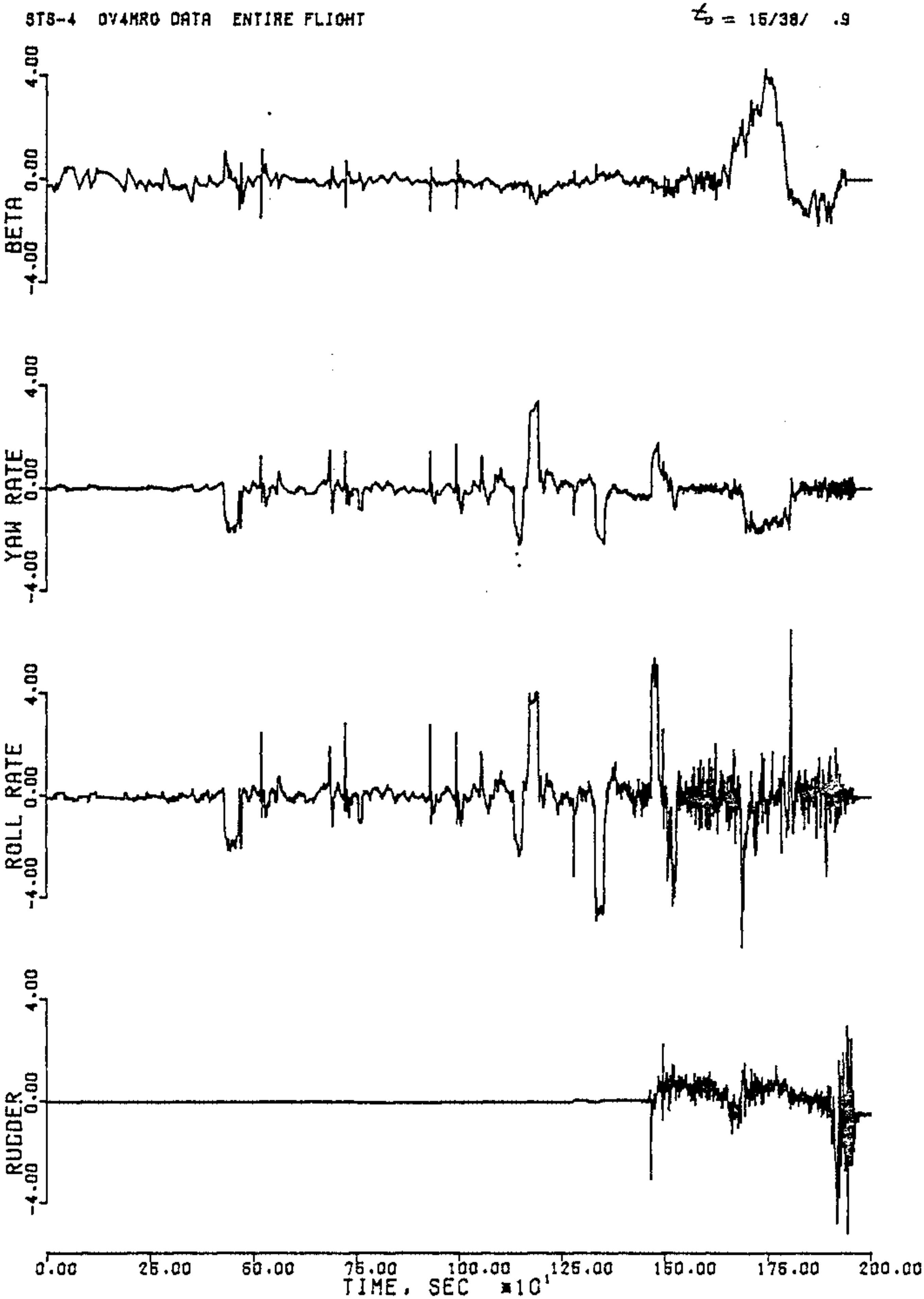

FIGURE 1c - (CONTINUED)

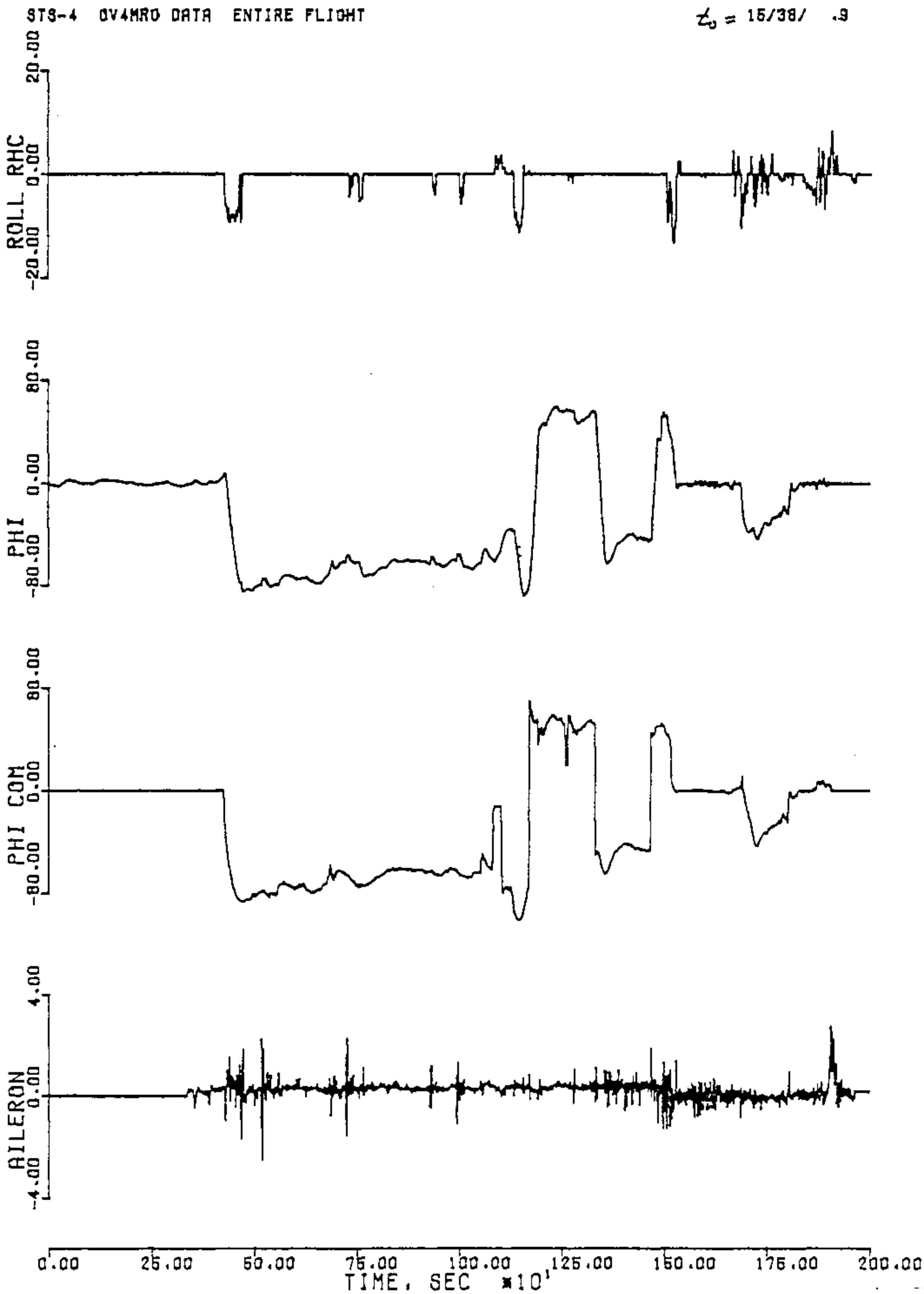

FIGURE 1d - (CONTINUED)

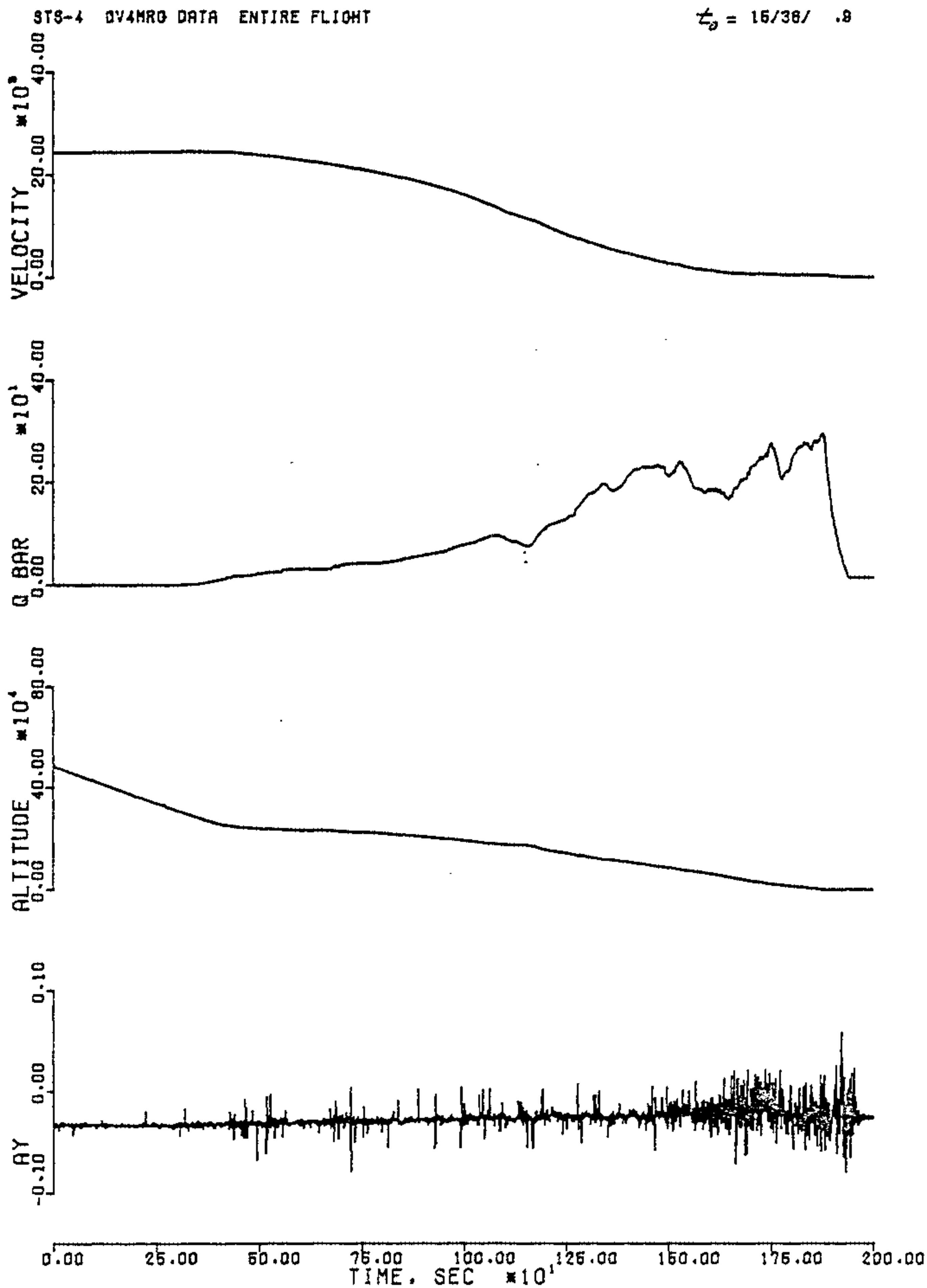

FIGURE 1e - (CONTINUED)

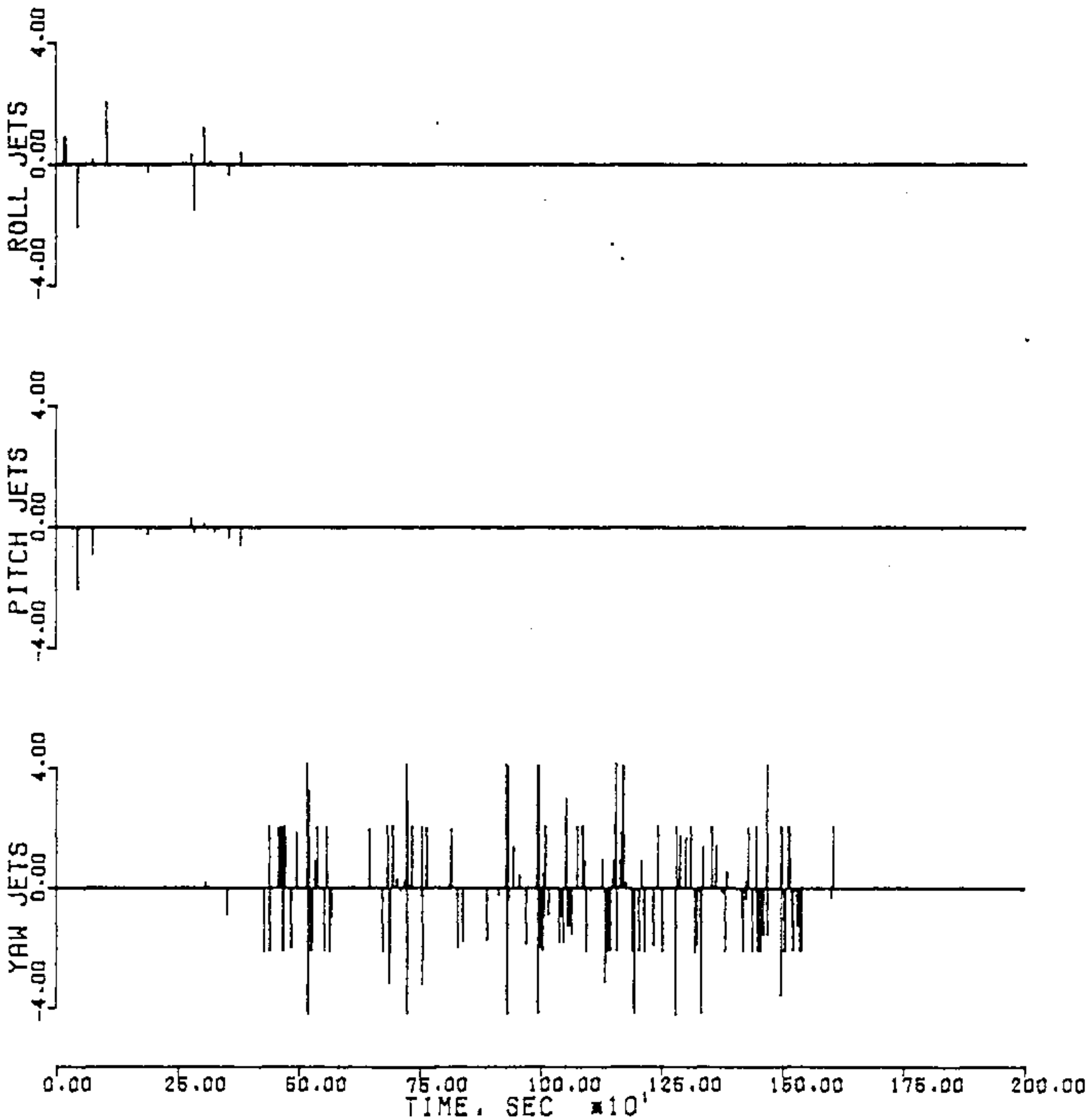

FIGURE 1f - (CONTINUED)

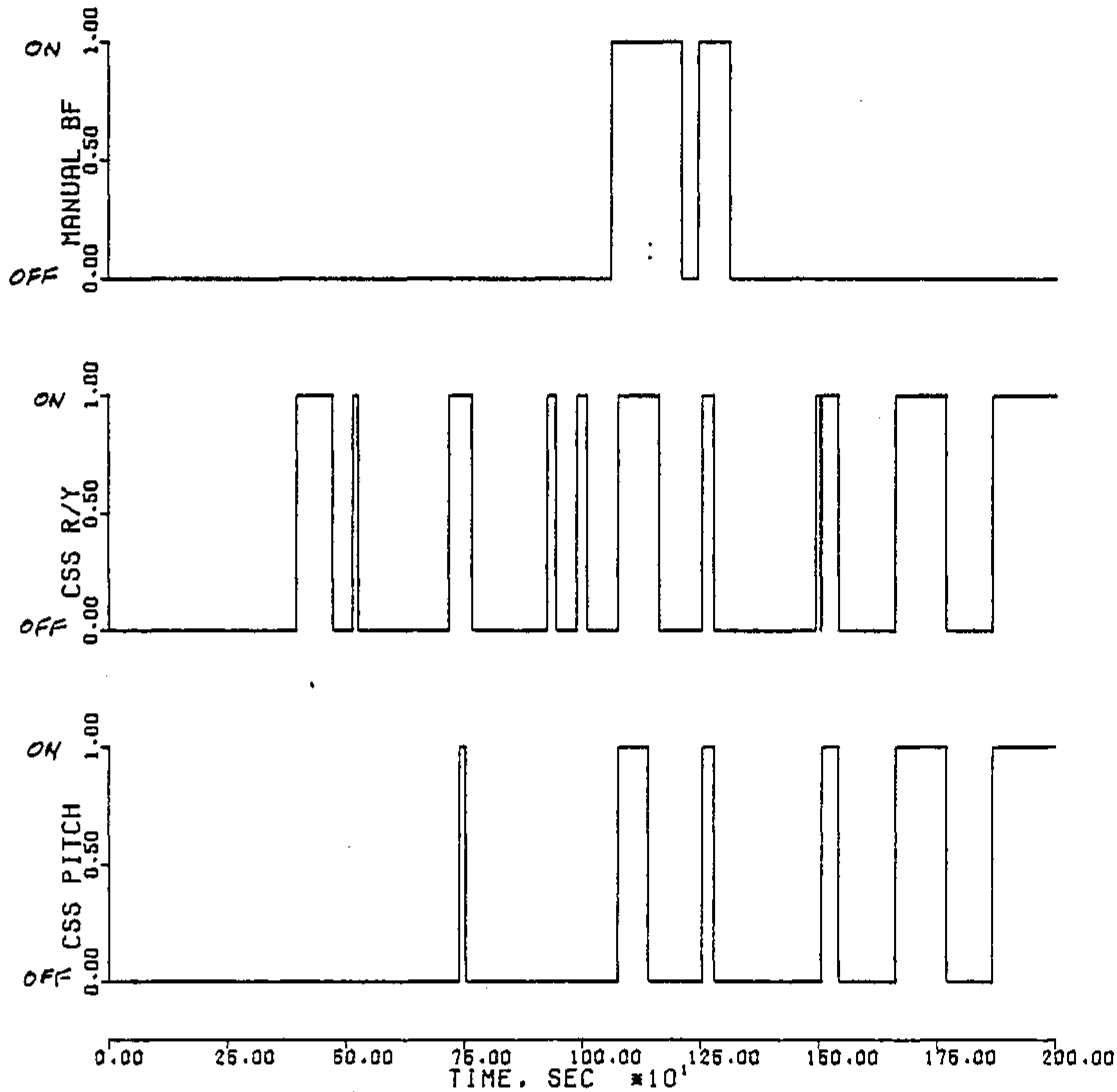

FIGURE 1g - (CONCLUDED)

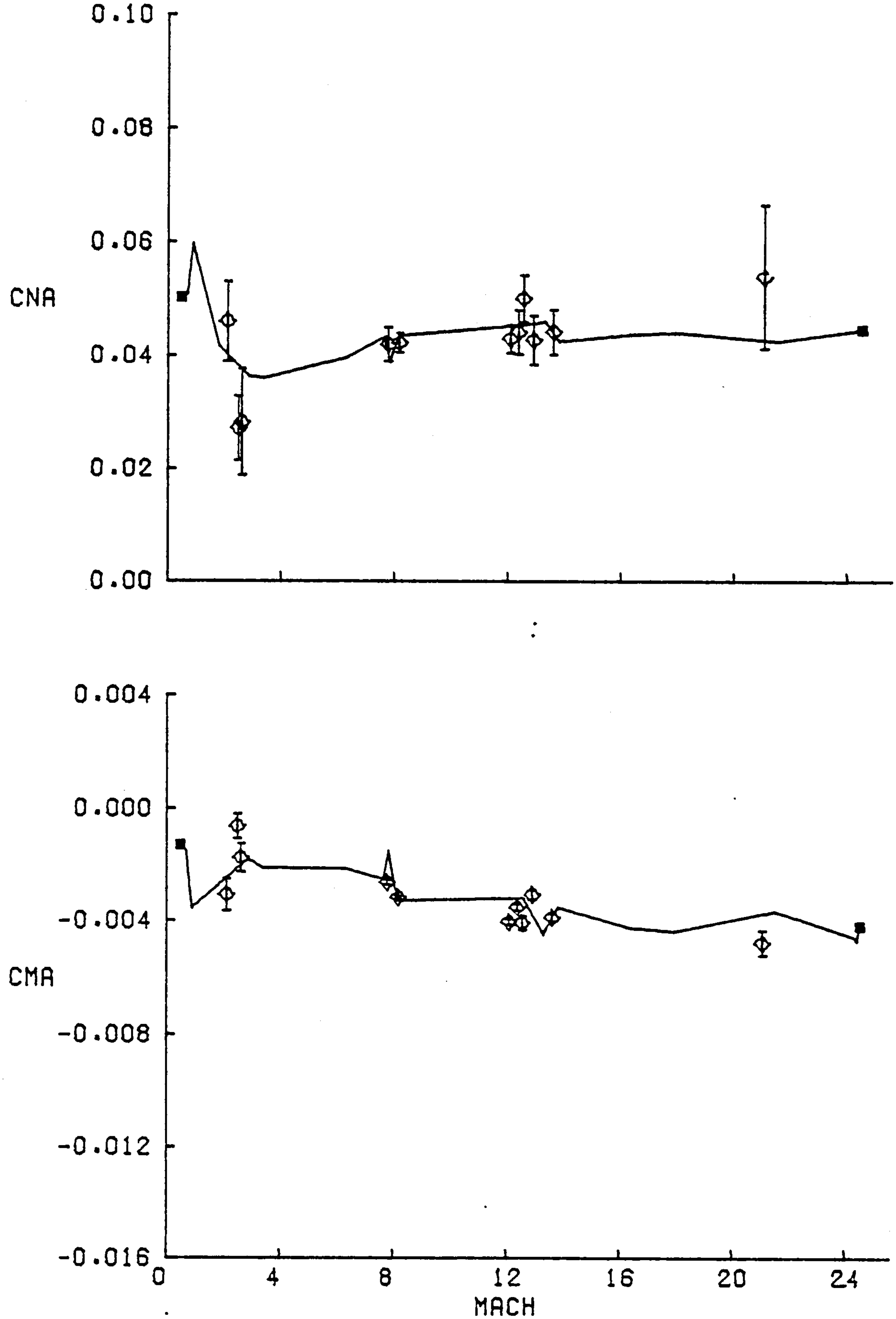

FIGURE 2a - LONGITUDINAL DERIVATIVE ESTIMATES, MACH = 24-1

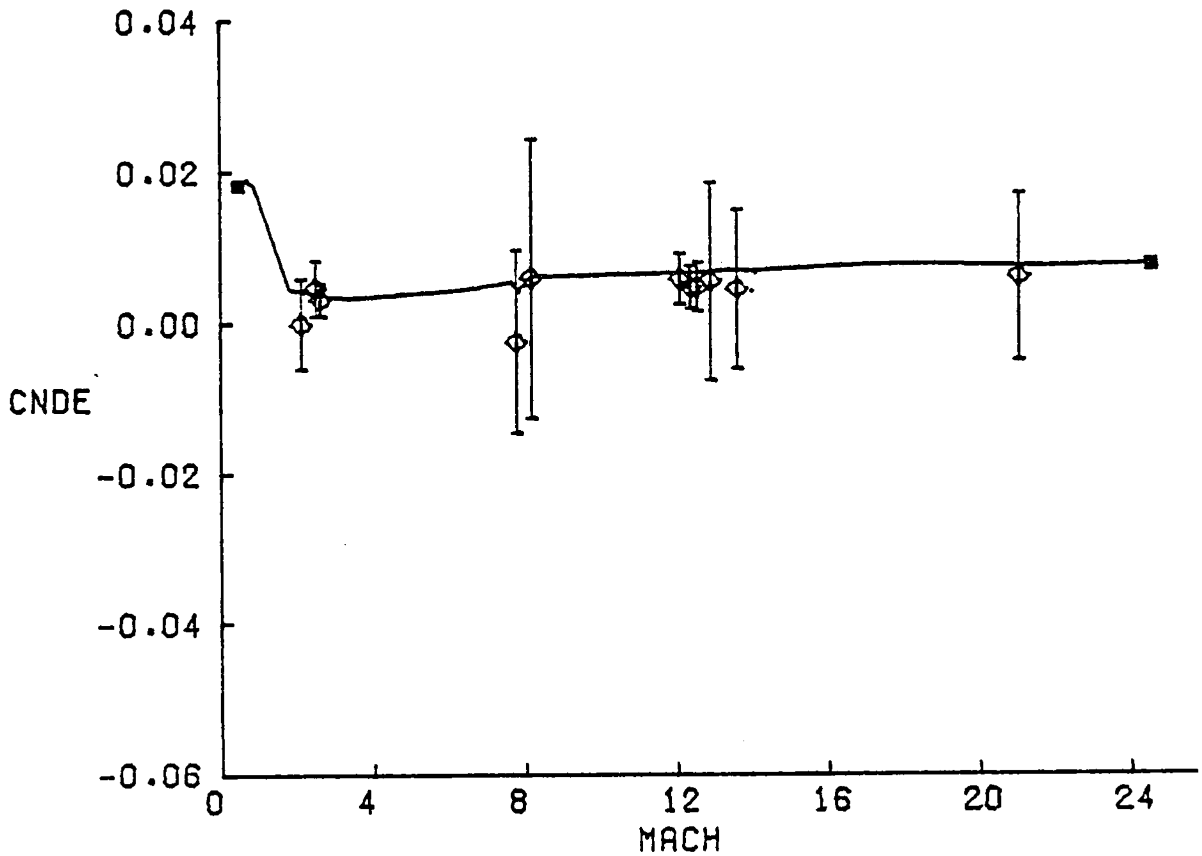

FIGURE 2b - (CONTINUED)

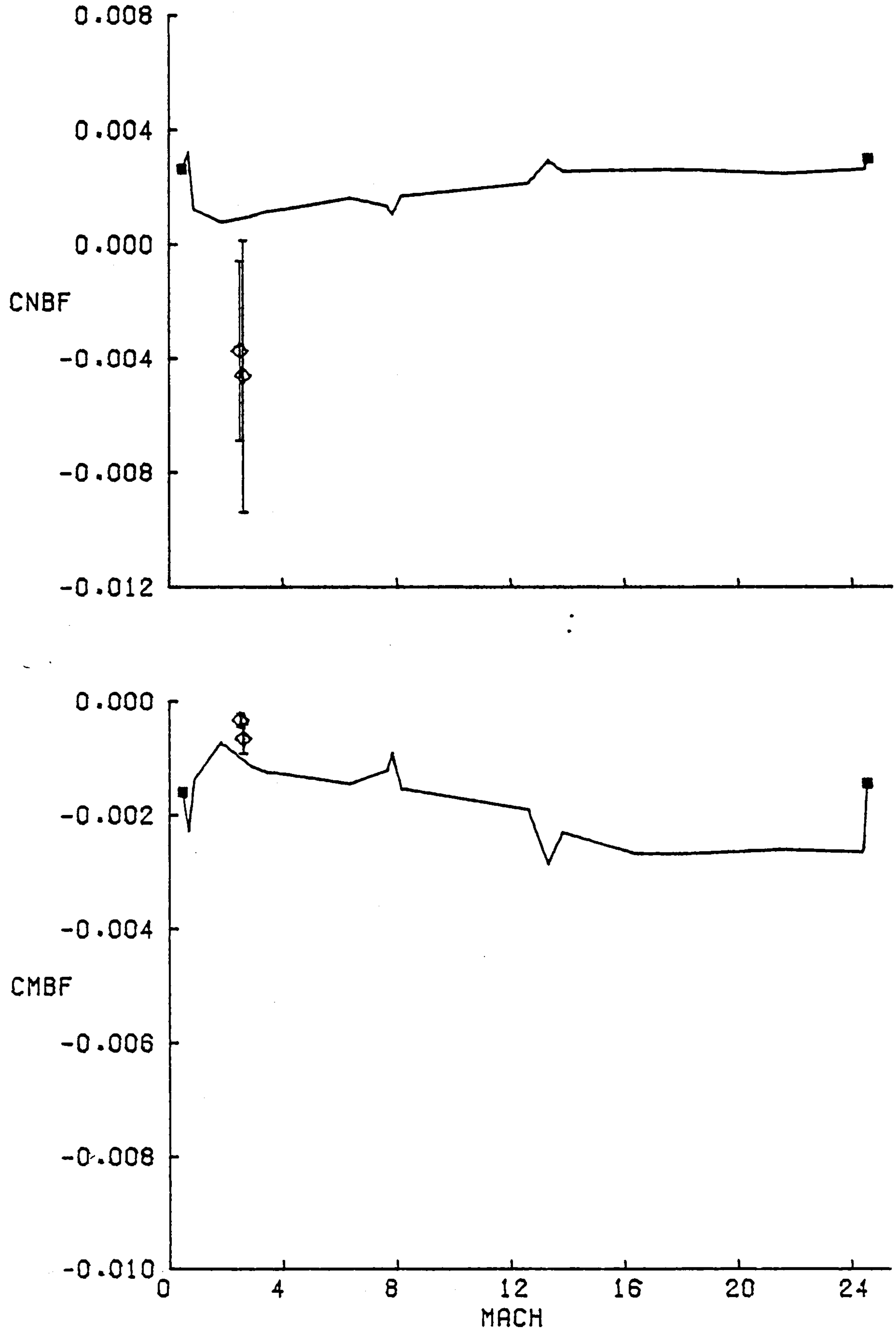

FIGURE 2c - (CONTINUED)

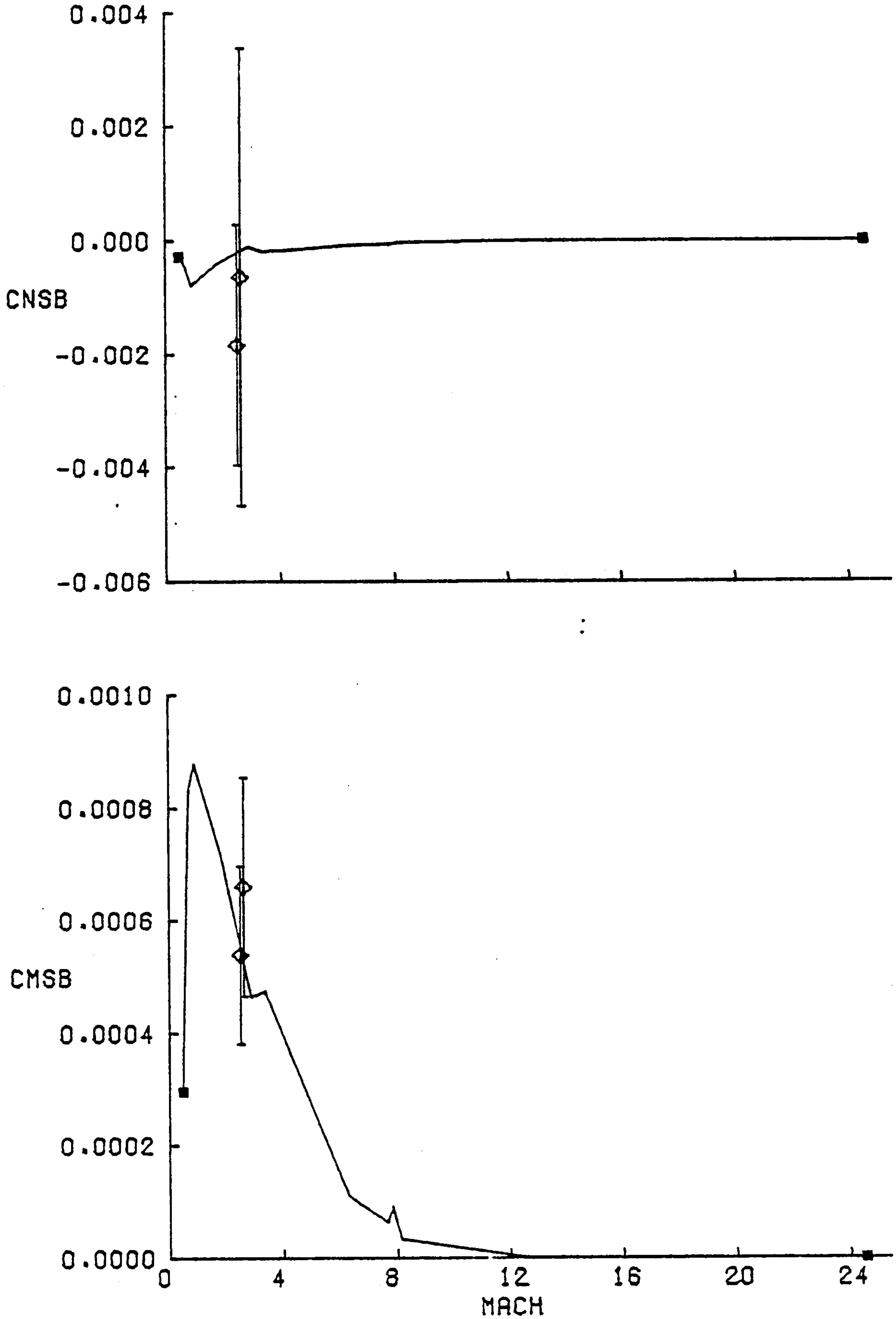

 FIGURE 2d - (CONTINUED)

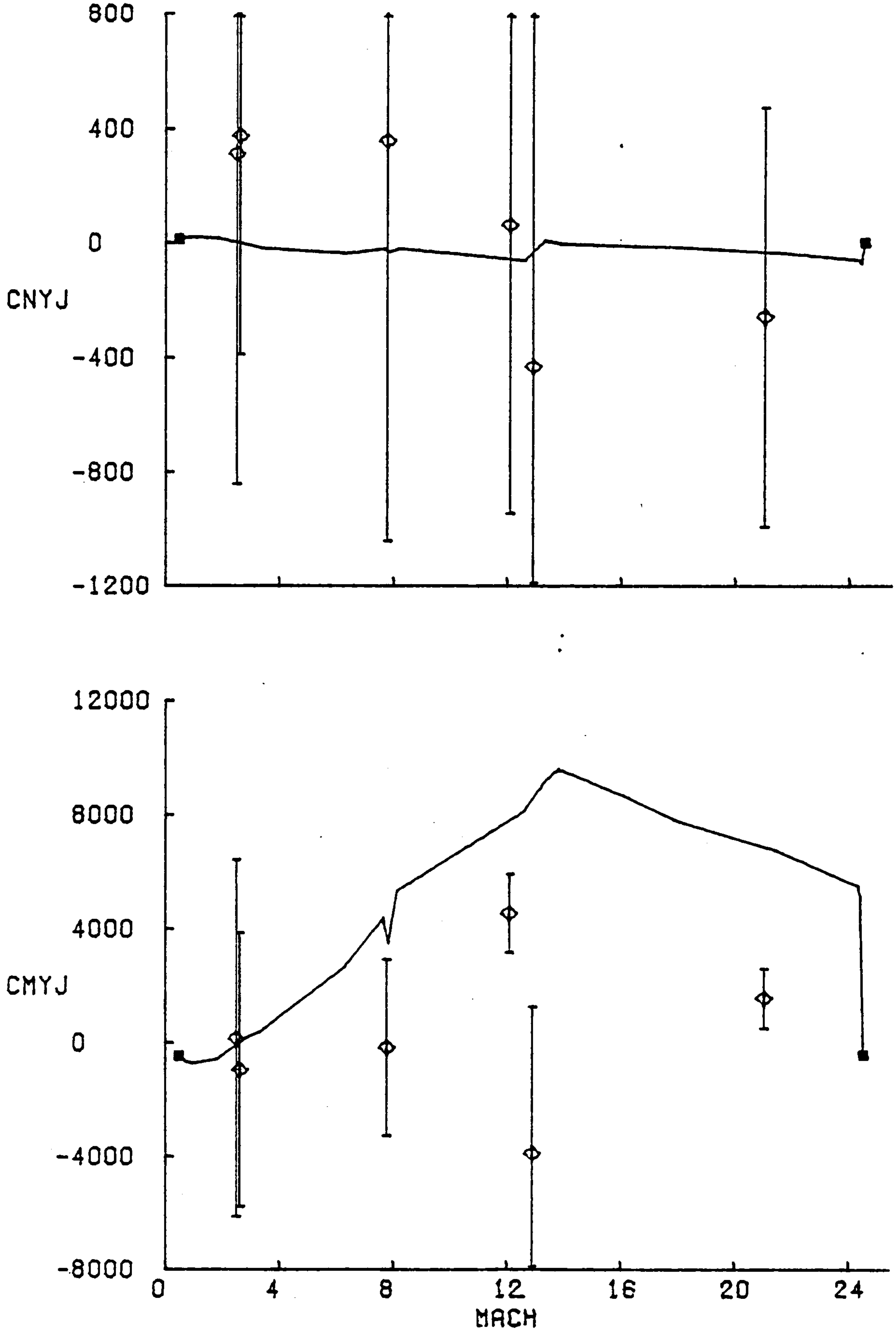

FIGURE 2e - (CONTINUED)

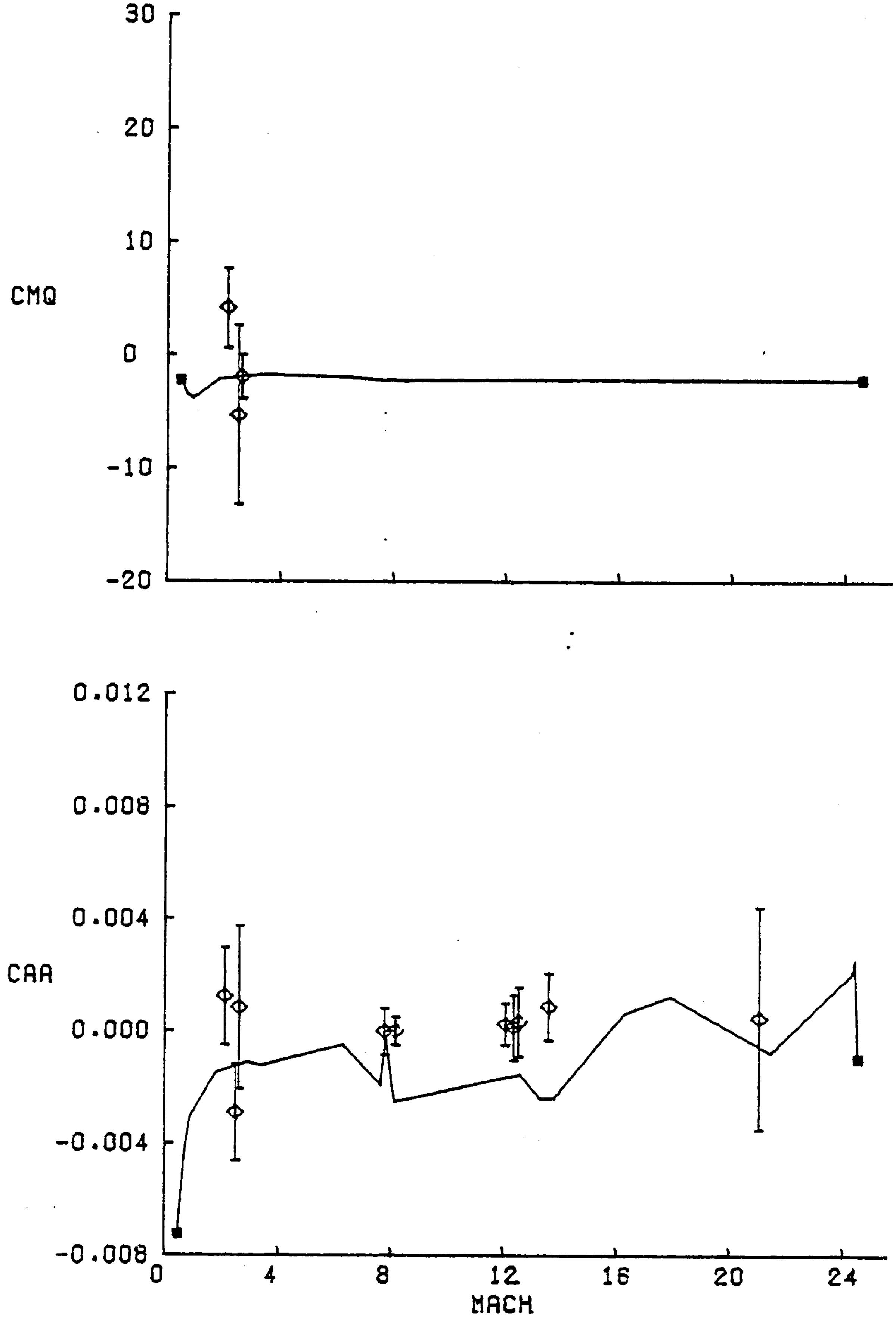

FIGURE 2f - (CONTINUED)

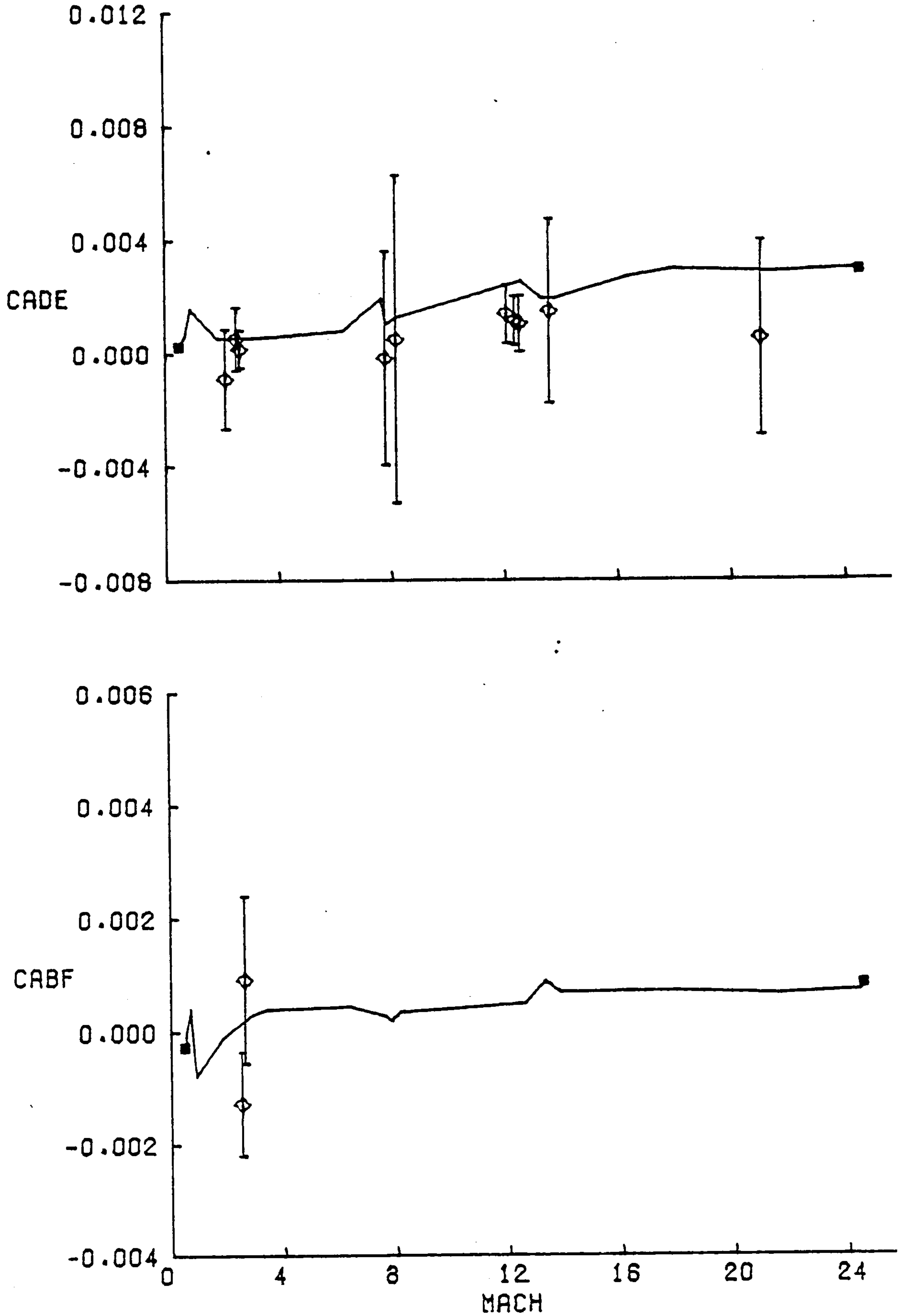

FIGURE 2g - (CONTINUED)

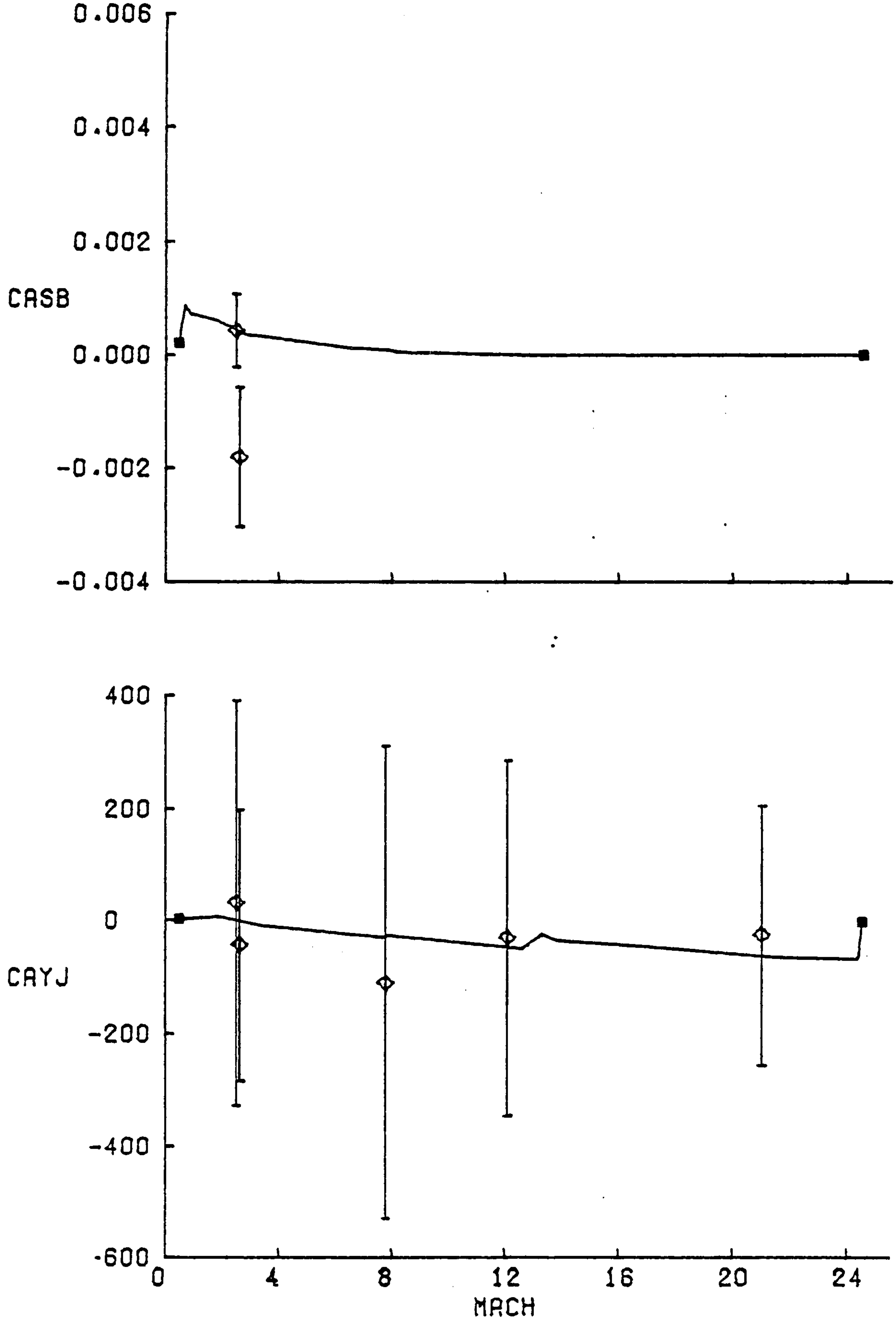

FIGURE 2h - (CONCLUDED)

ELEVATOR EFFECTIVENESS, MACH > 2.5

NASA
DFRF82-557

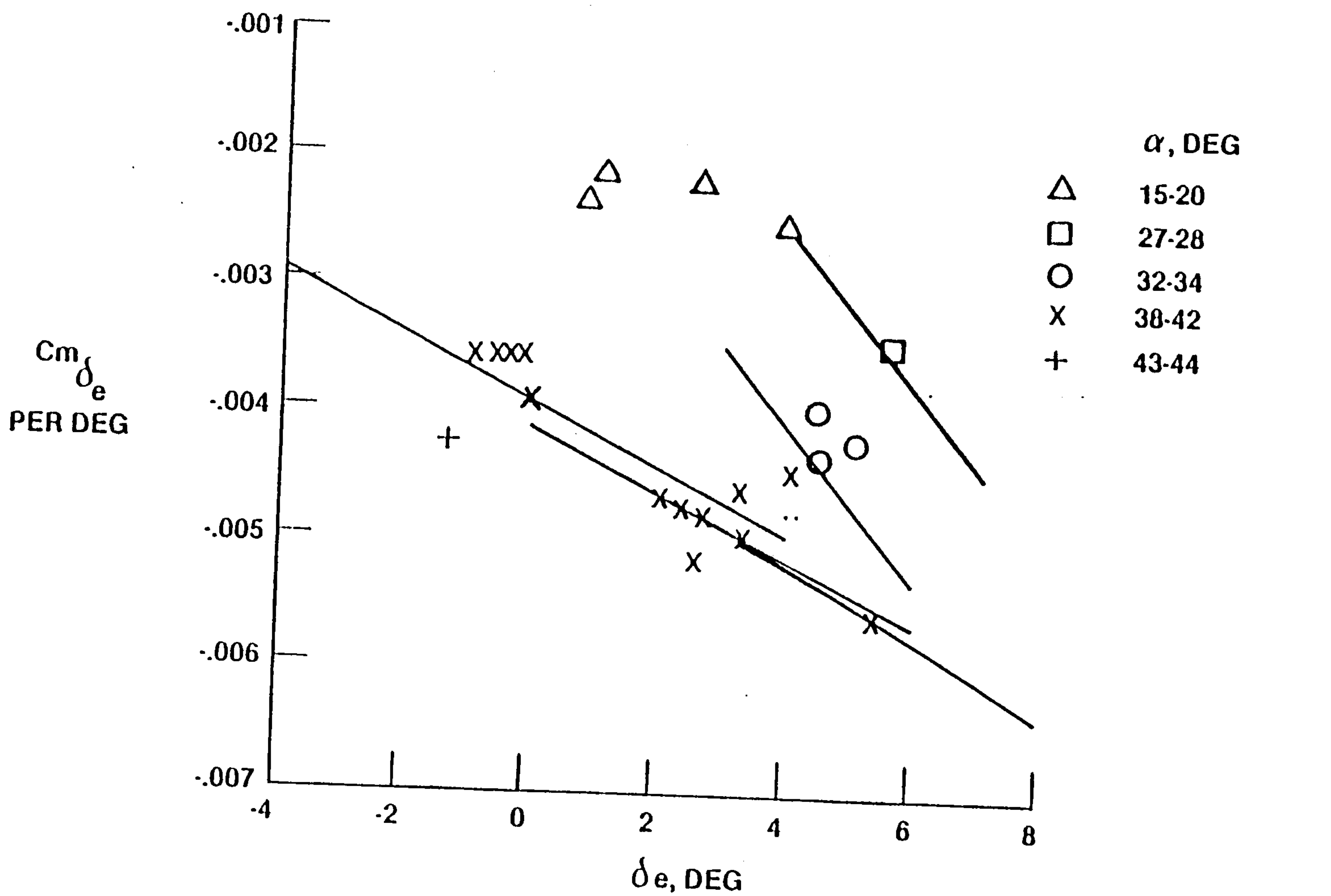

FIGURE 3 - PITCHING MOMENT DUE TO ELEVON, STS-1 THRU STS-4

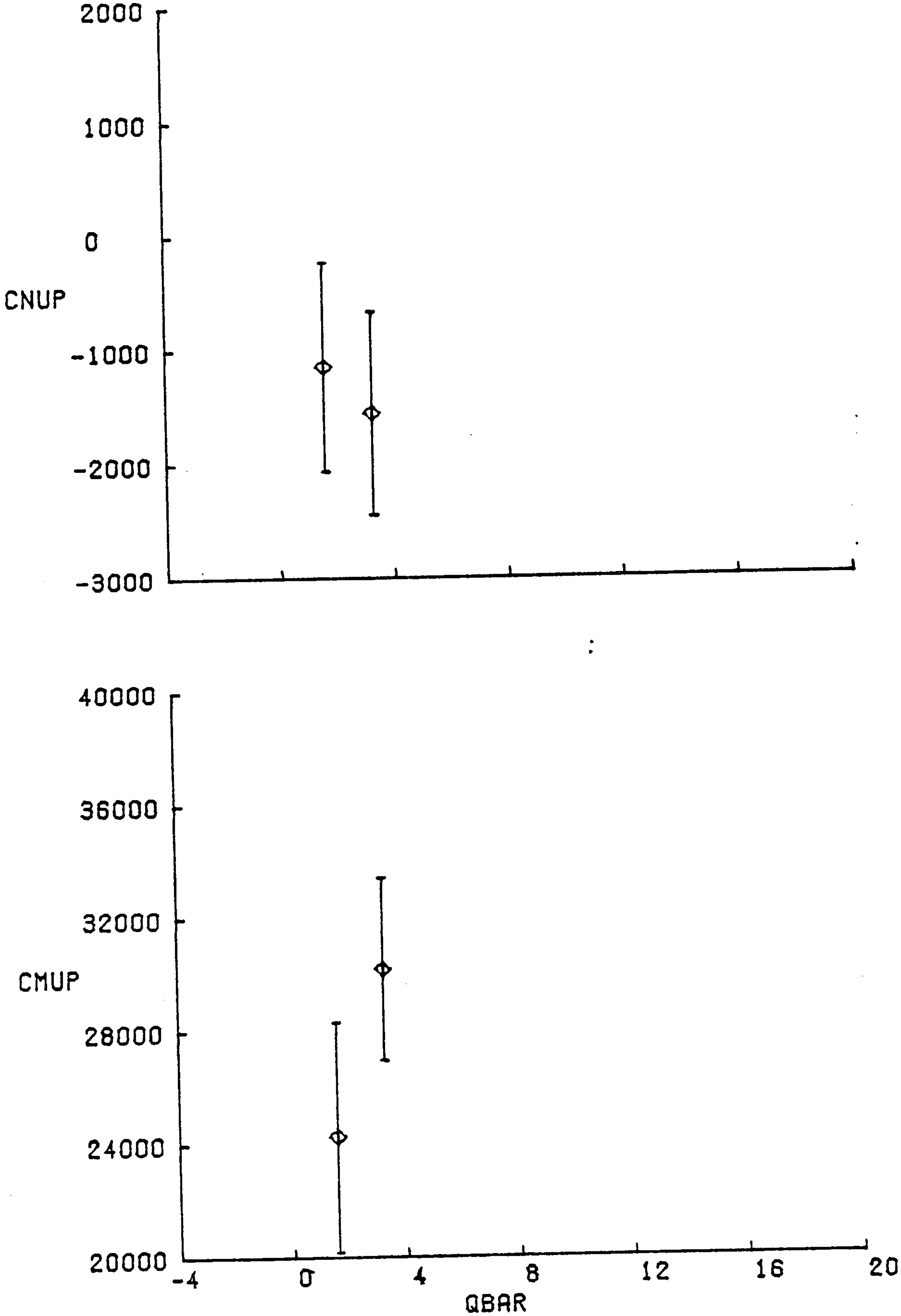

FIGURE 4a - PITCH JET DERIVATIVE ESTIMATES, STS-4

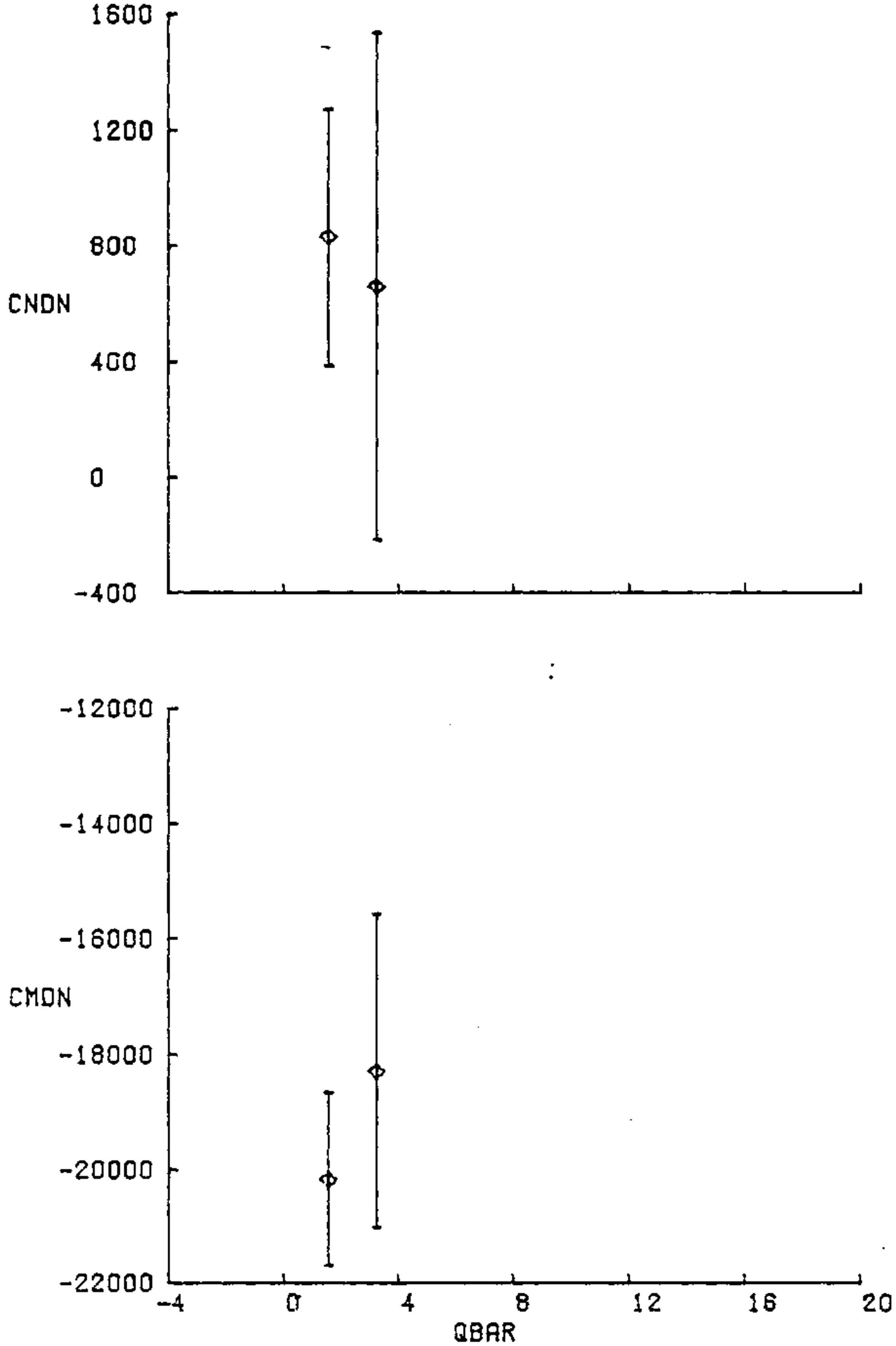

FIGURE 4b - (CONTINUED)

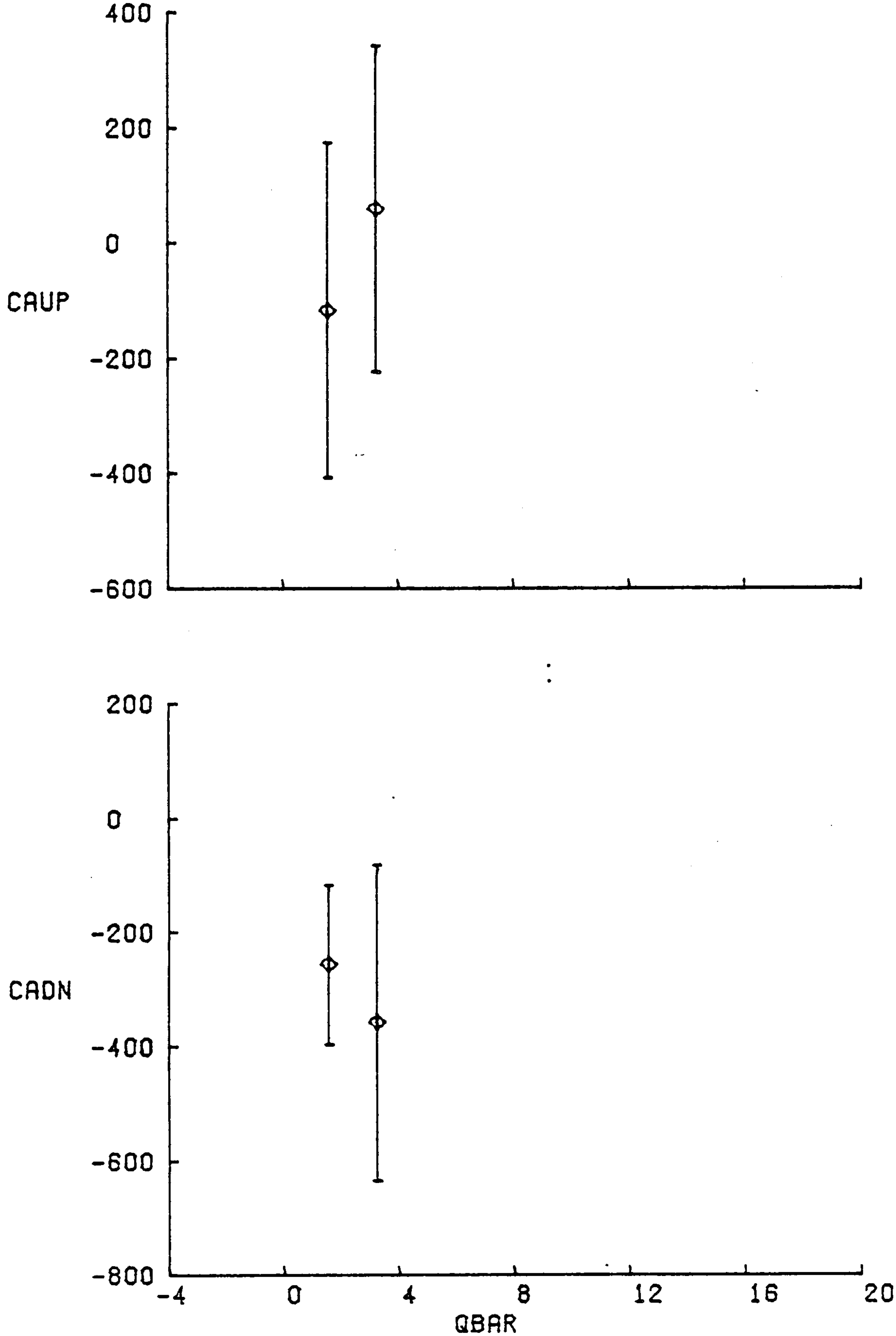

FIGURE 4c - (CONCLUDED)

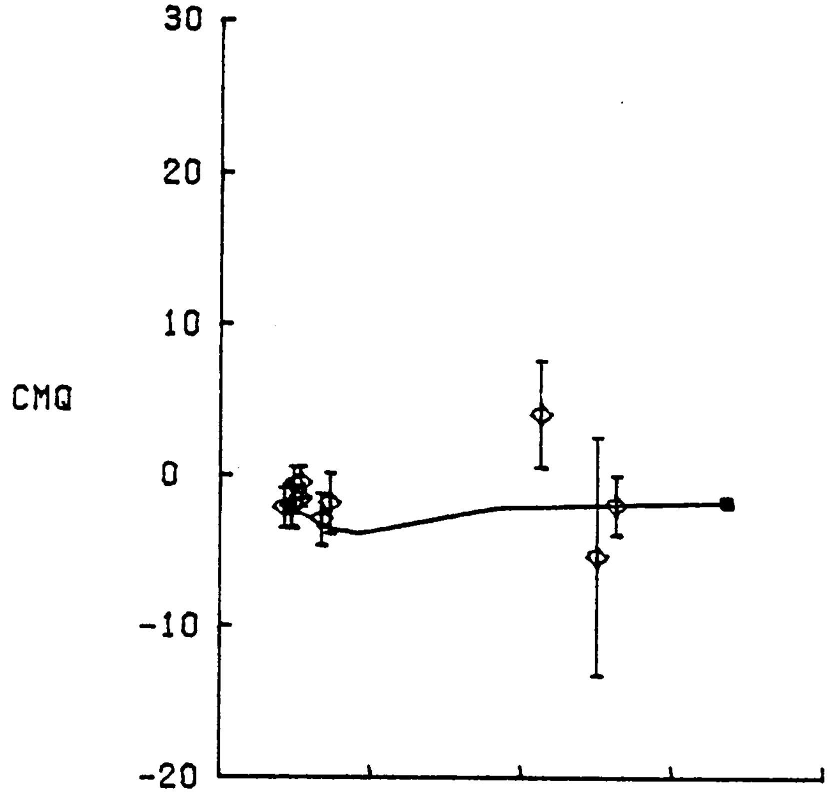

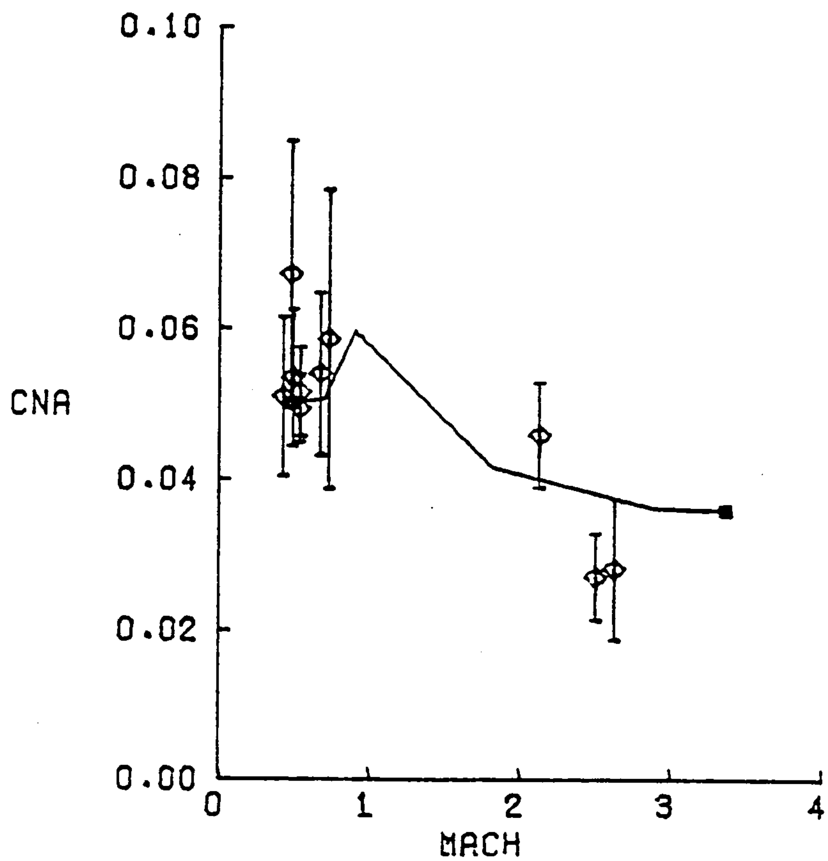

FIGURE 5a - LONGITUDINAL DERIVATIVE ESTIMATES, MACH = 4-0

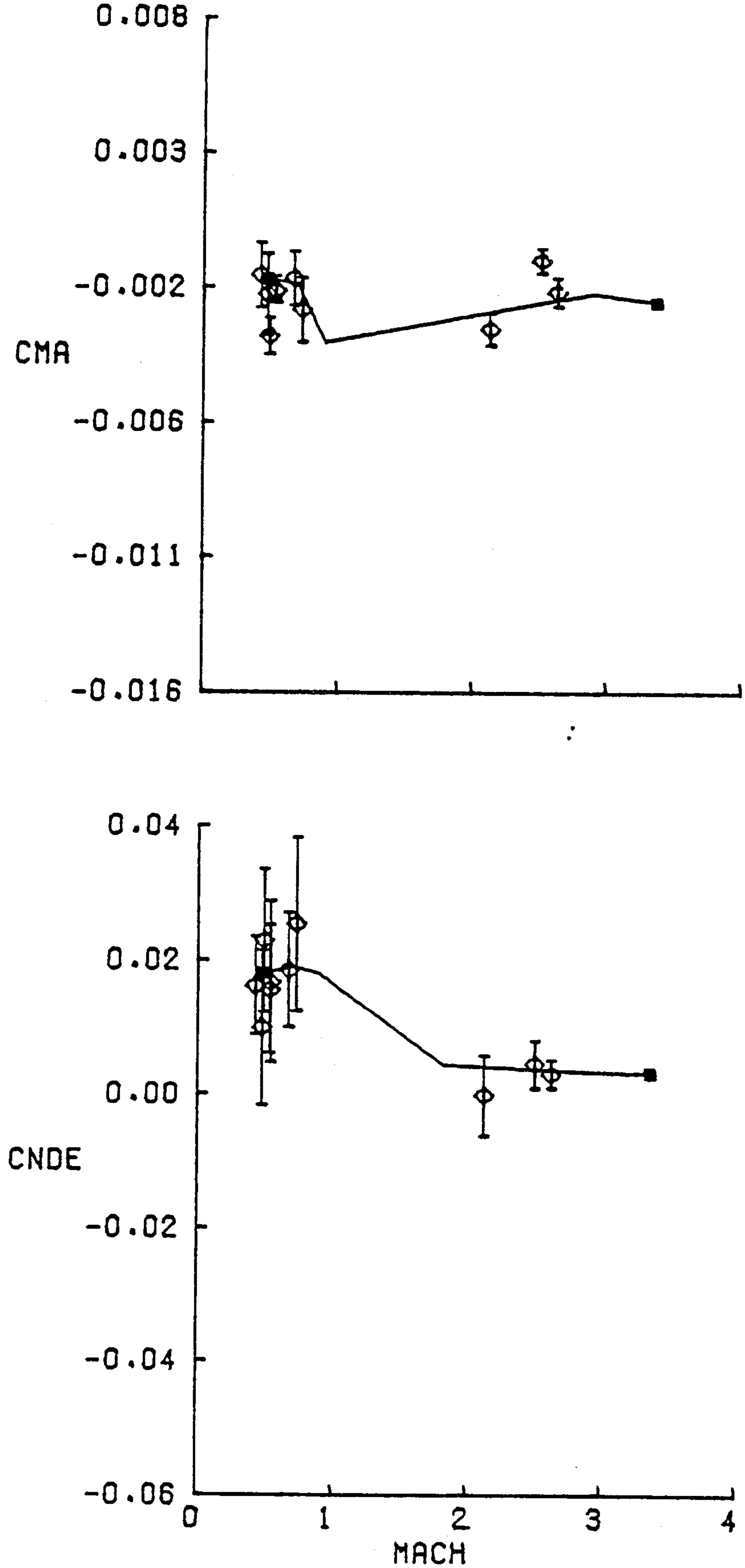

FIGURE 5b - (CONTINUED)

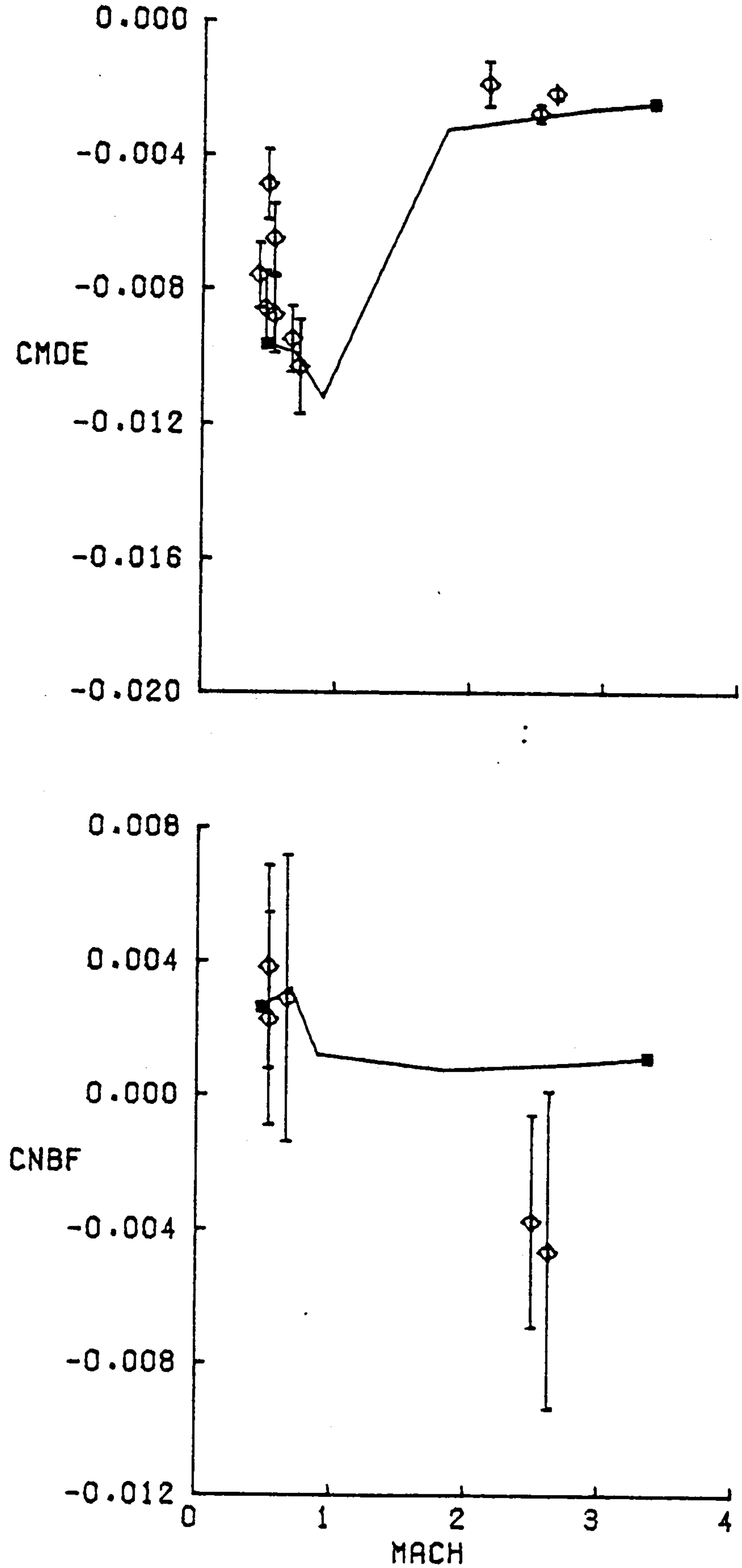

FIGURE 5c - (CONTINUED)

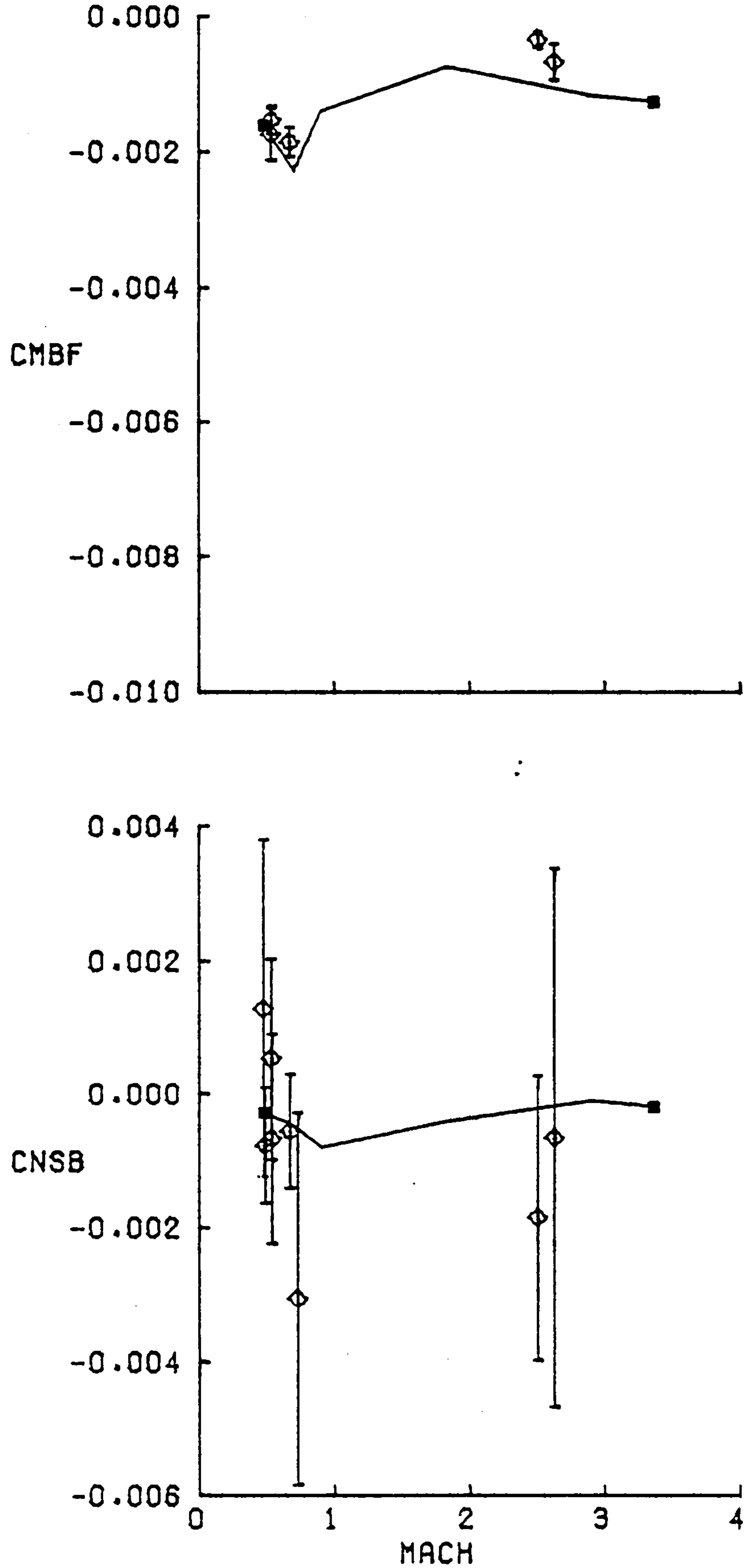

FIGURE 5d - (CONTINUED)

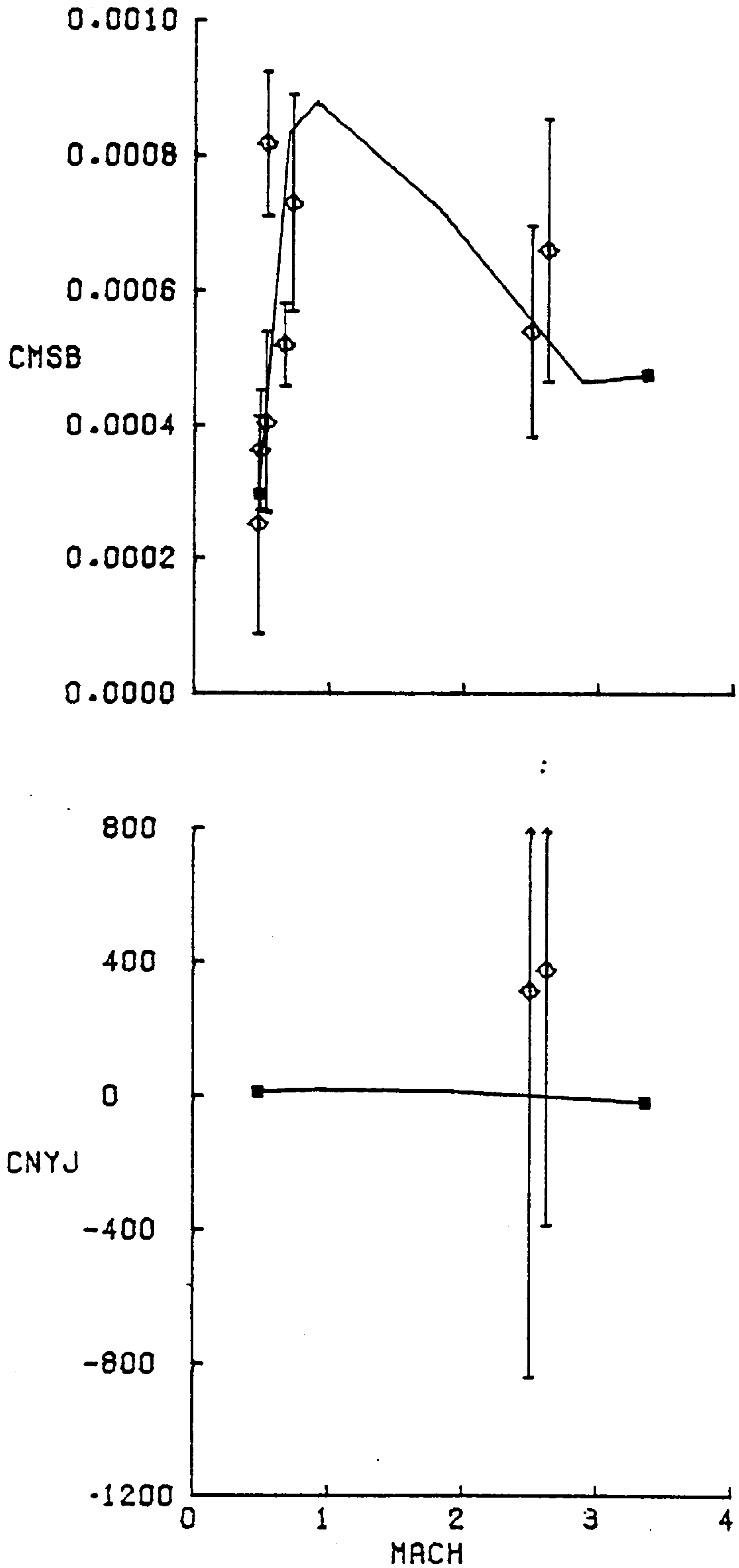

FIGURE 5e - (CONTINUED)

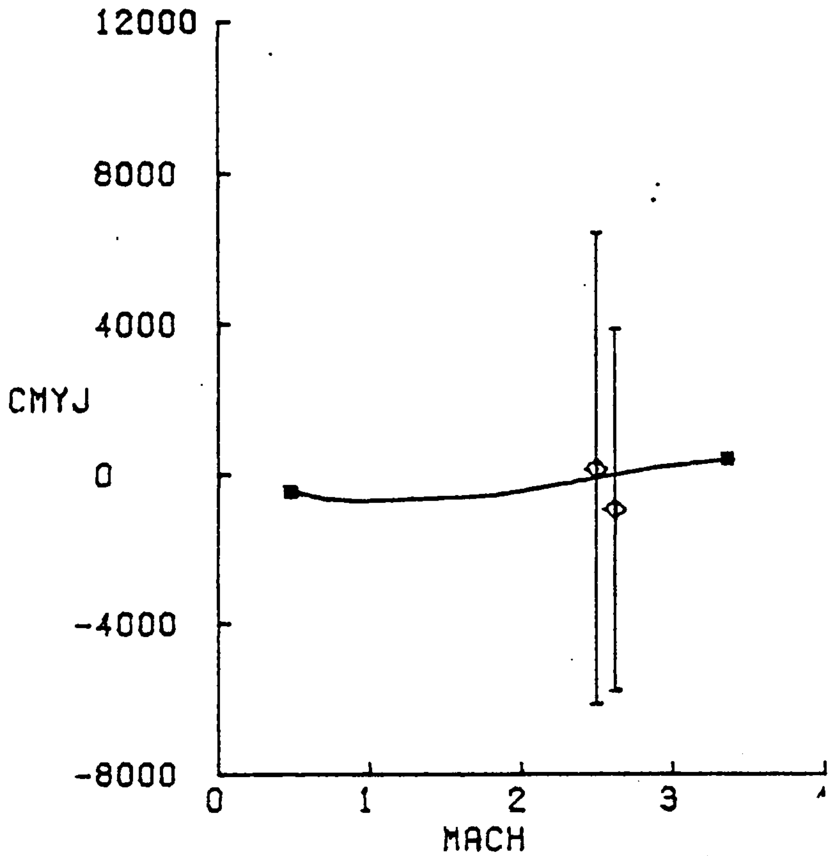

FIGURE 5f - (CONCLUDED)

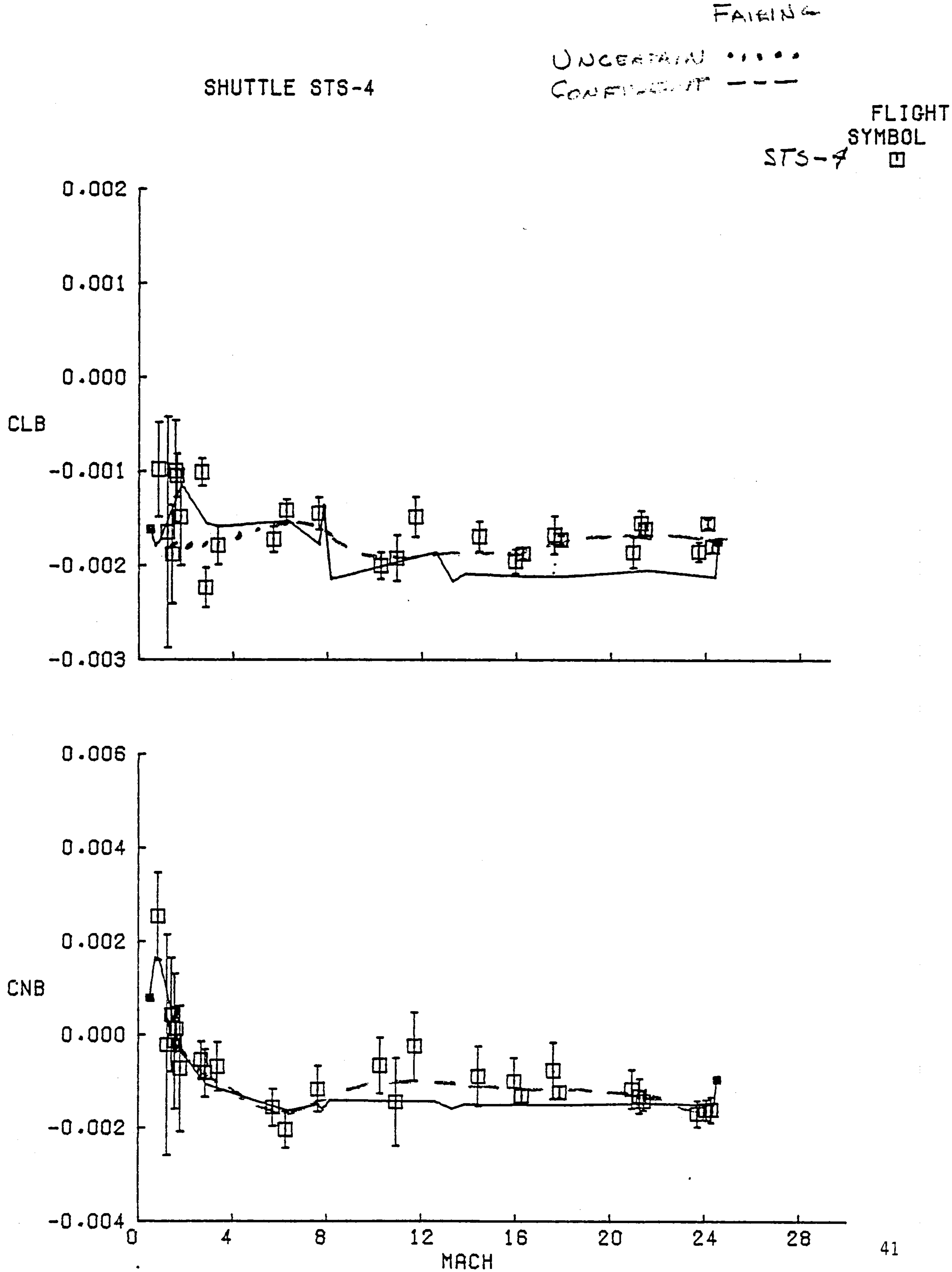

FIGURE 6a - LATERAL-DIRECTIONAL DERIVATIVE ESTIMATES, STS-1

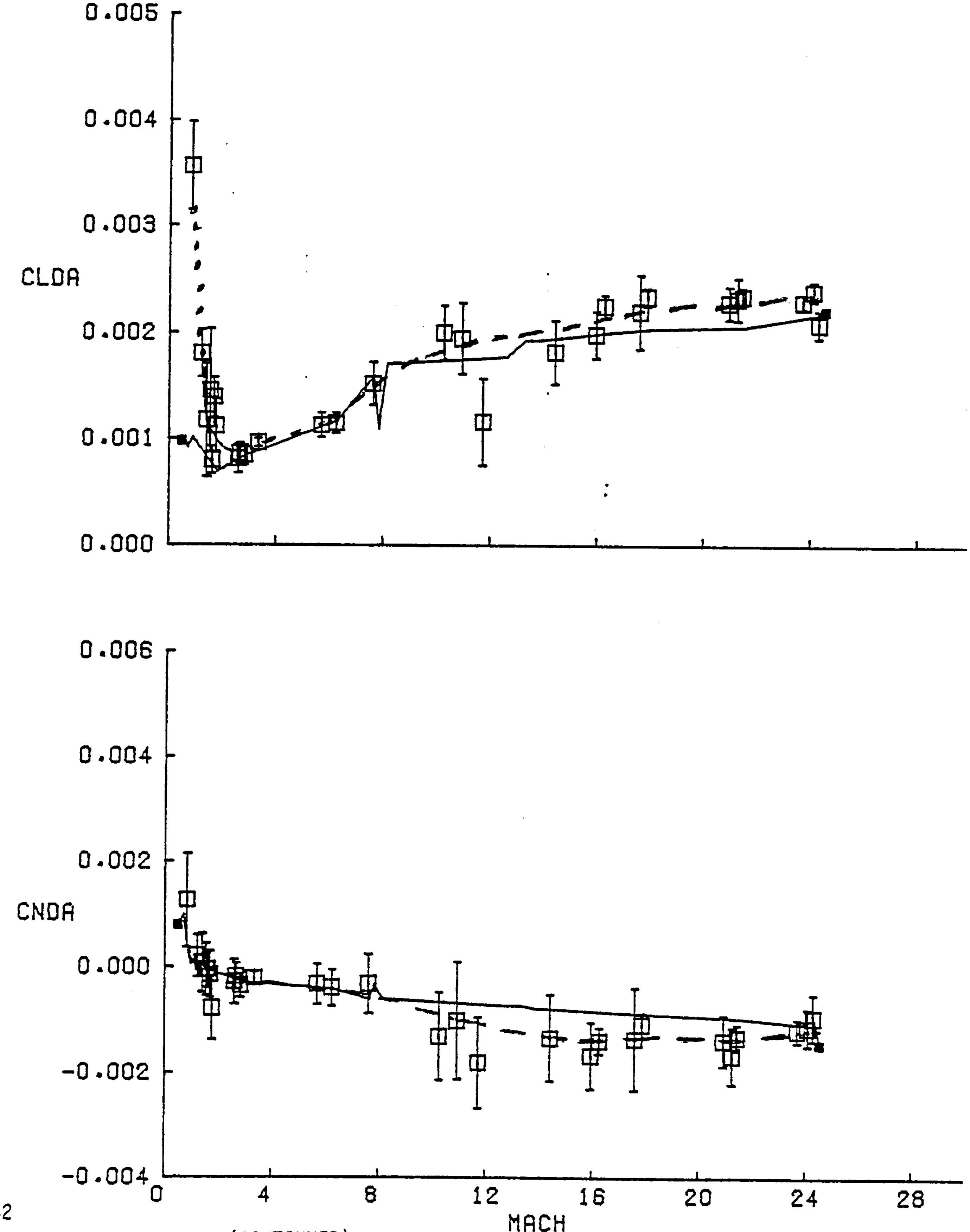

FIGURE 6b - (CONTINUED)

SHUTTLE STS-4

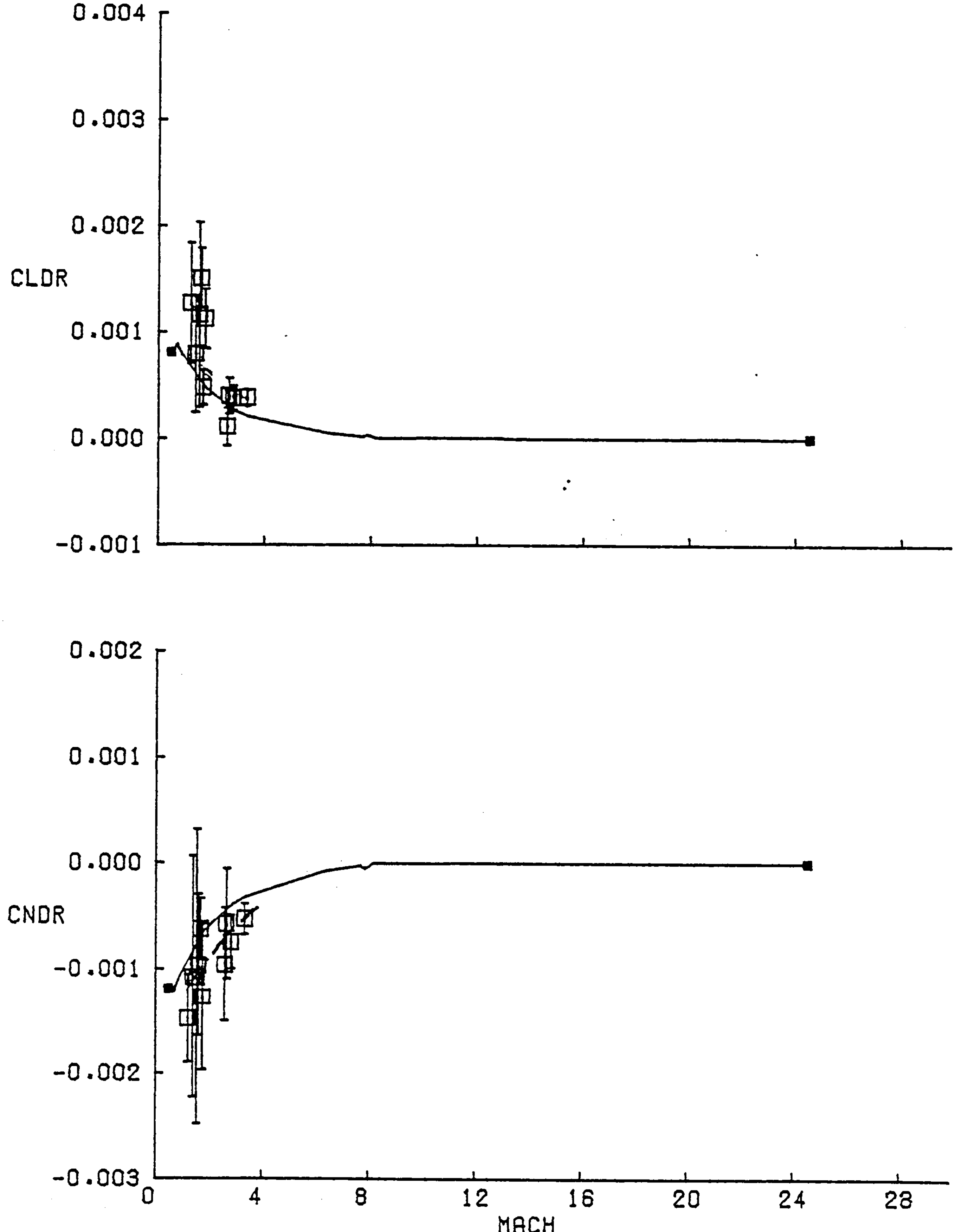

FIGURE 6c - (CONTINUED)

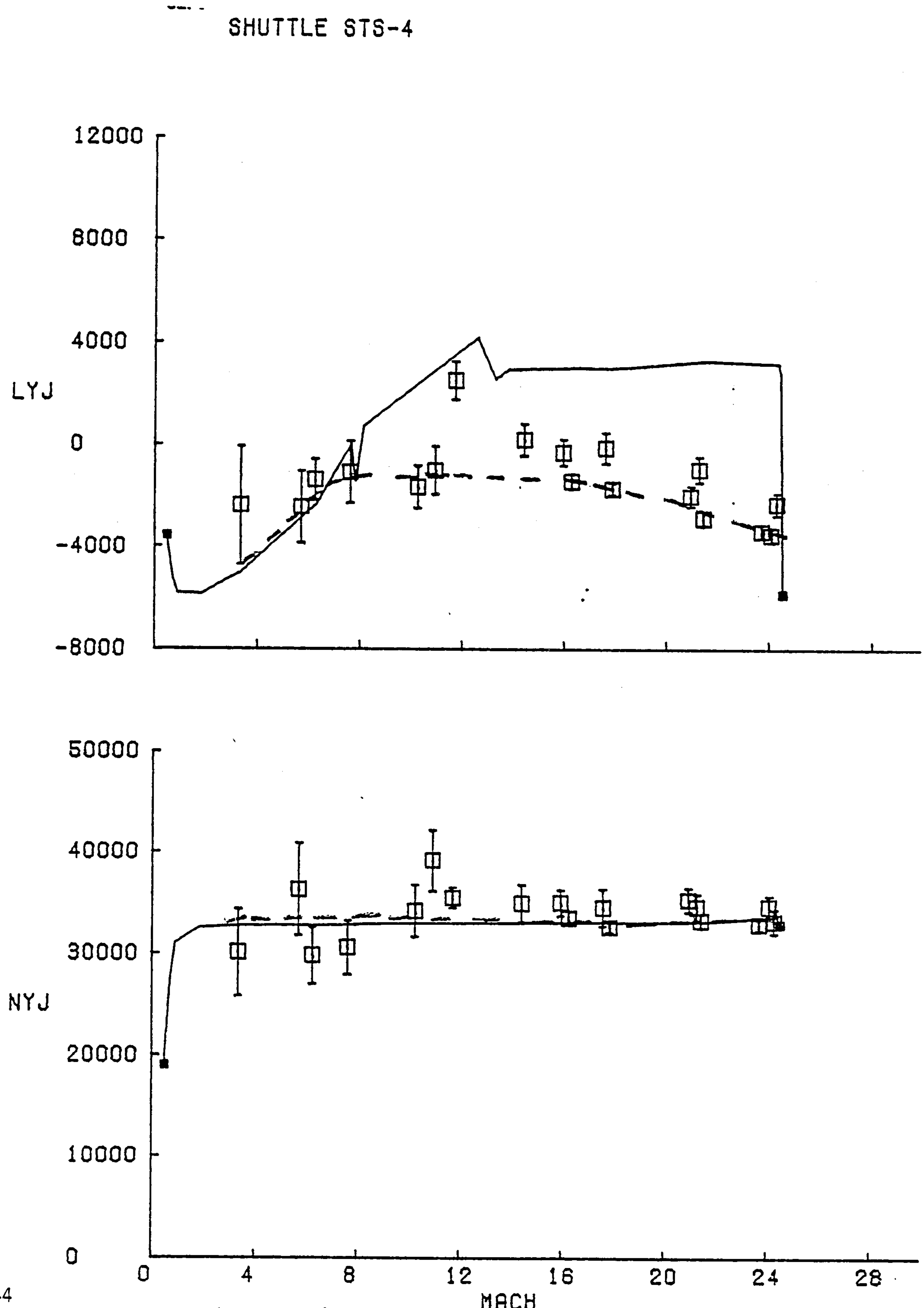

FIGURE 6d - (CONTINUED)

SHUTTLE STS-4

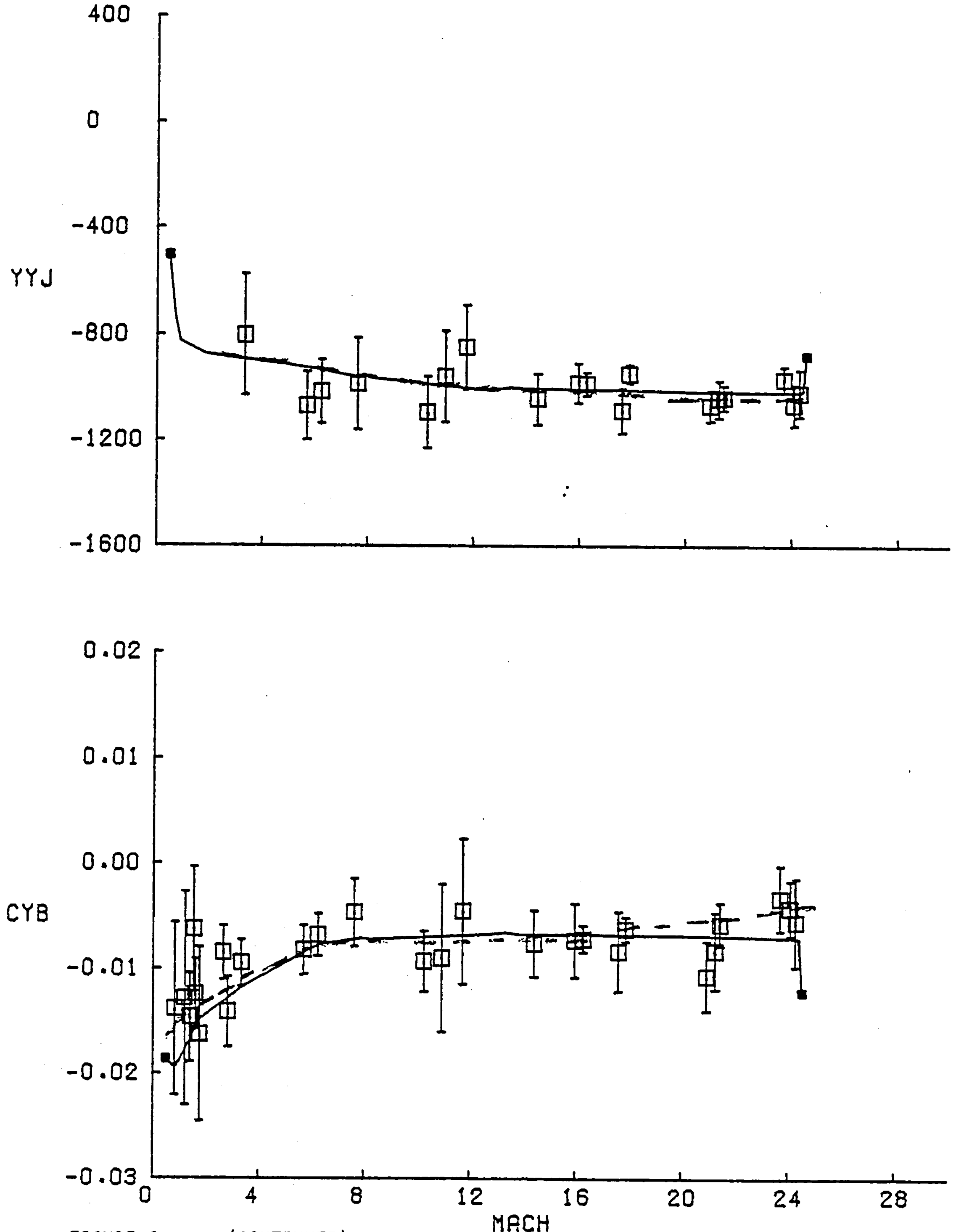

FIGURE 6e - (CONTINUED)

SHUTTLE STS-4

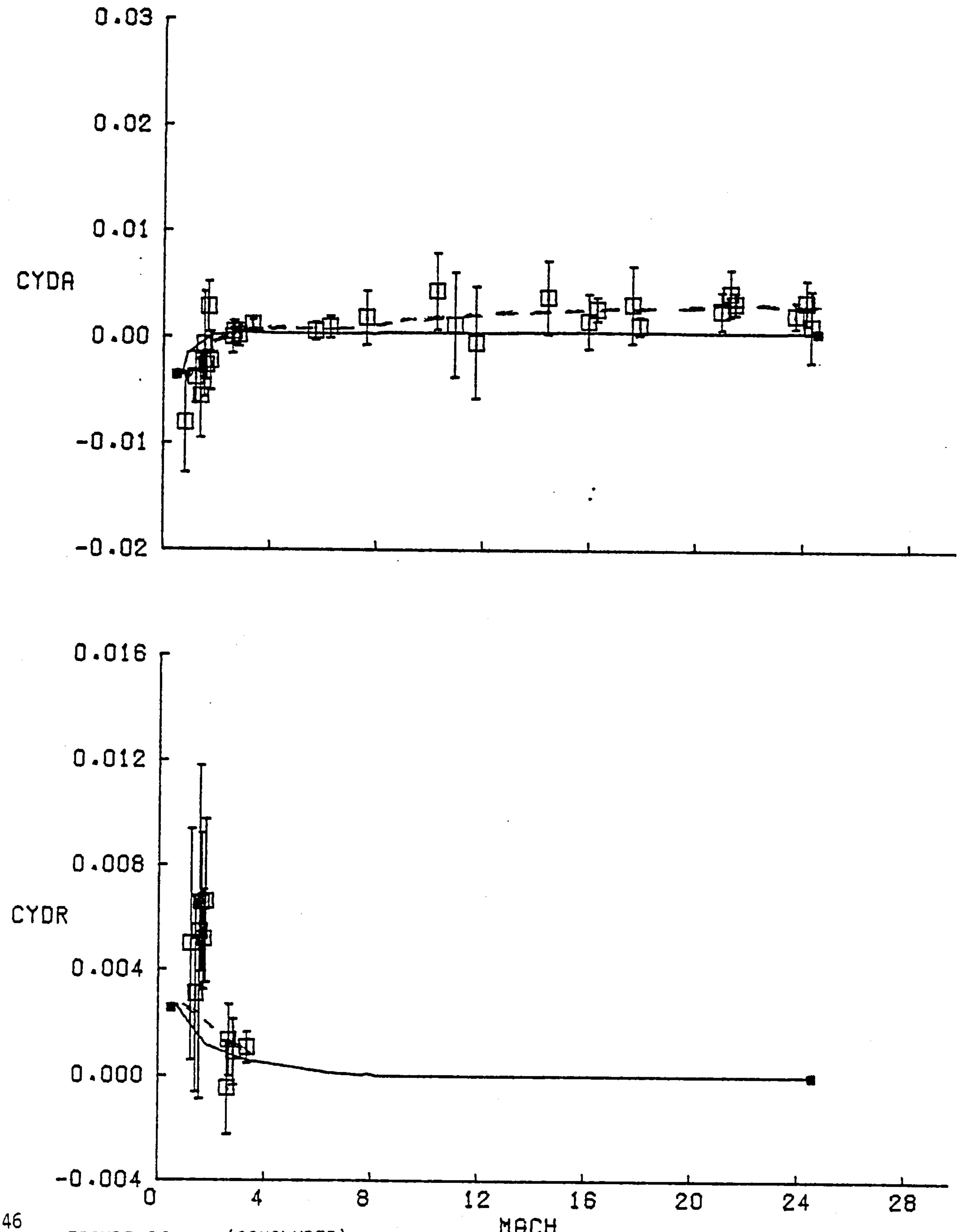

FIGURE 6f - (CONCLUDED)

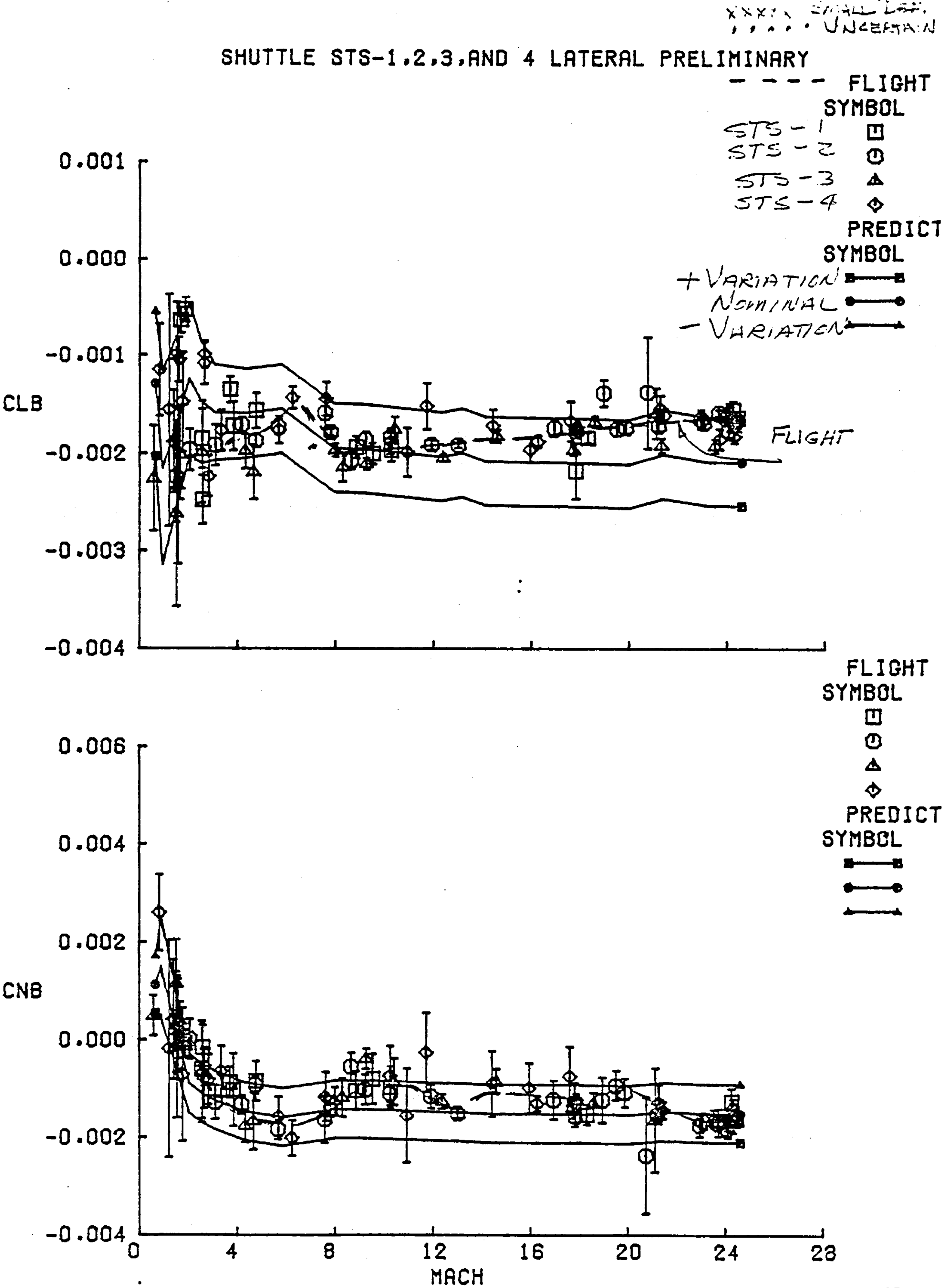

FIGURE 7a - LATERAL-DIRECTIONAL DERIVATIVE COMPARISONS, STS-1 THRU STS-4

SHUTTLE STS-1,2,3,AND 4 LATERAL PRELIMINARY

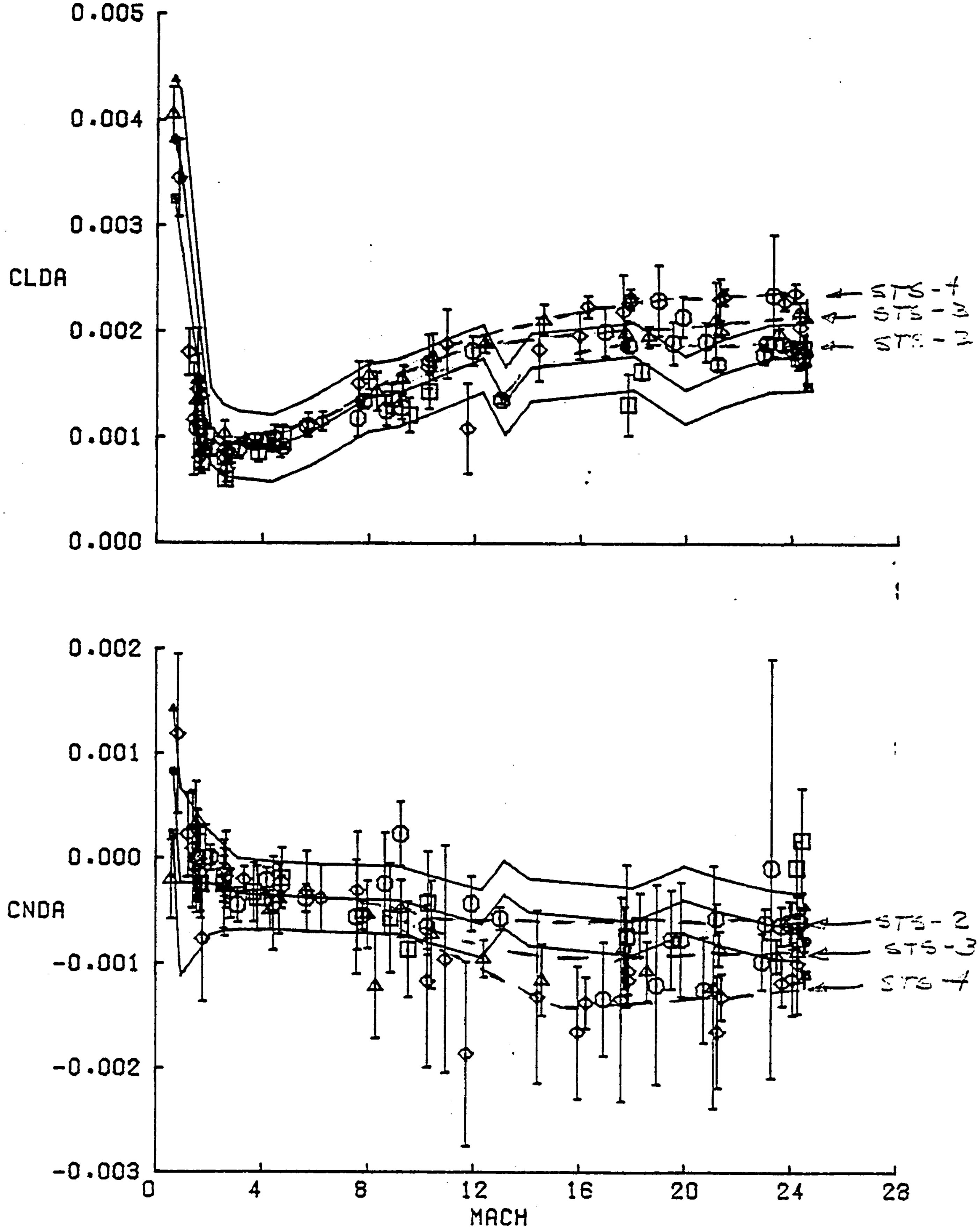

FIGURE 7b - (CONTINUED)

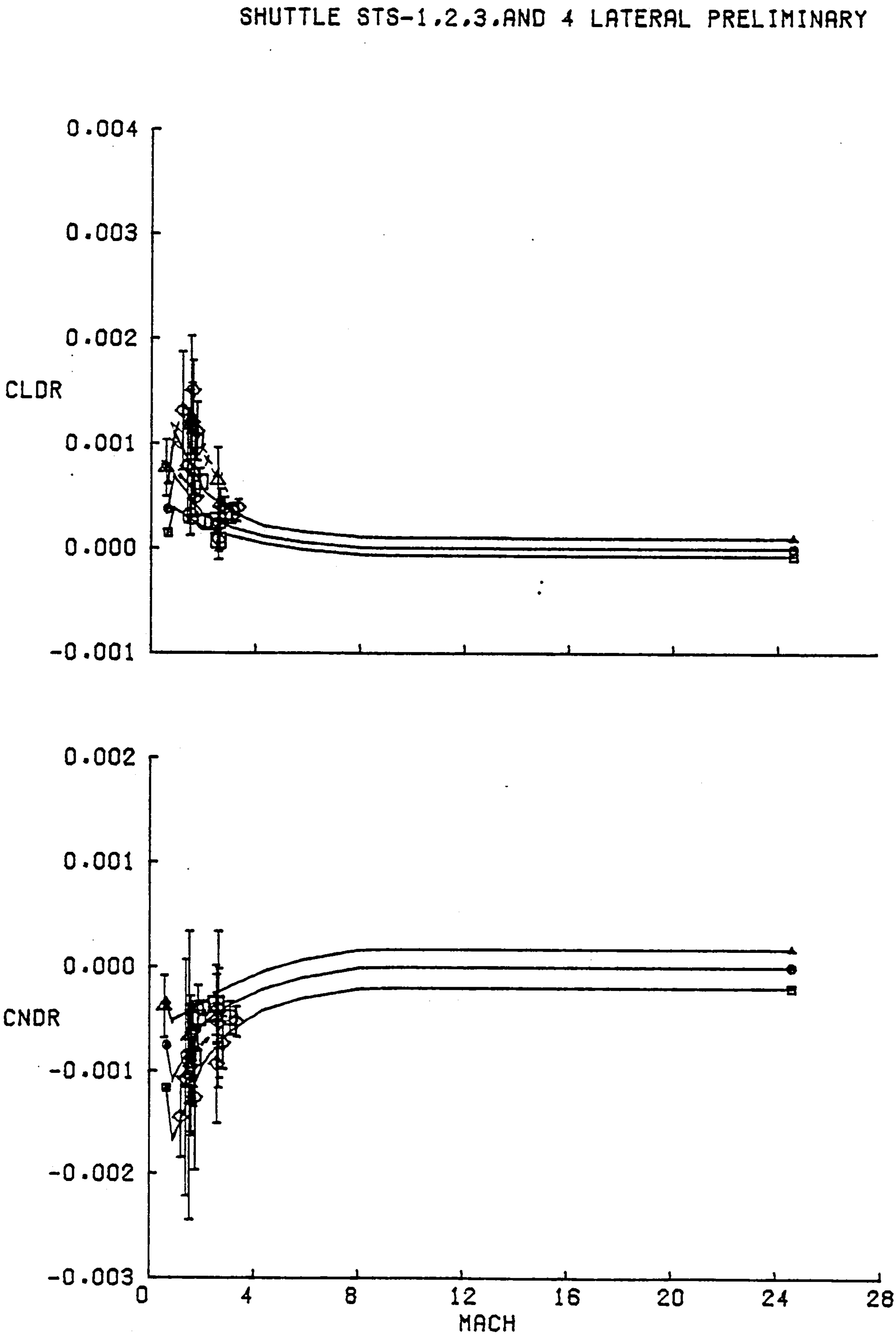

FIGURE 7c - (CONTINUED)

SHUTTLE STS-1,2,3,AND 4 LATERAL PRELIMINARY

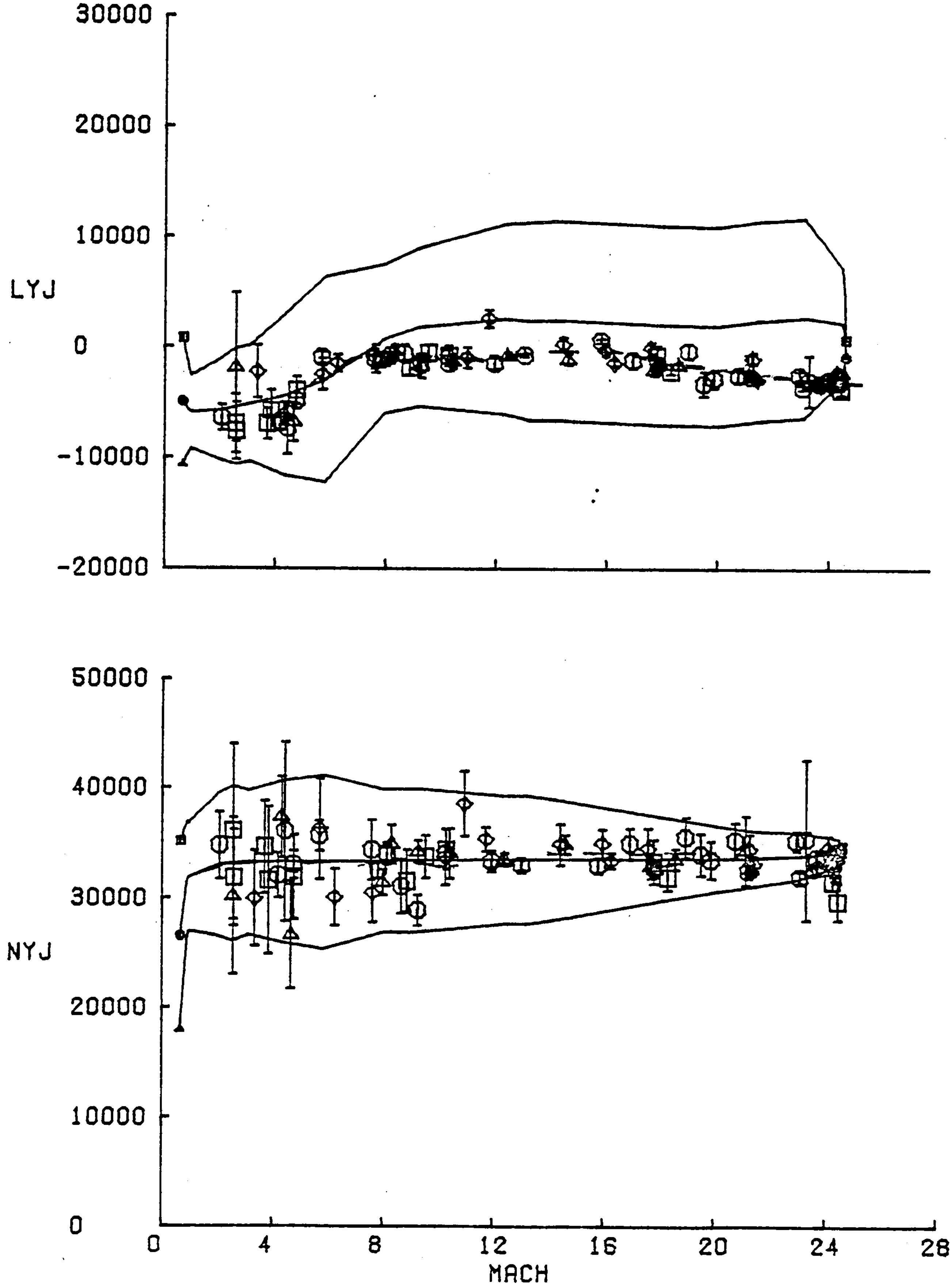

FIGURE 7d - (CONTINUED)

SHUTTLE STS-1,2,3,AND 4 LATERAL PRELIMINARY

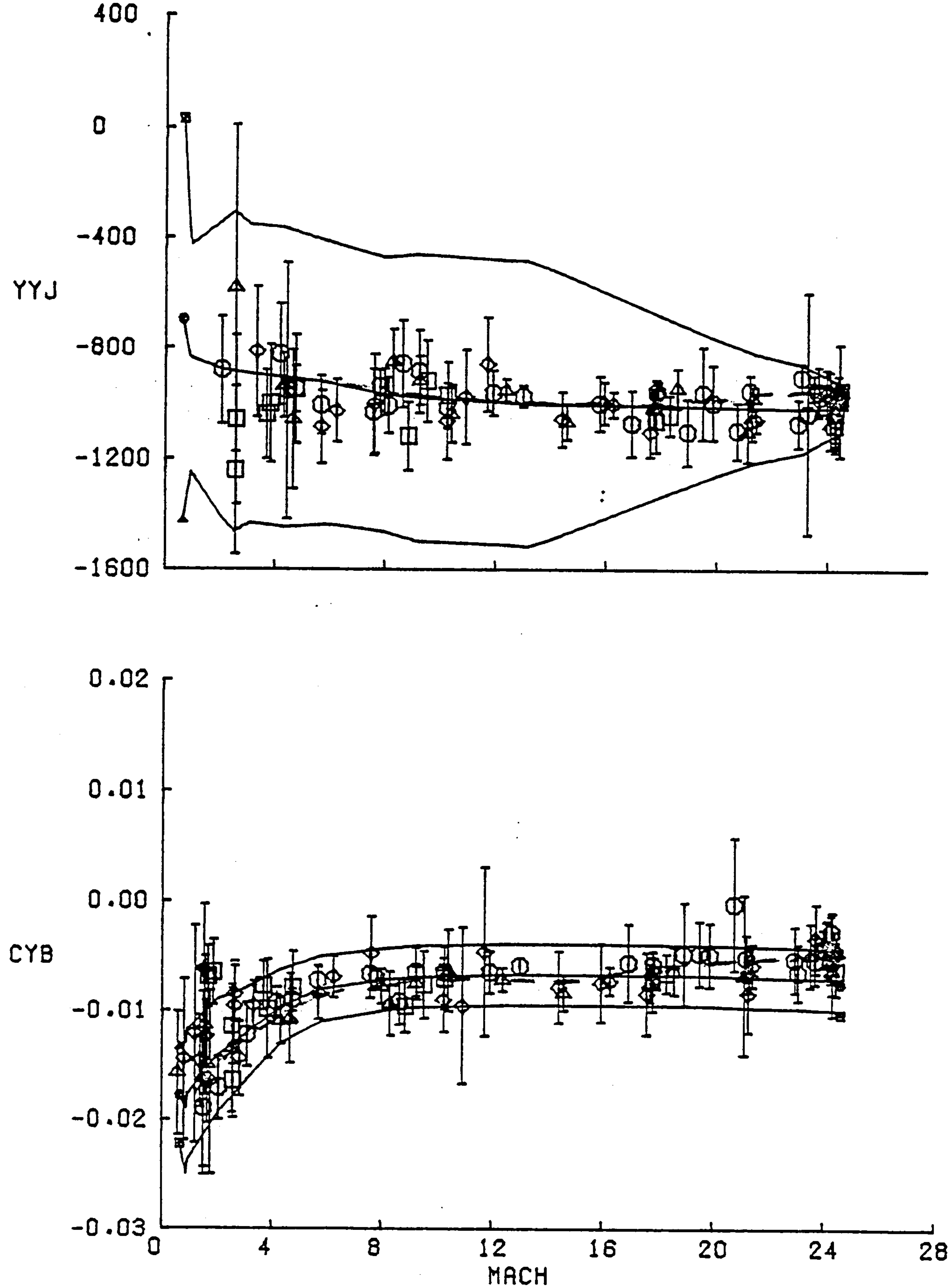

FIGURE 7e - (CONTINUED)

SHUTTLE STS-1,2,3,AND 4 LATERAL PRELIMINARY

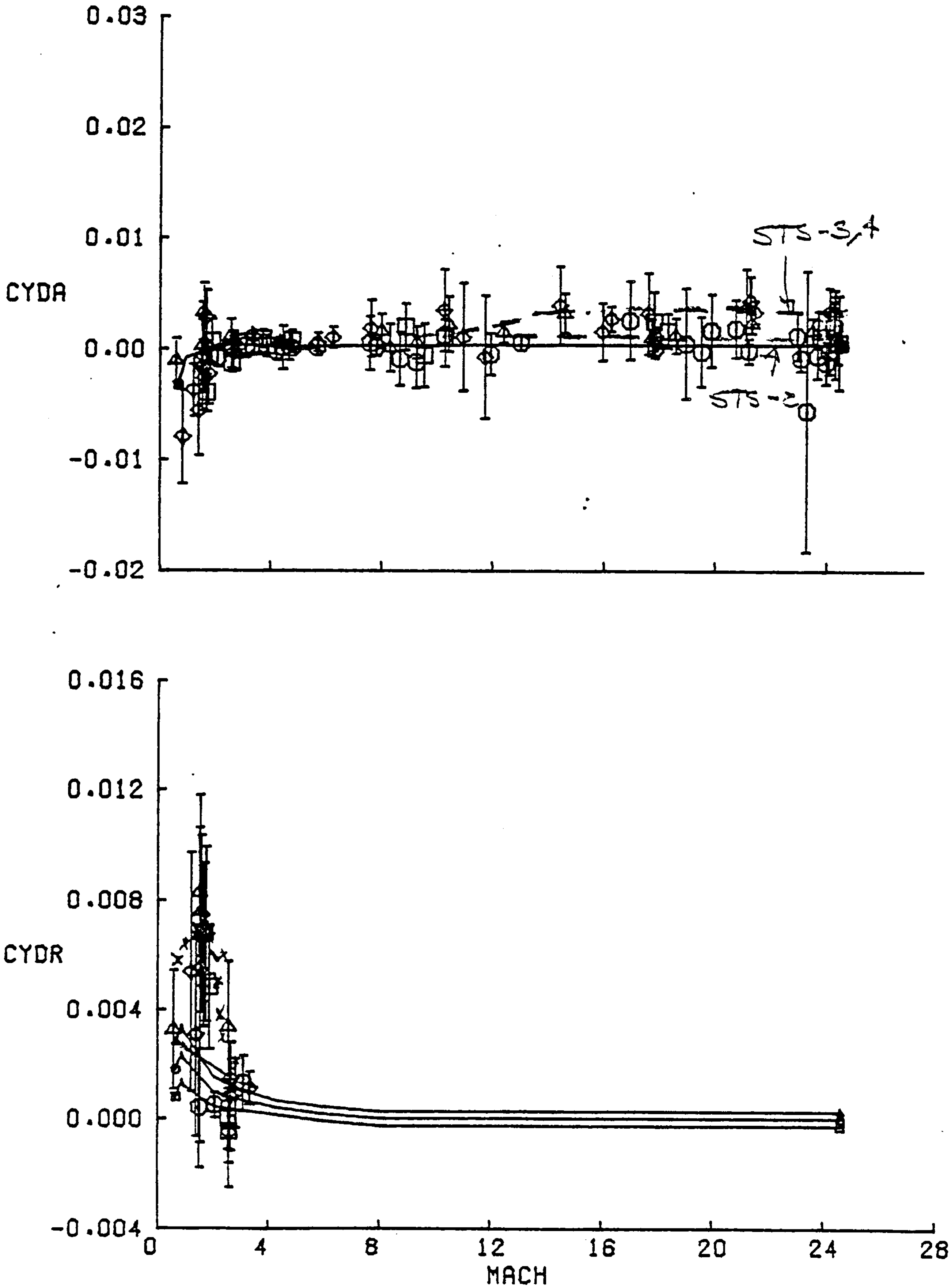

FIGURE 7f - (CONCLUDED)

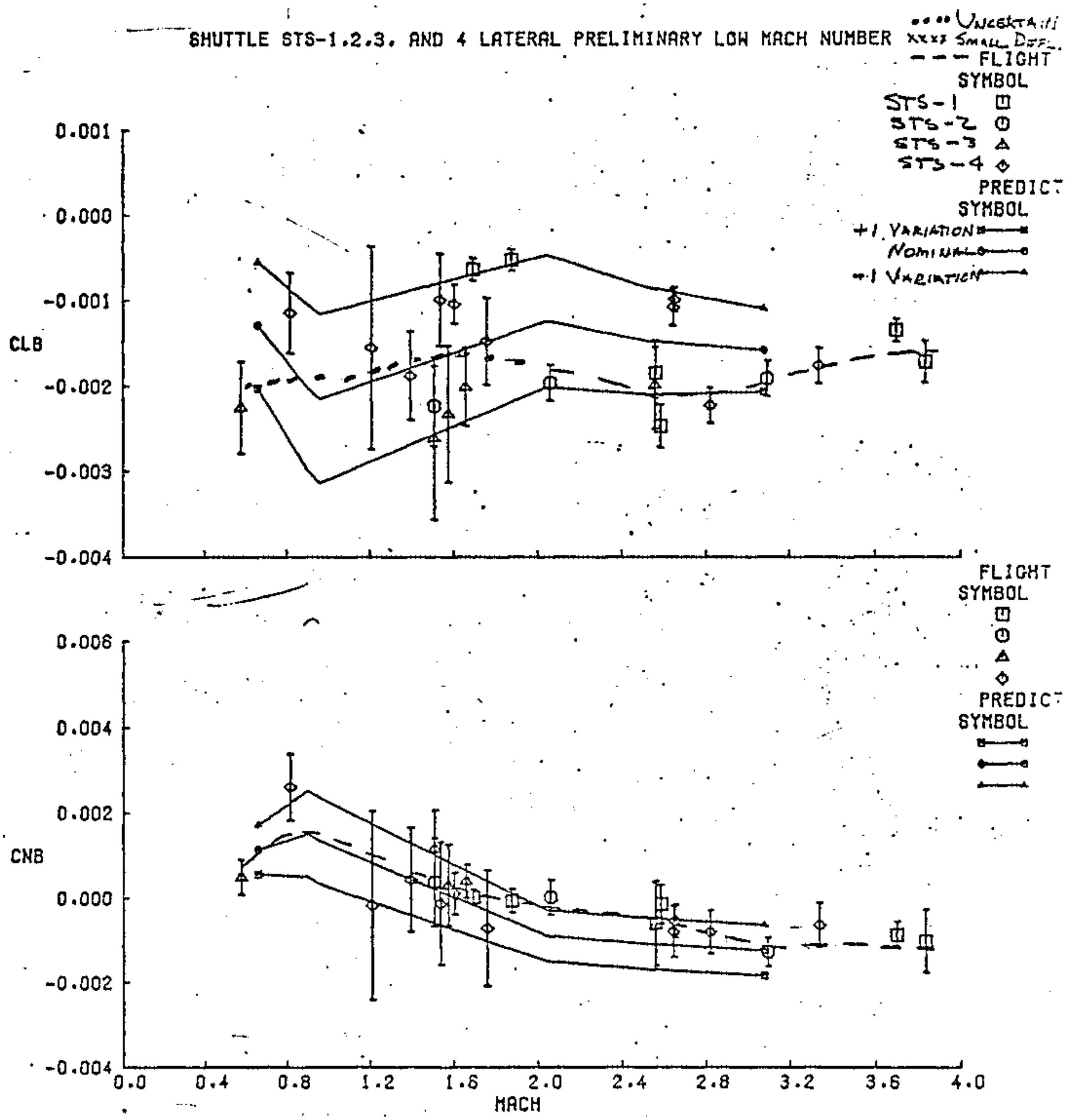

FIGURE 8a - LATERAL-DIRECTIONAL DERIVATIVE ESTIMATES, MACH = 0-4

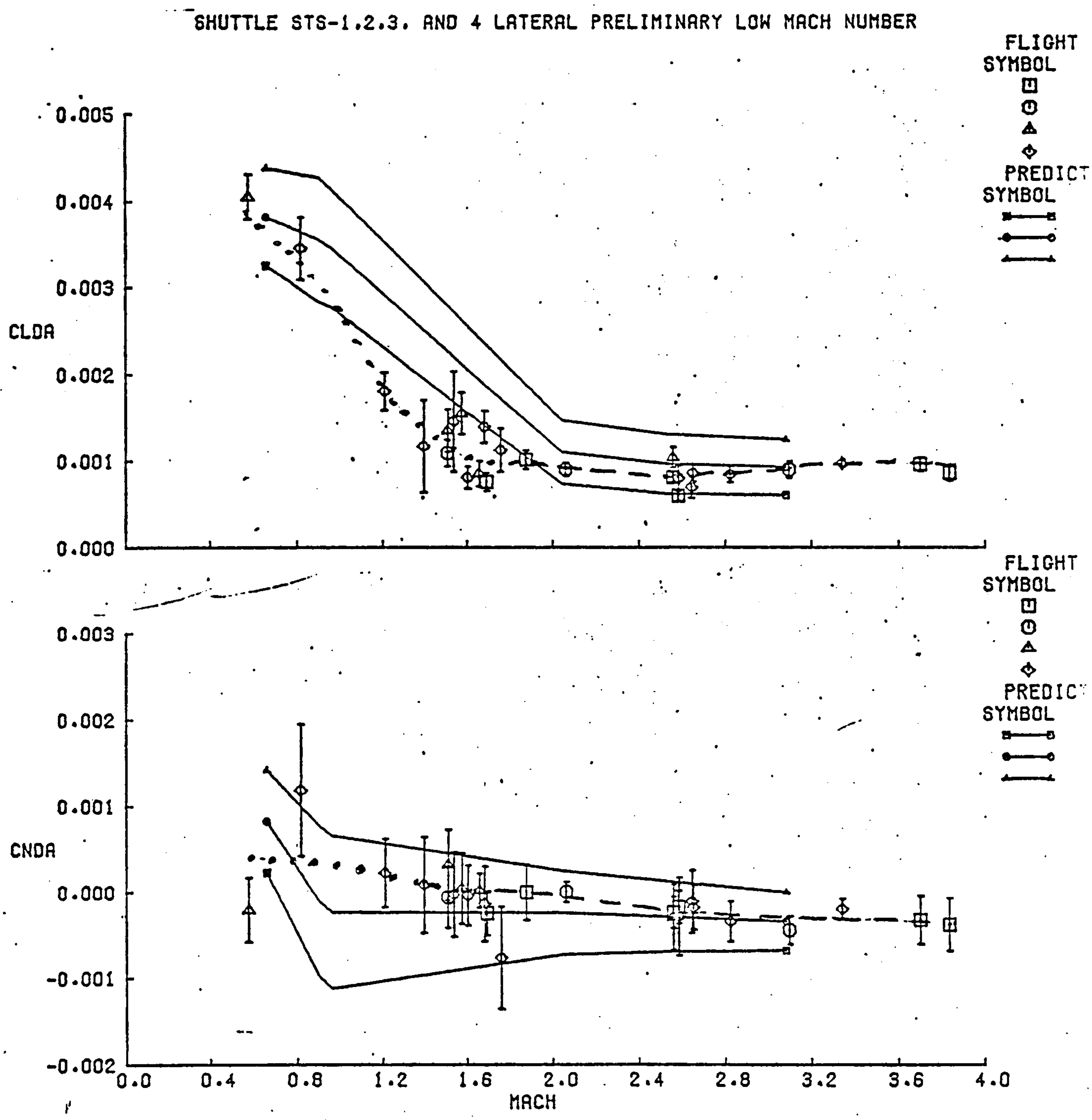

FIGURE 8b - (CONTINUED)

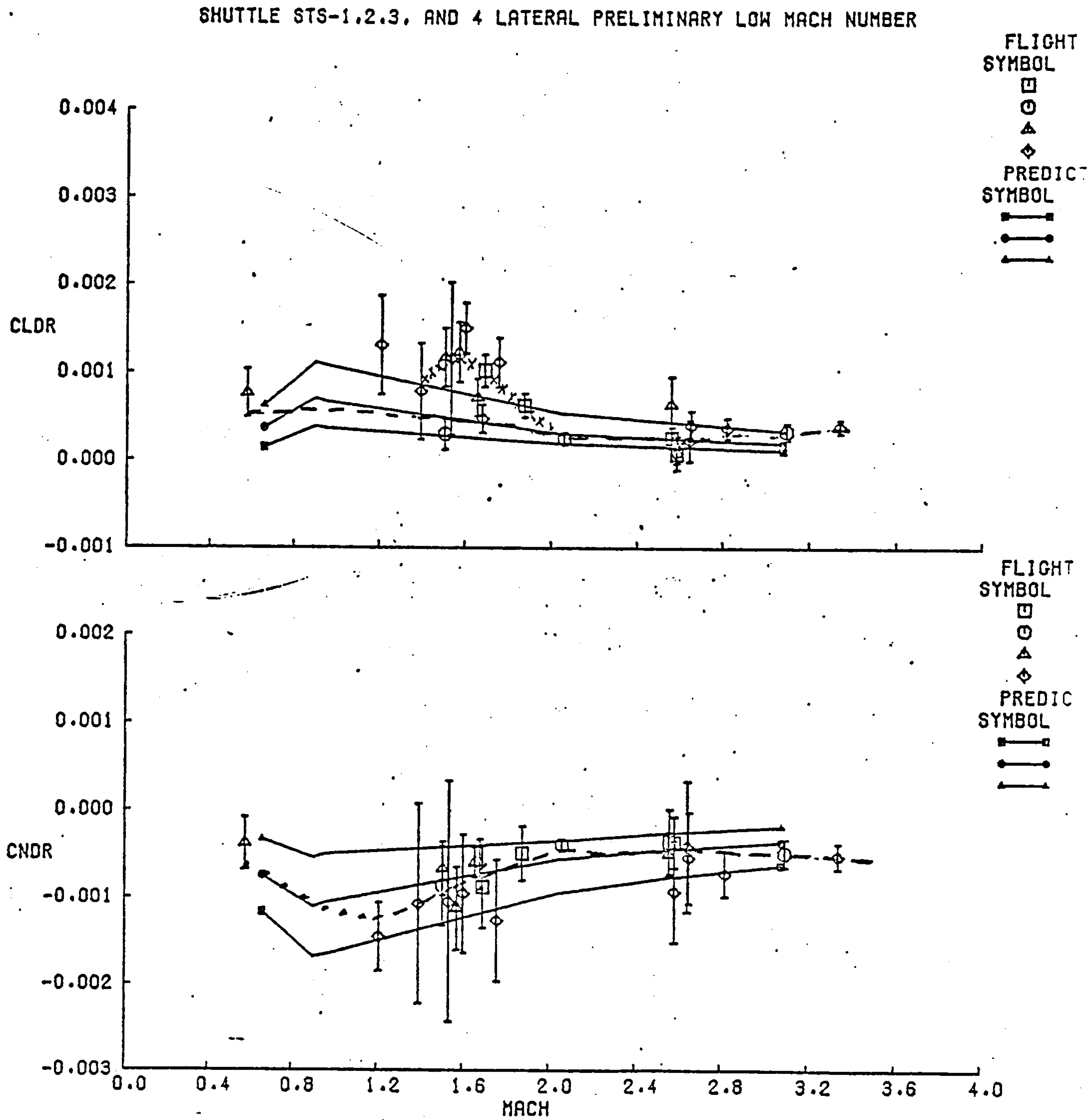

FIGURE 8c - (CONTINUED)

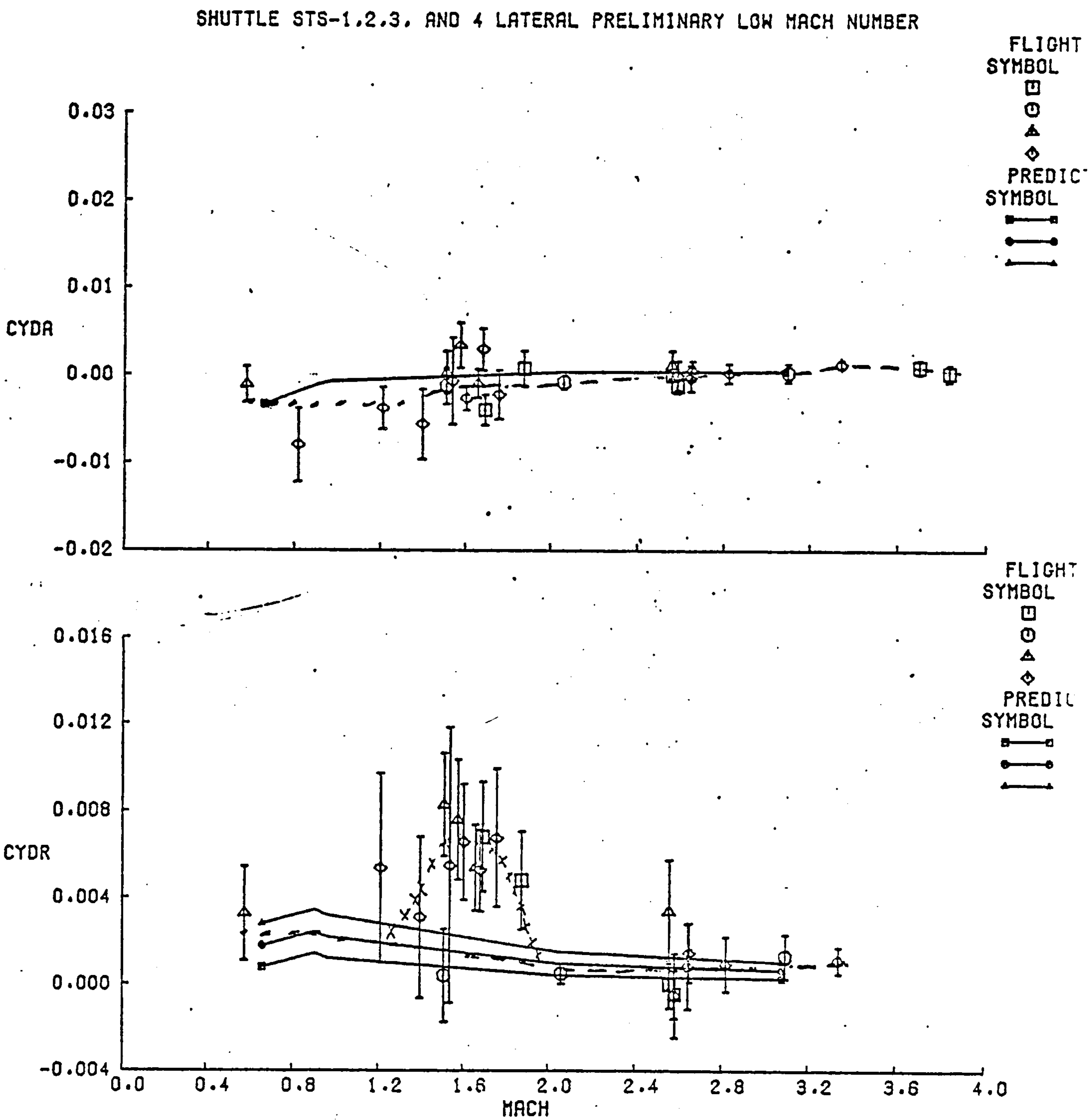

FIGURE 8d - (CONCLUDED)

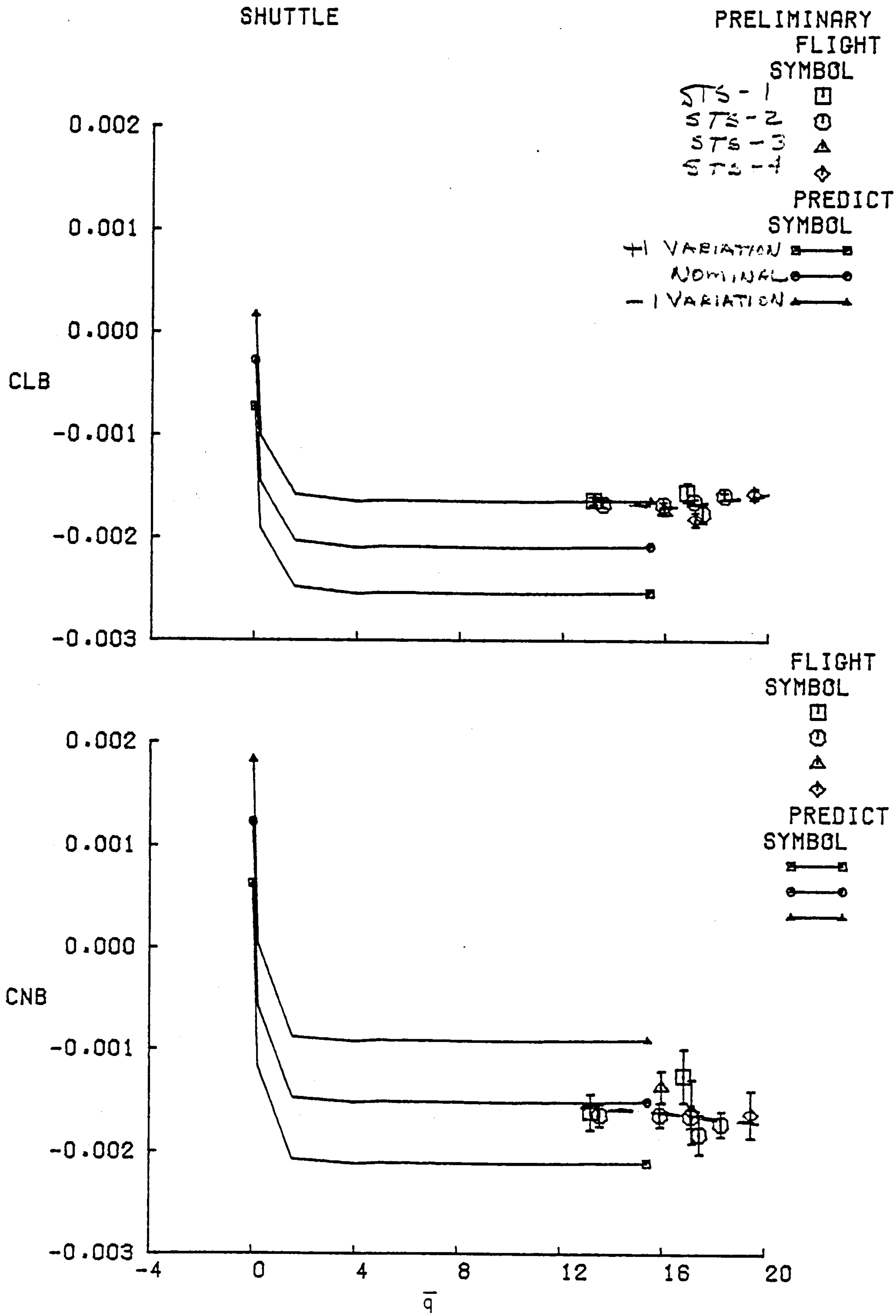

FIGURE 9a - LATERAL-DIRECTIONAL DERIVATIVES VS DYNAMIC PRESSURE

SHUTTLE

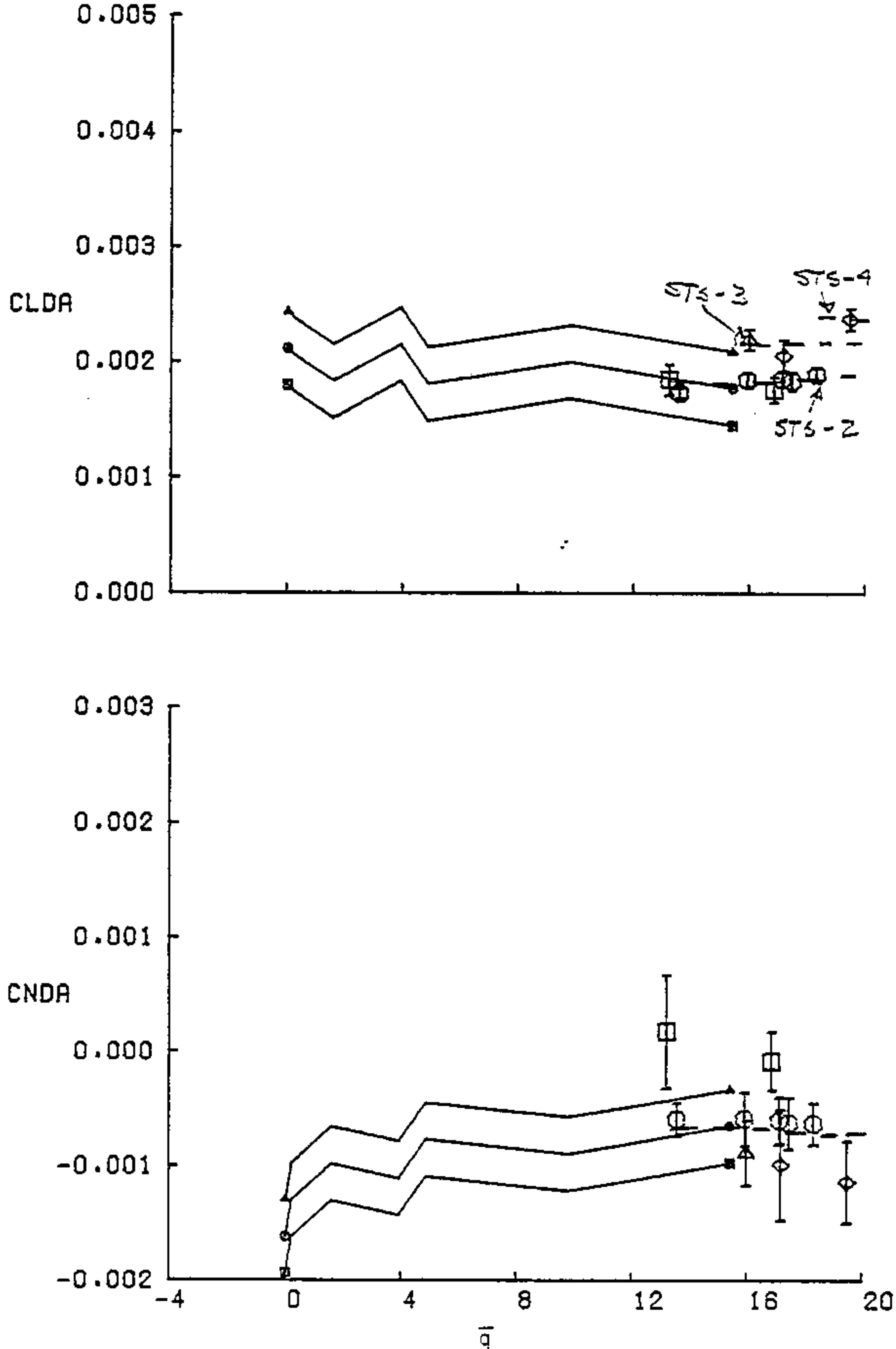

FIGURE 9b - (CONTINUED)

SHUTTLE

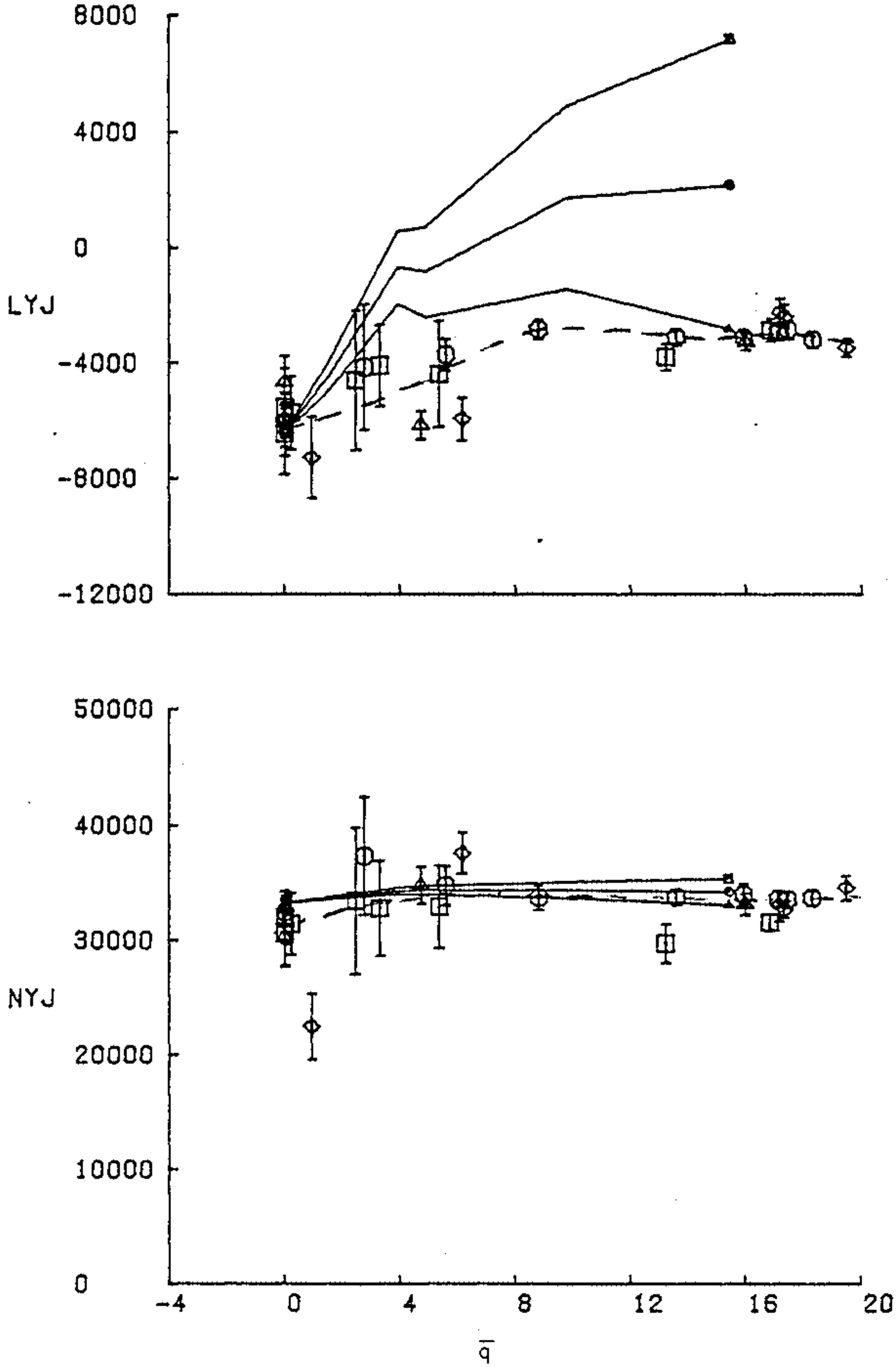

FIGURE 9c - (CONTINUED)

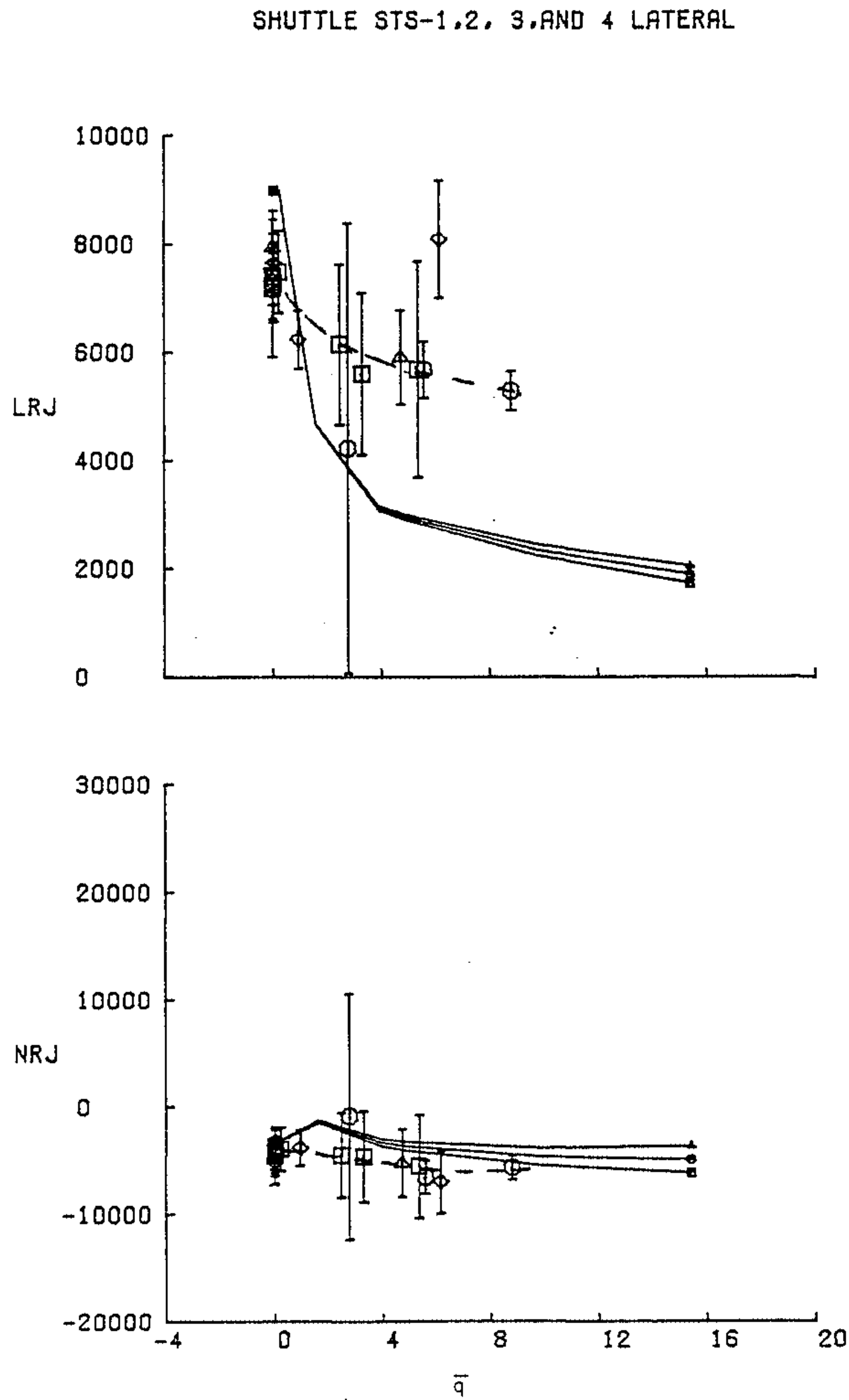

 FIGURE 9d - (CONTINUED)

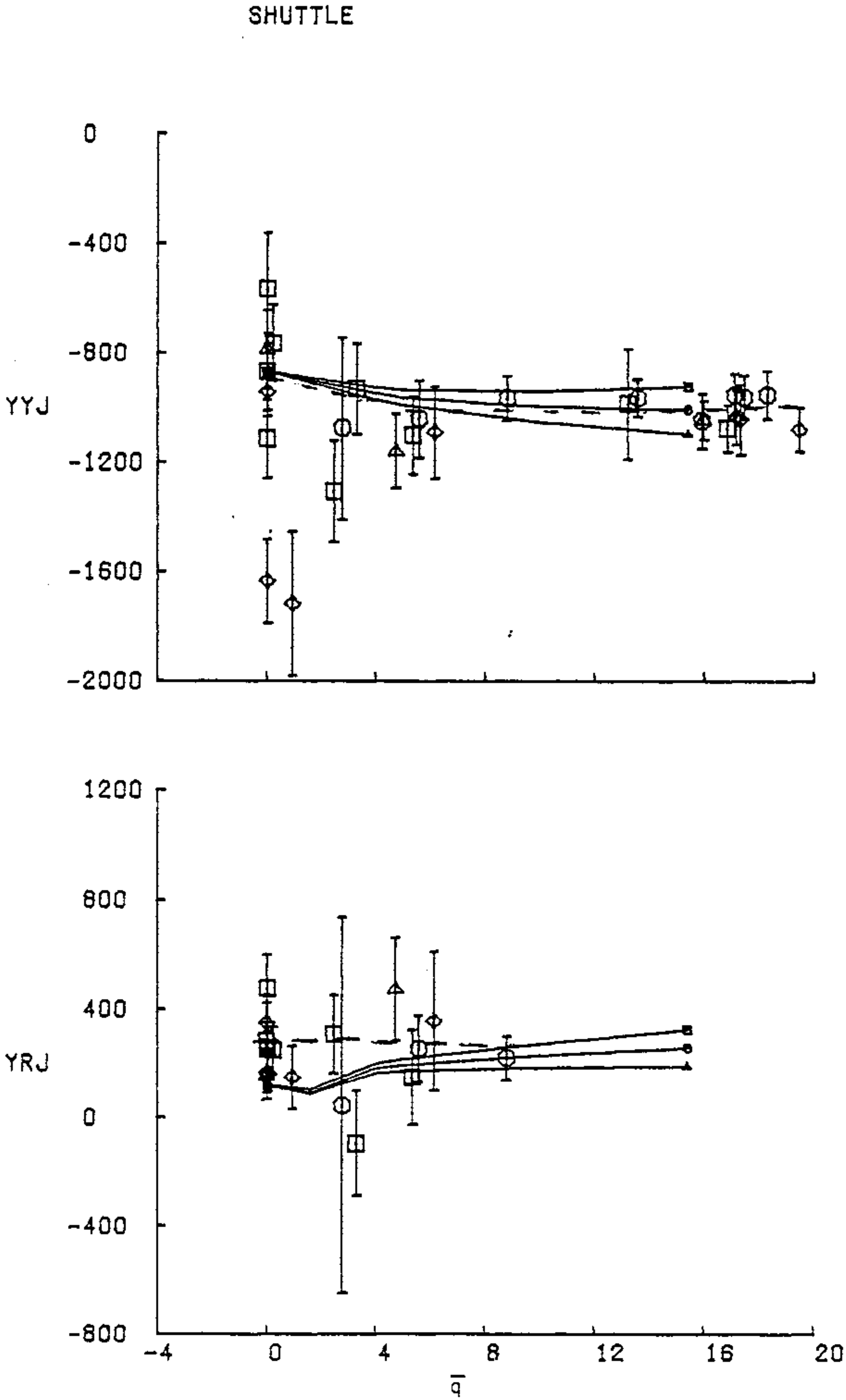

FIGURE 9e - (CONCLUDED)

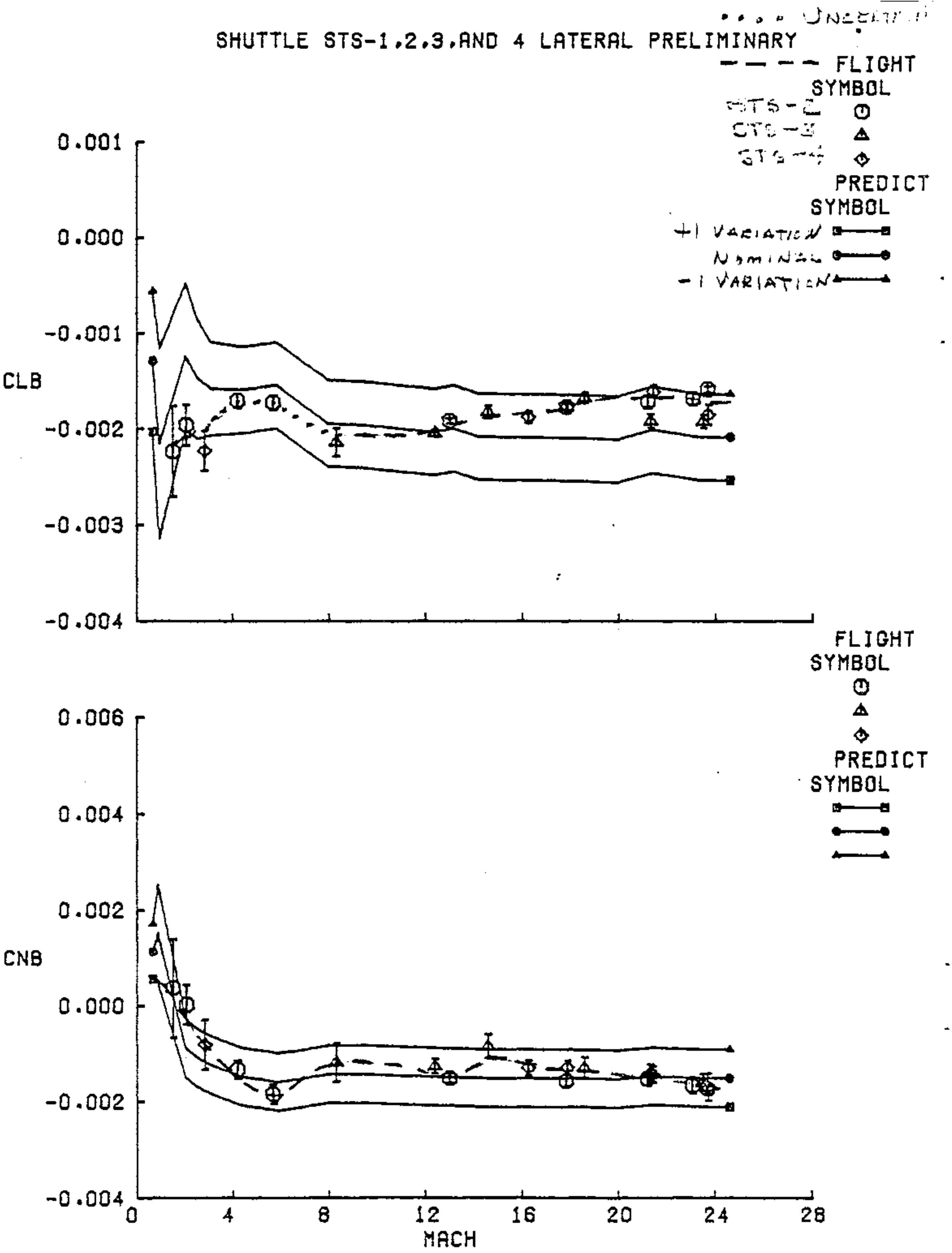

FIGURE 10a - LATERAL-DIRECTIONAL ESTIMATES FROM PROGRAMMED TEST INPUTS

SHUTTLE STS-1,2,3,AND 4 LATERAL PRELIMINARY

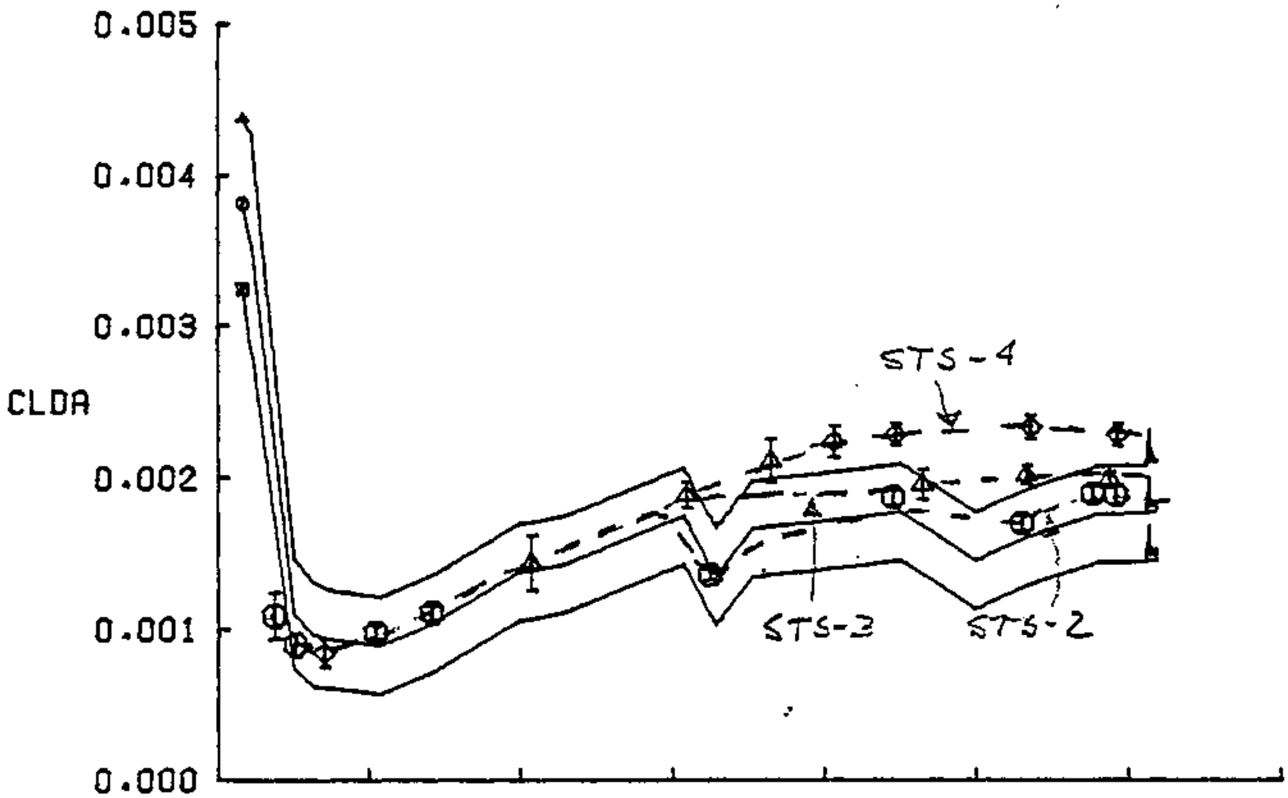

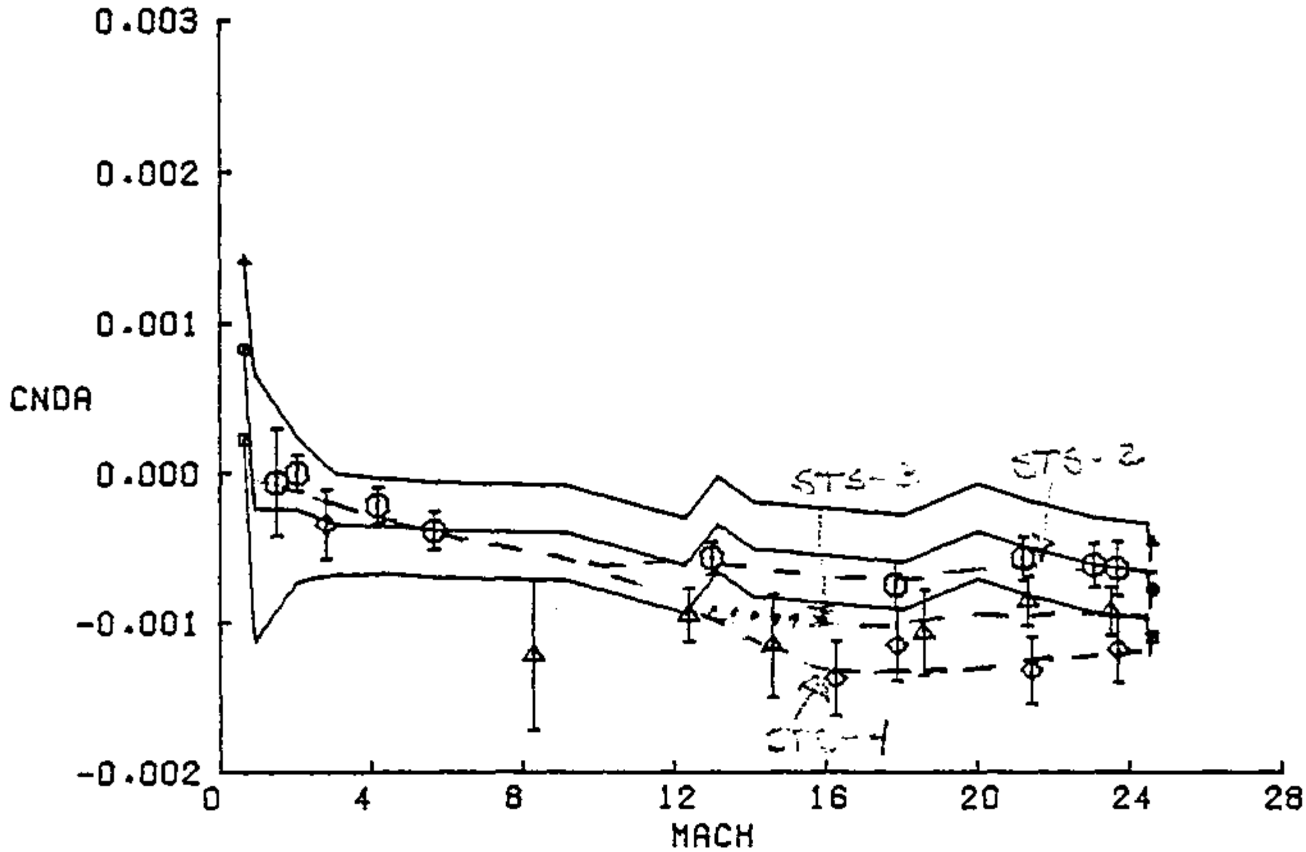

FIGURE 10b - (CONTINUED)

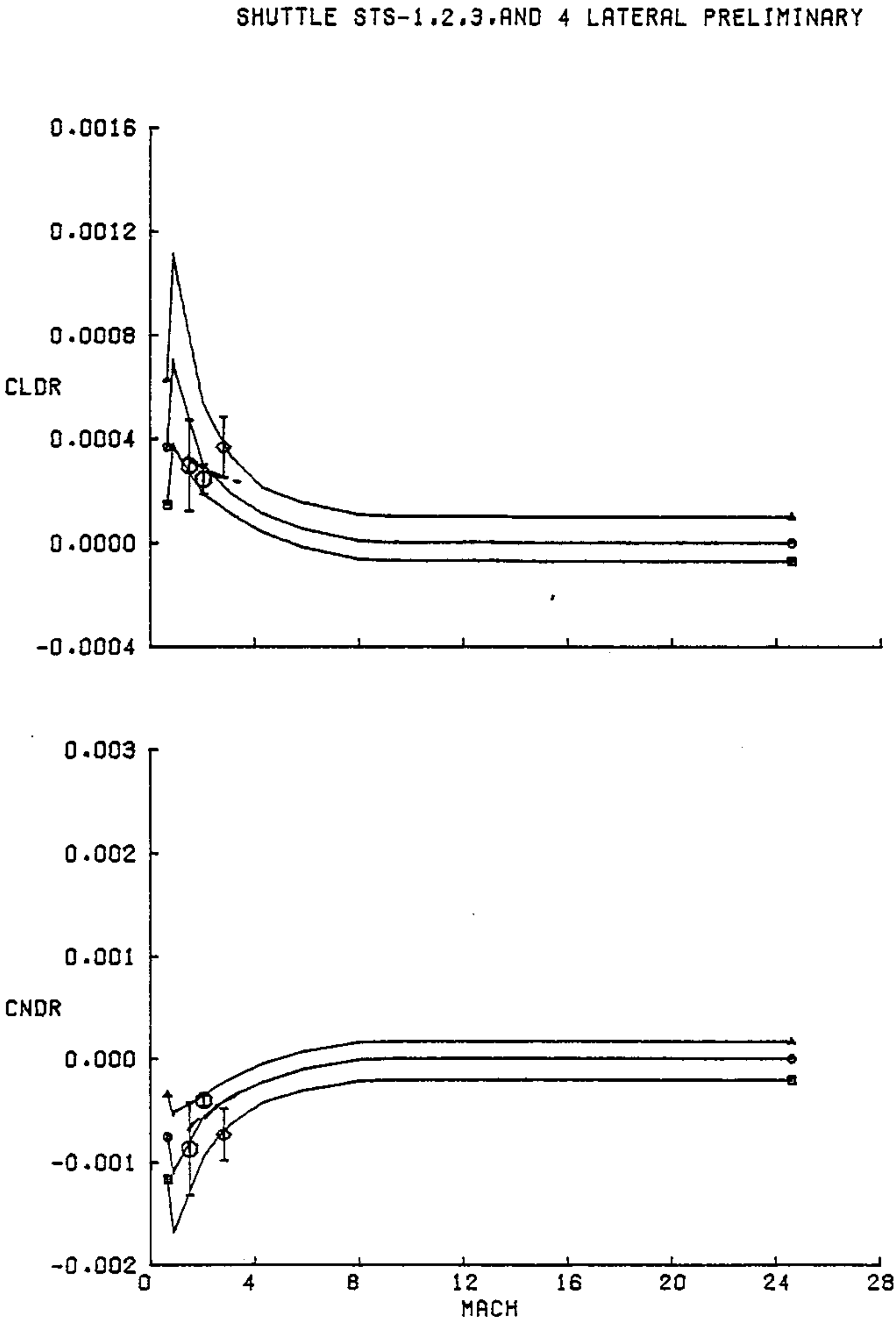

FIGURE 10c - (CONTINUED)

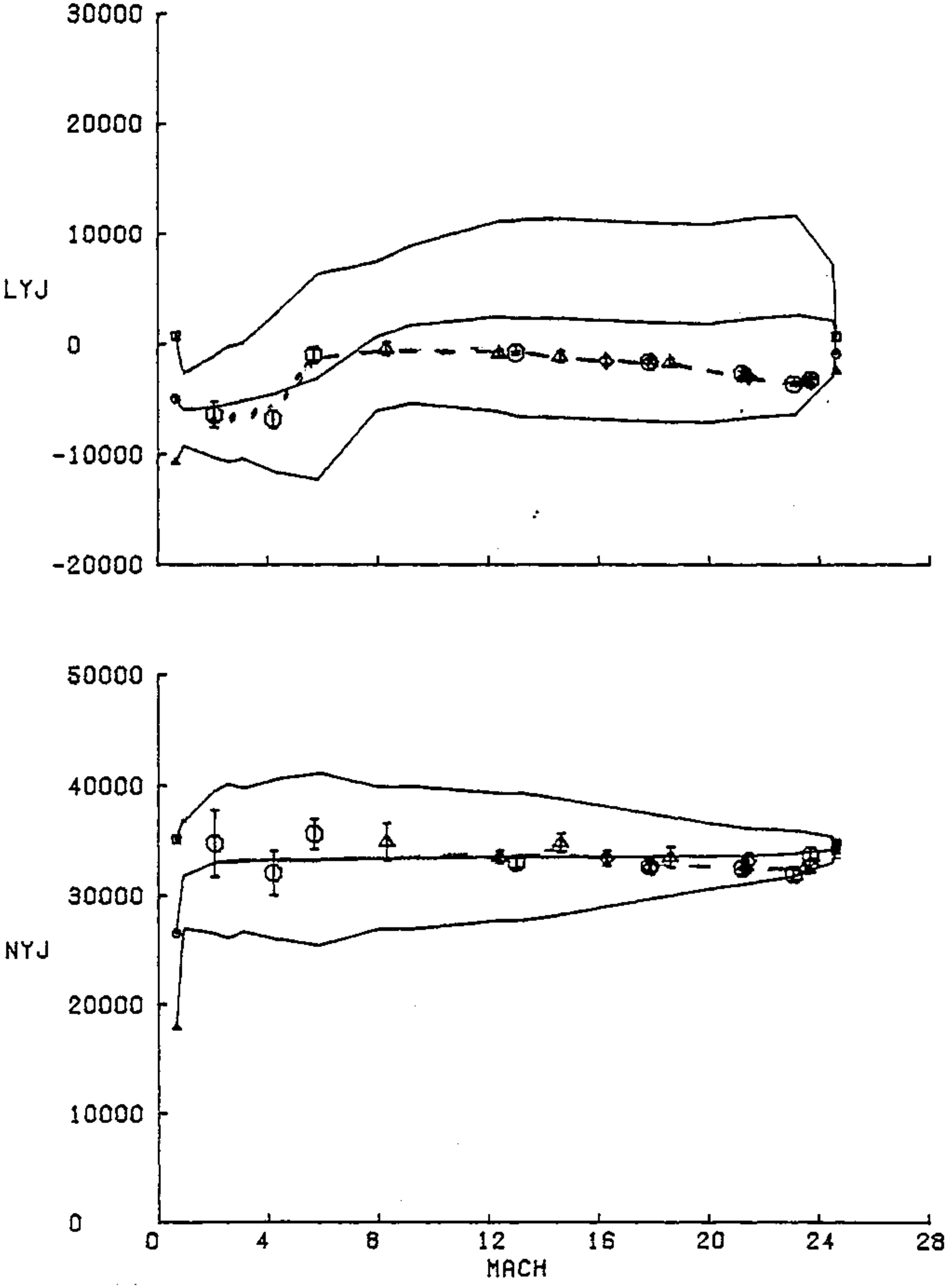

FIGURE 10d - (CONTINUED)

SHUTTLE STS-1,2,3,AND 4 LATERAL PRELIMINARY

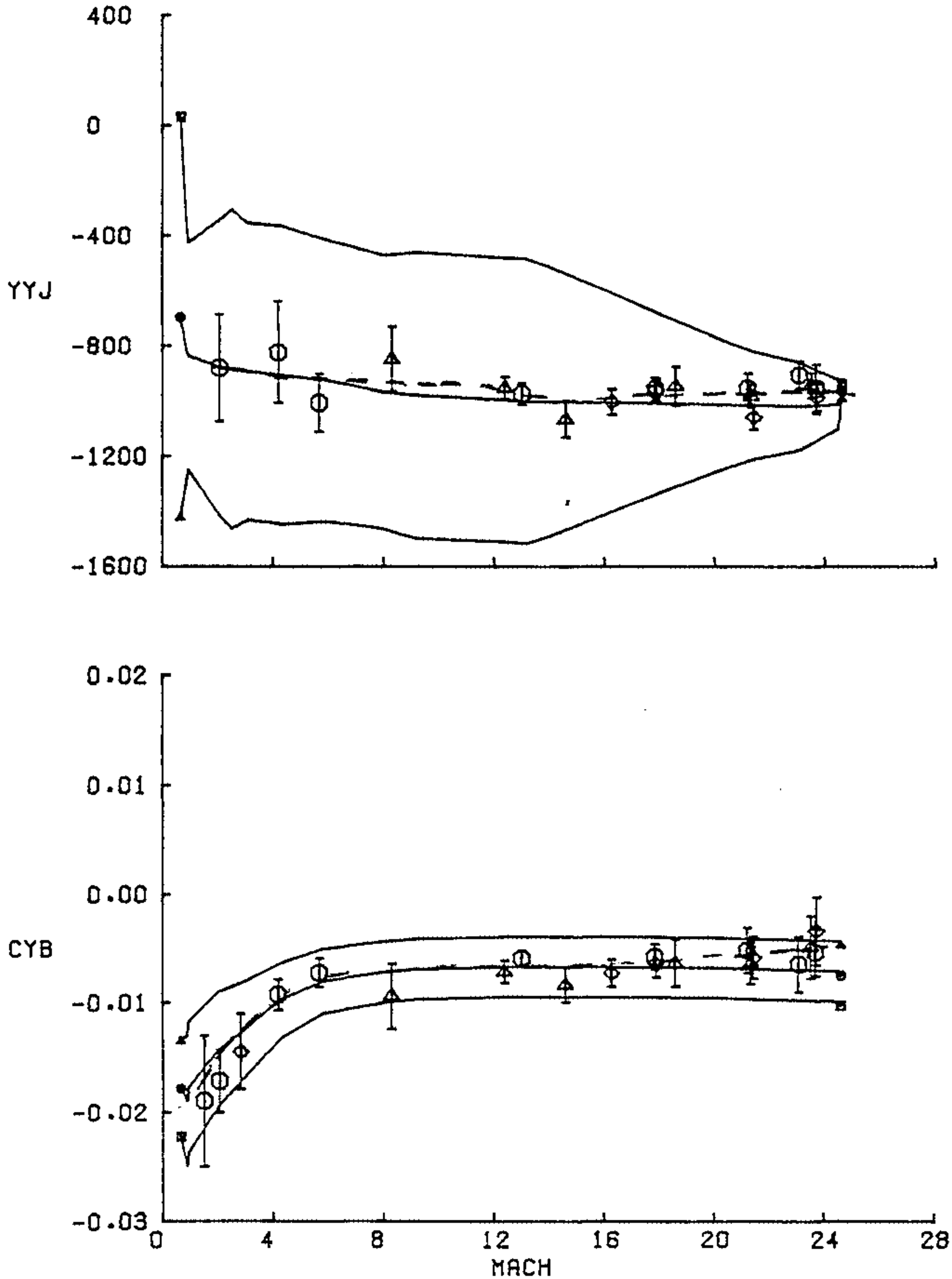

FIGURE 10e - (CONTINUED)

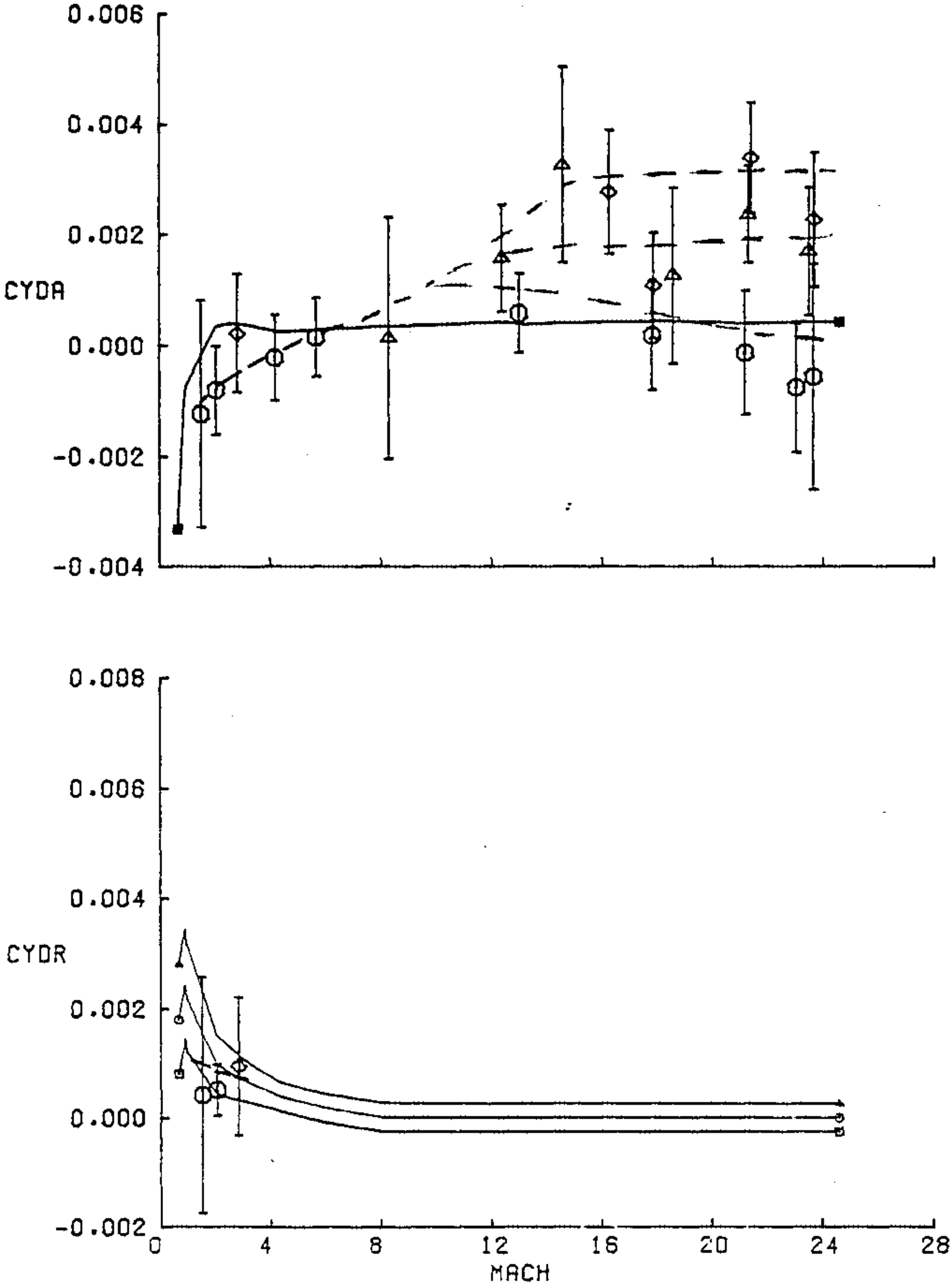

FIGURE 10f - (CONCLUDED)

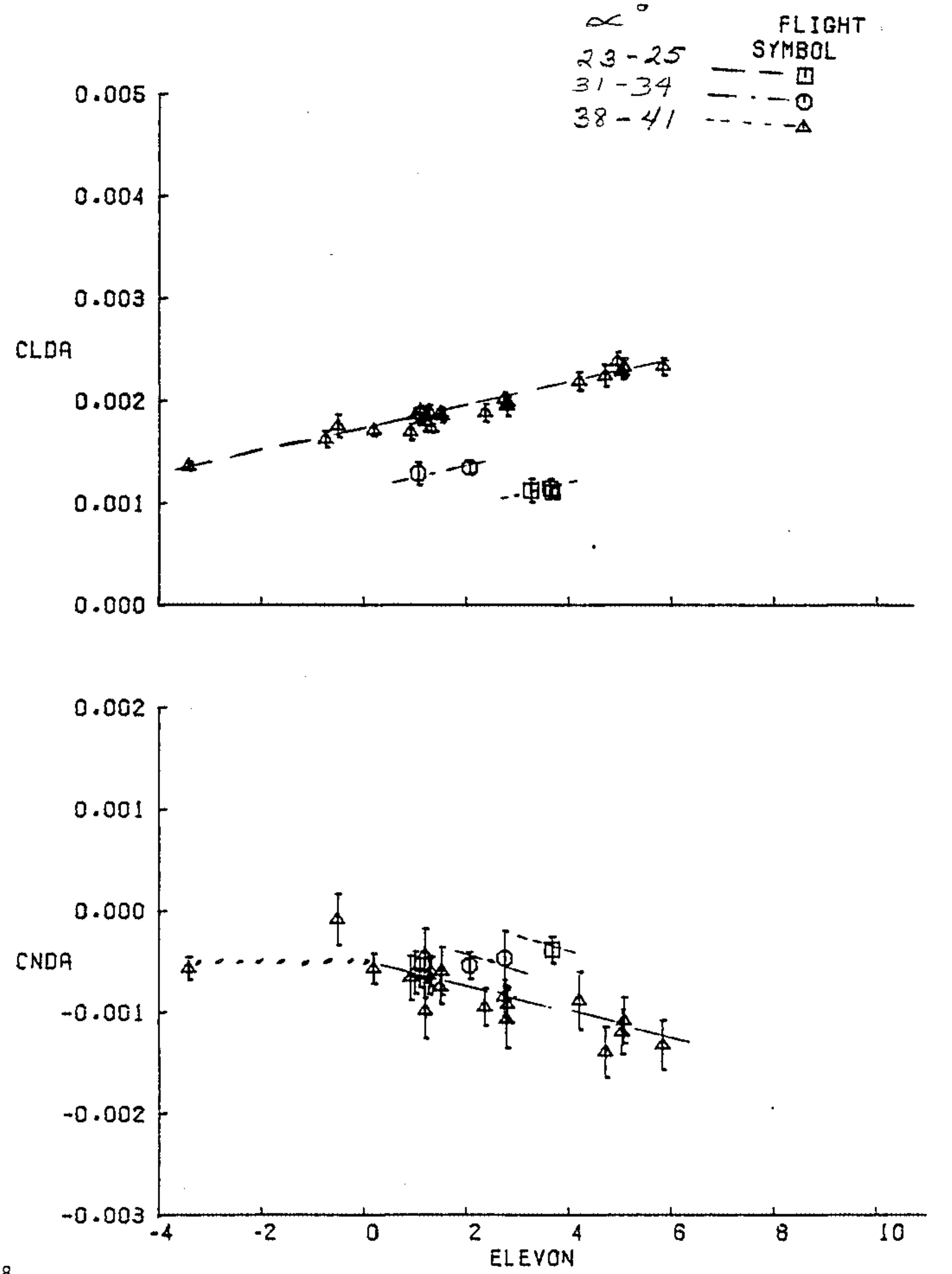

FIGURE 11 - AILERON EFFECTIVENESS AS A FUNCITON OF ELEVATOR POSITION, MACH > 10

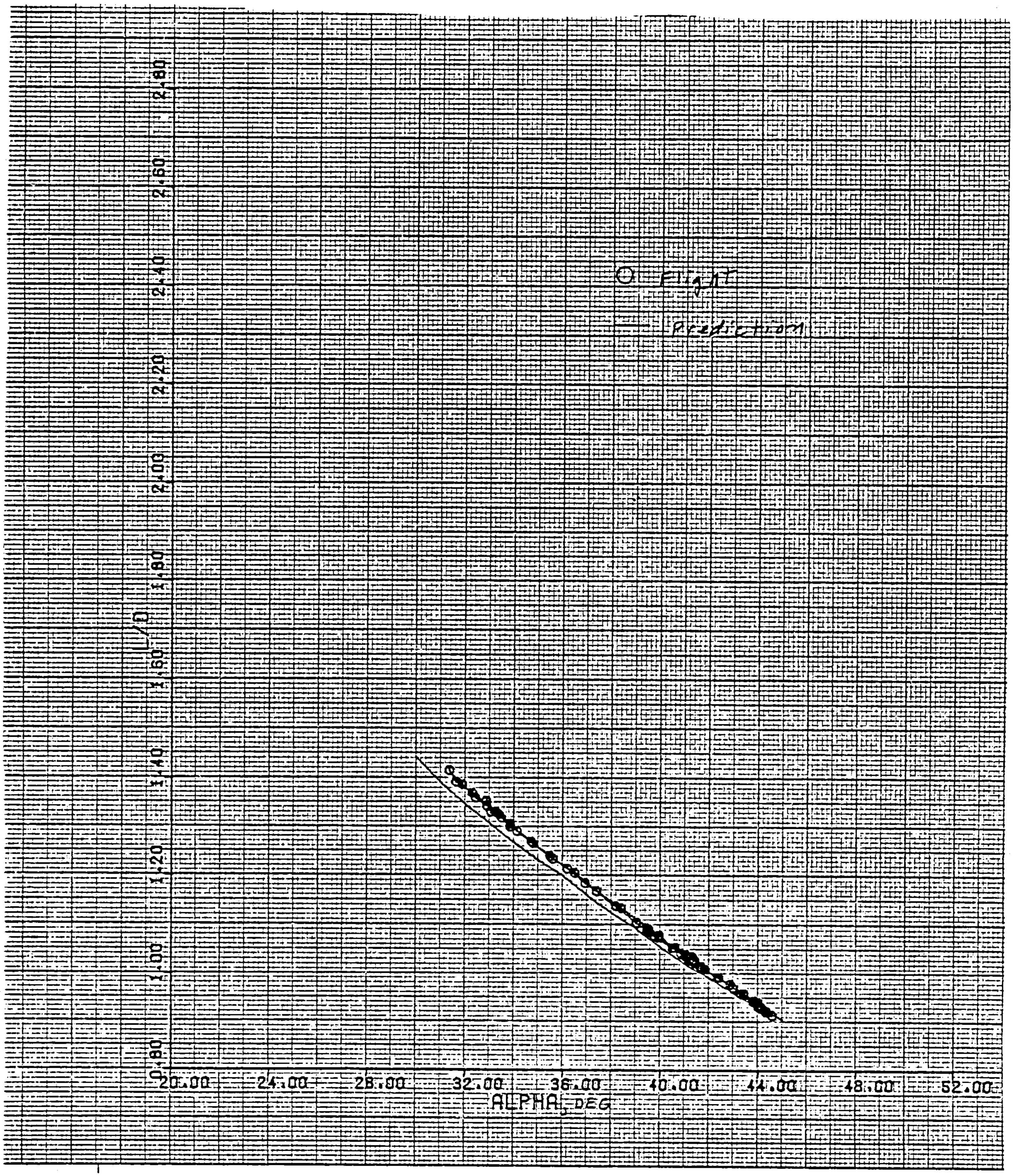

FIGURE 12 - LIFT/DRAG VS ANGLE OF ATTACK, MACH = 11.8 - 14.0

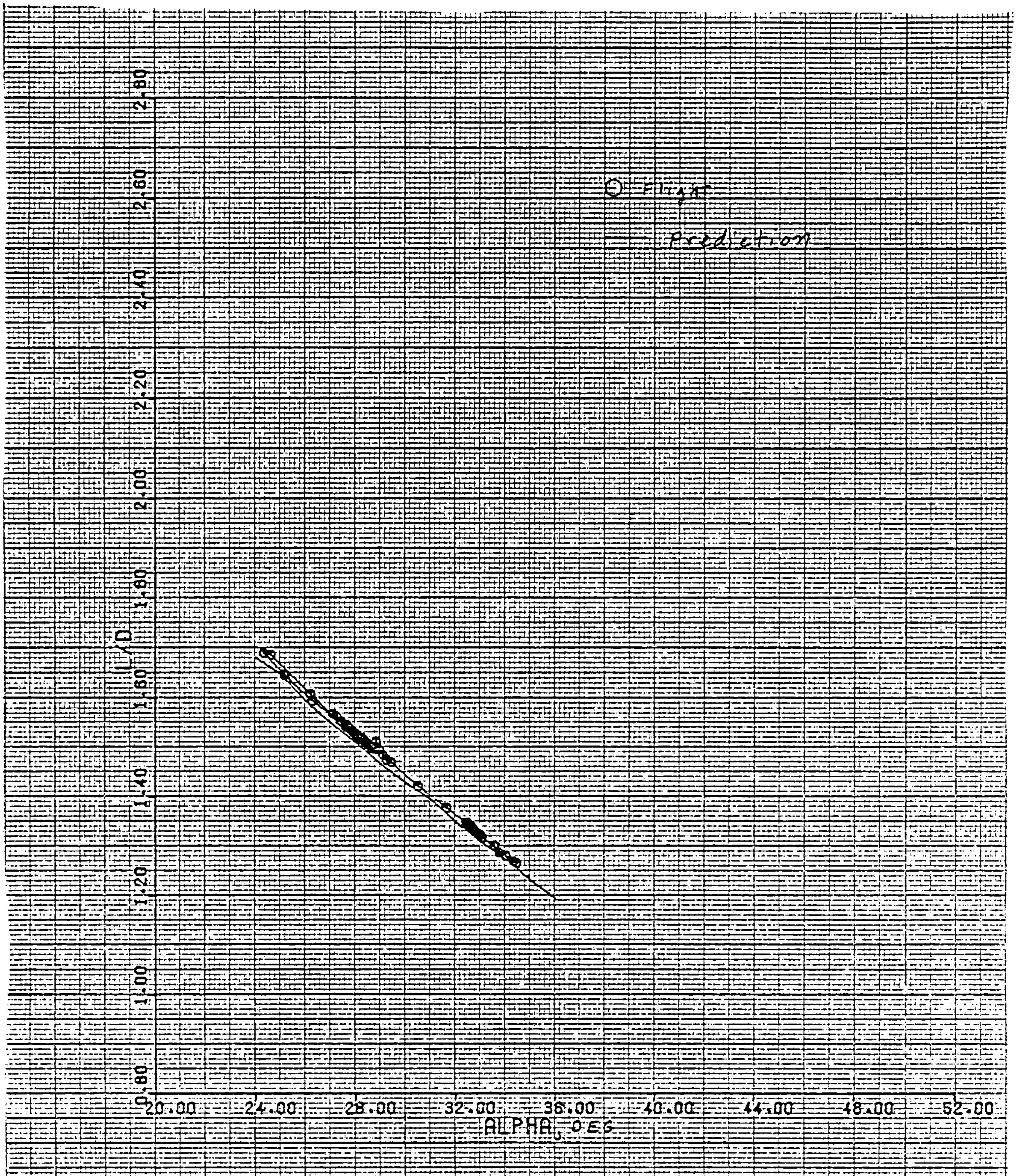

 FIGURE 13 - LIFT/DRAG VS ANGLE OF ATTACK, MACH = 7.7 - 8.6

FIGURE 14a - CSS MANEUVERING AROUND THE HEADING ALIGNMENT CIRCLE

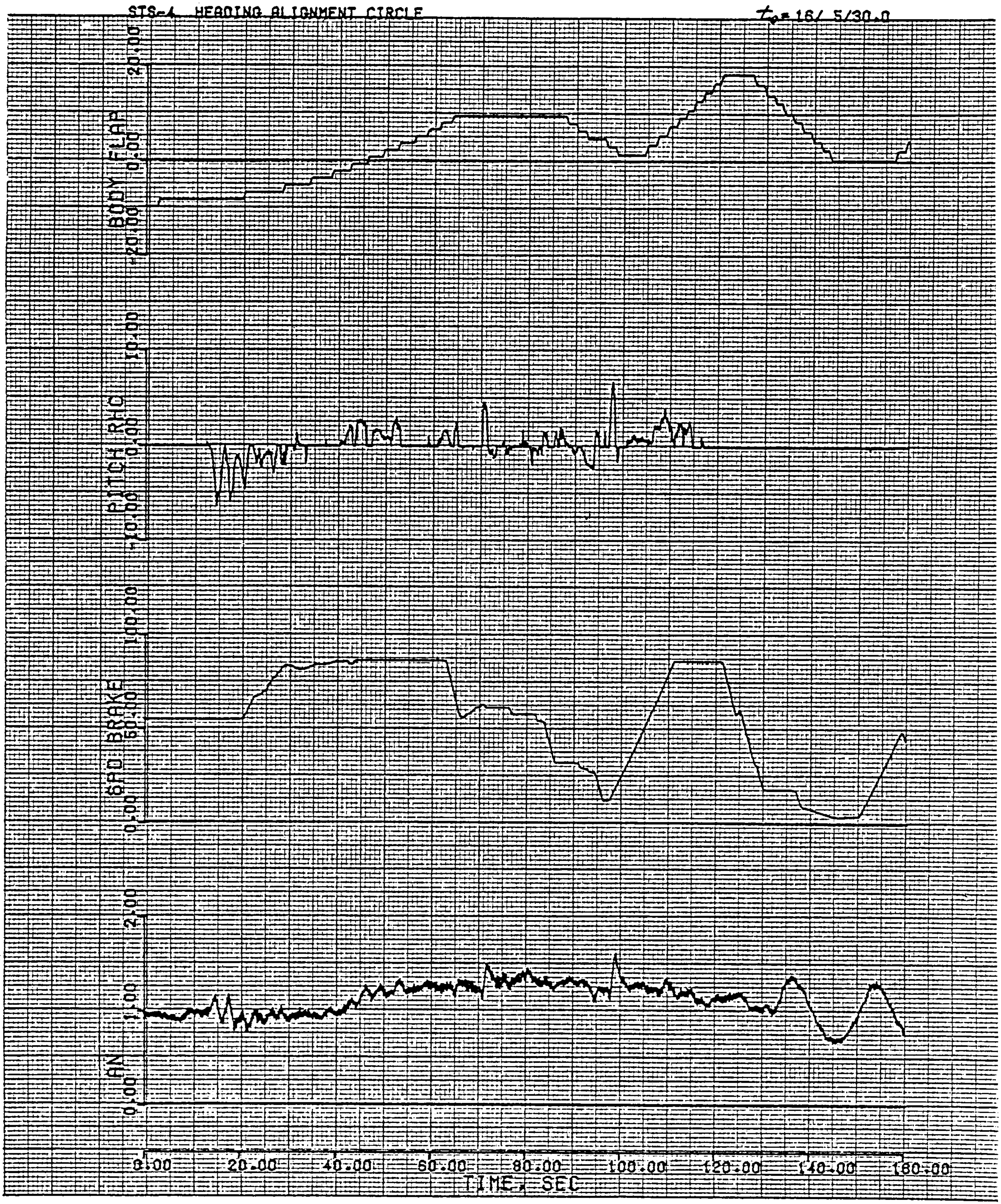

FIGURE 14b - (CONTINUED)

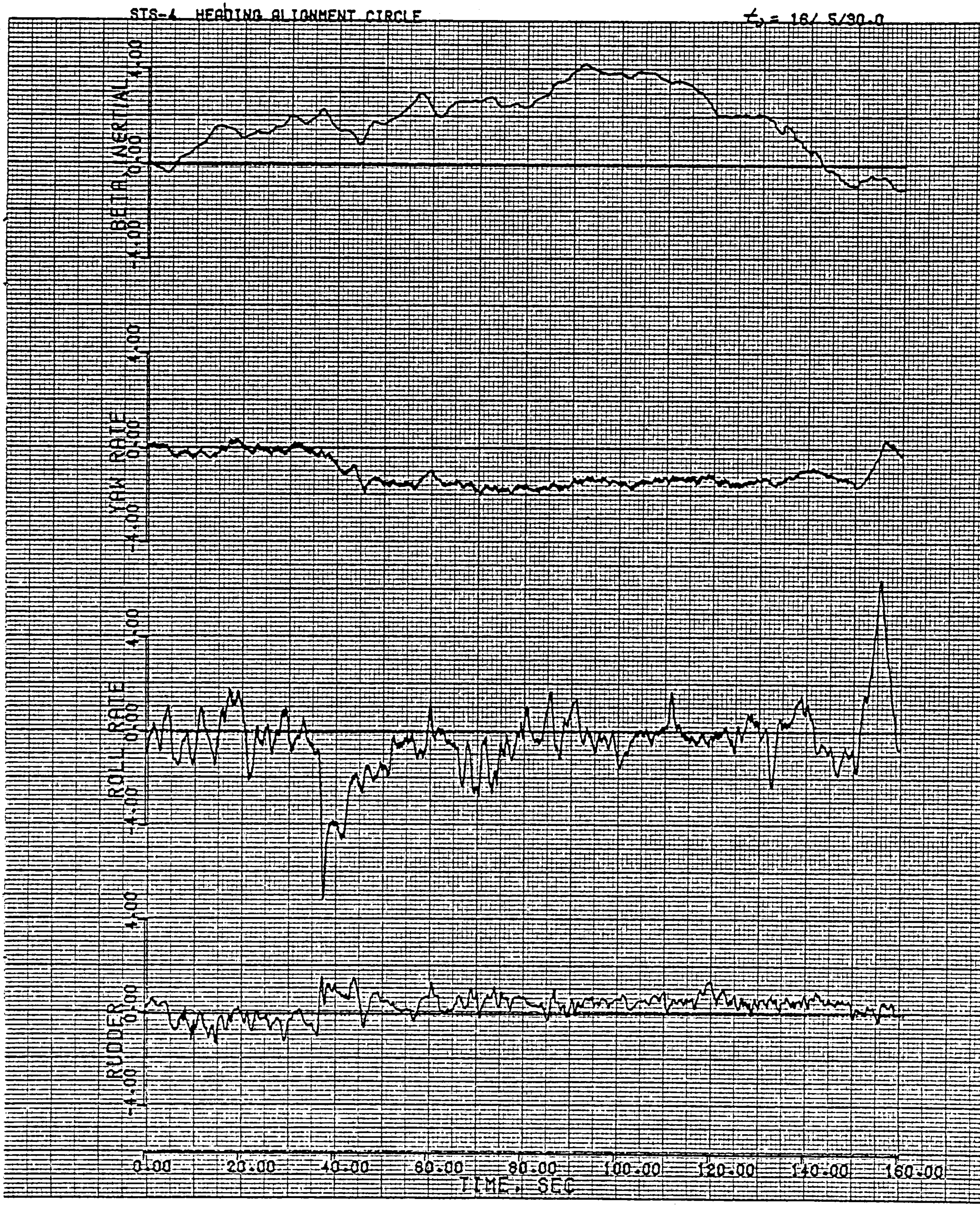

FIGURE 14c - (CONTINUED)

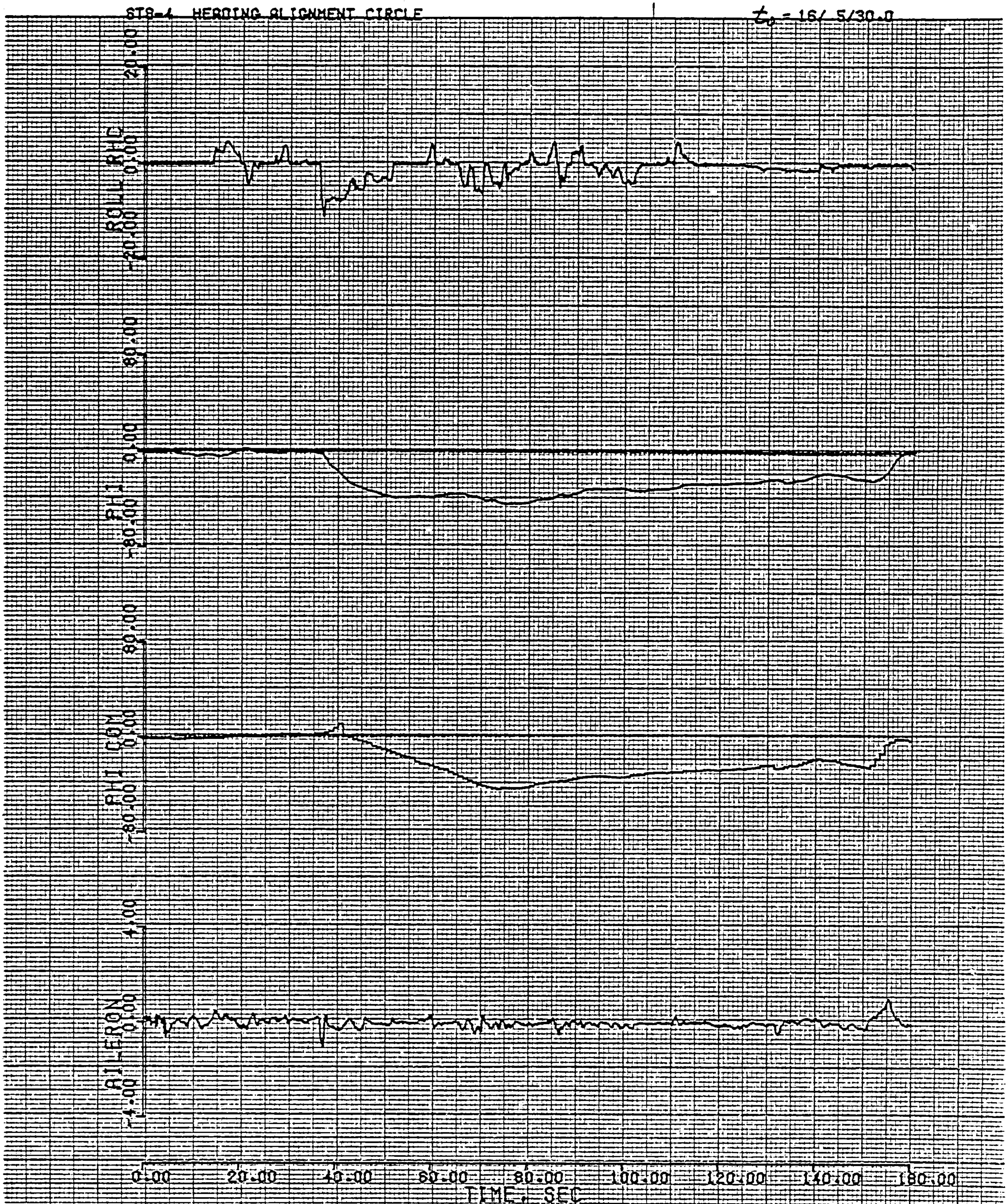

FIGURE 14d - (CONTINUED)

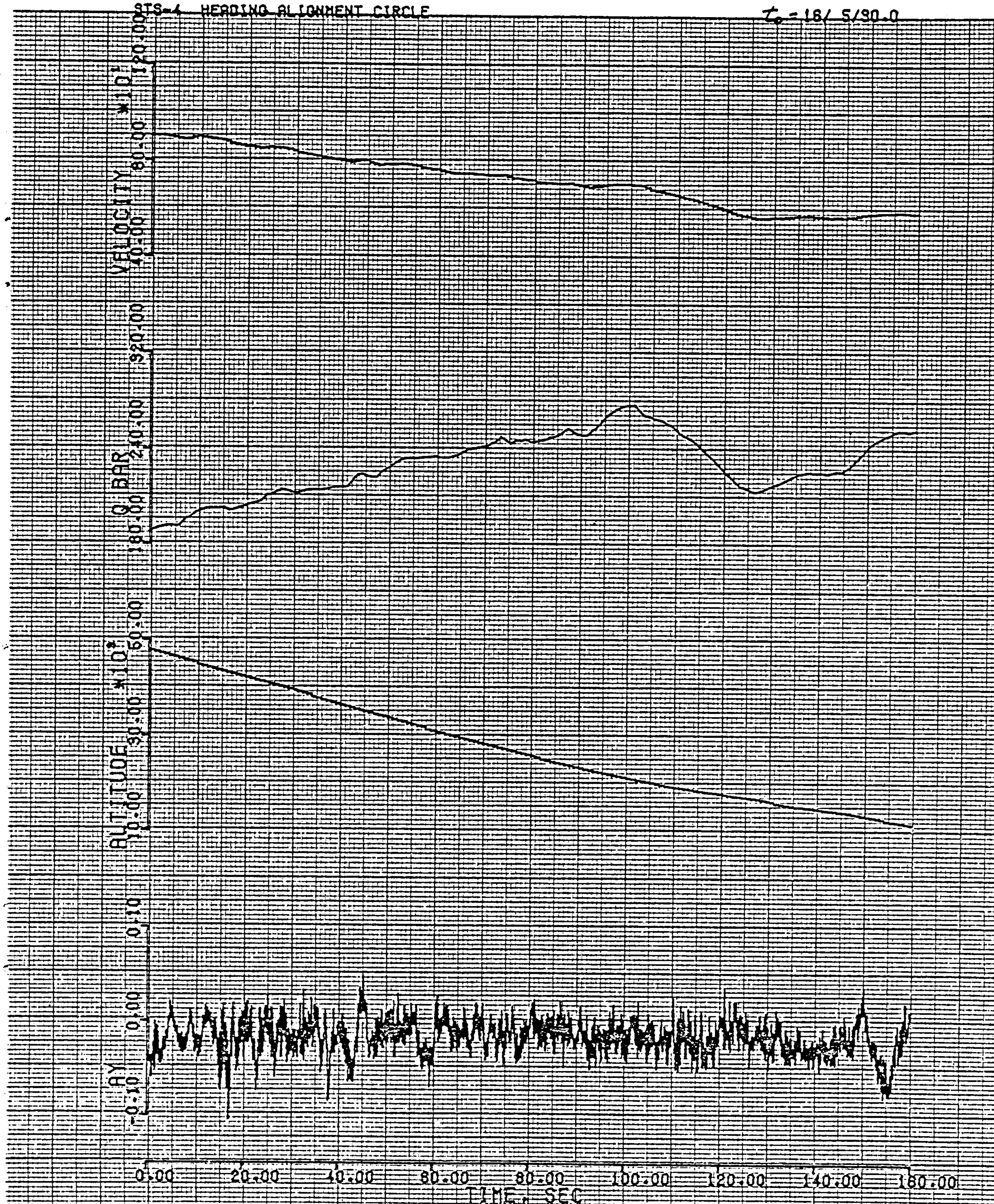

FIGURE 14e - (CONCLUDED)

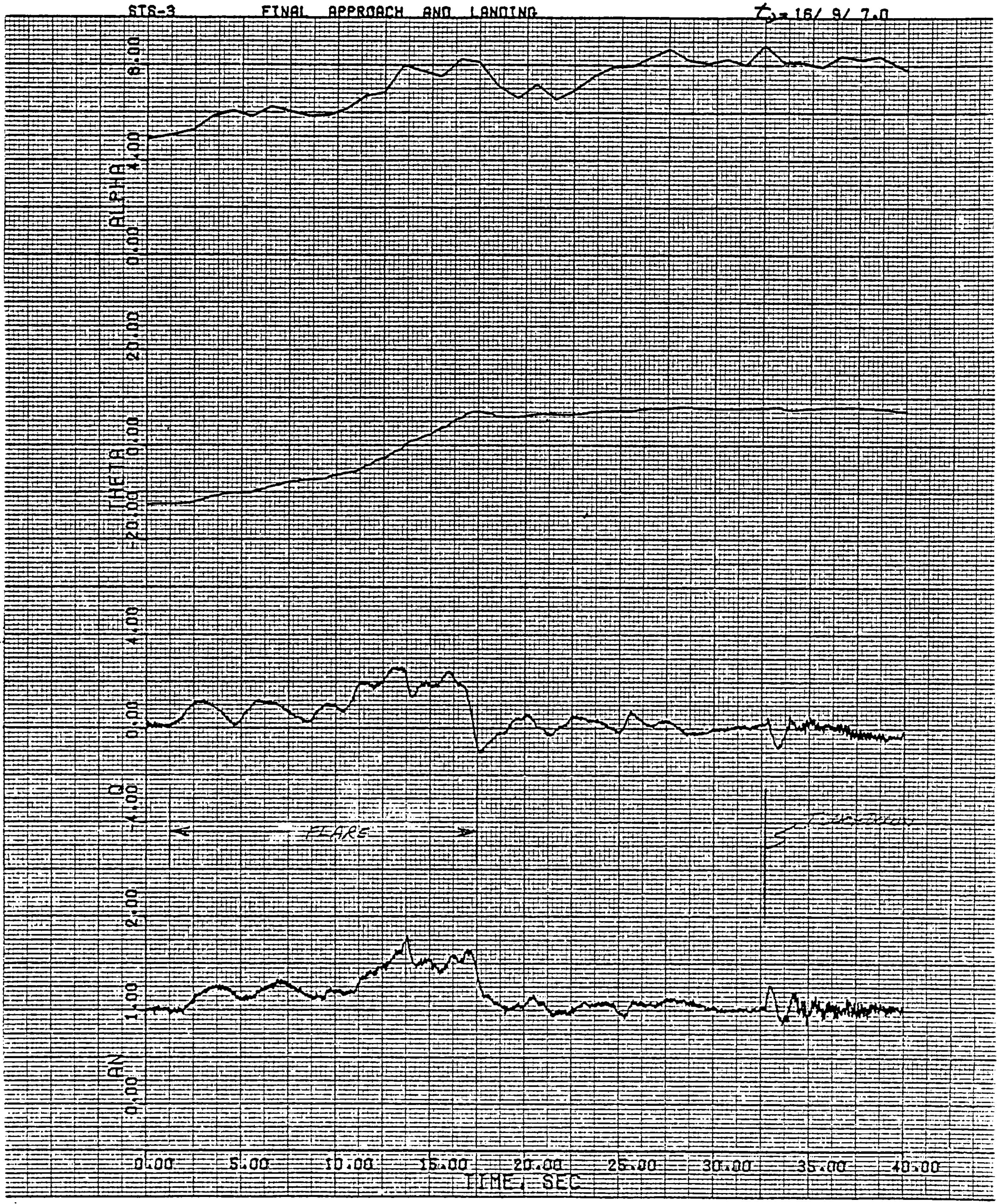

FIGURE 15a - LANDING TIME HISTORY, PRE-FLARE TO TOUCHDOWN

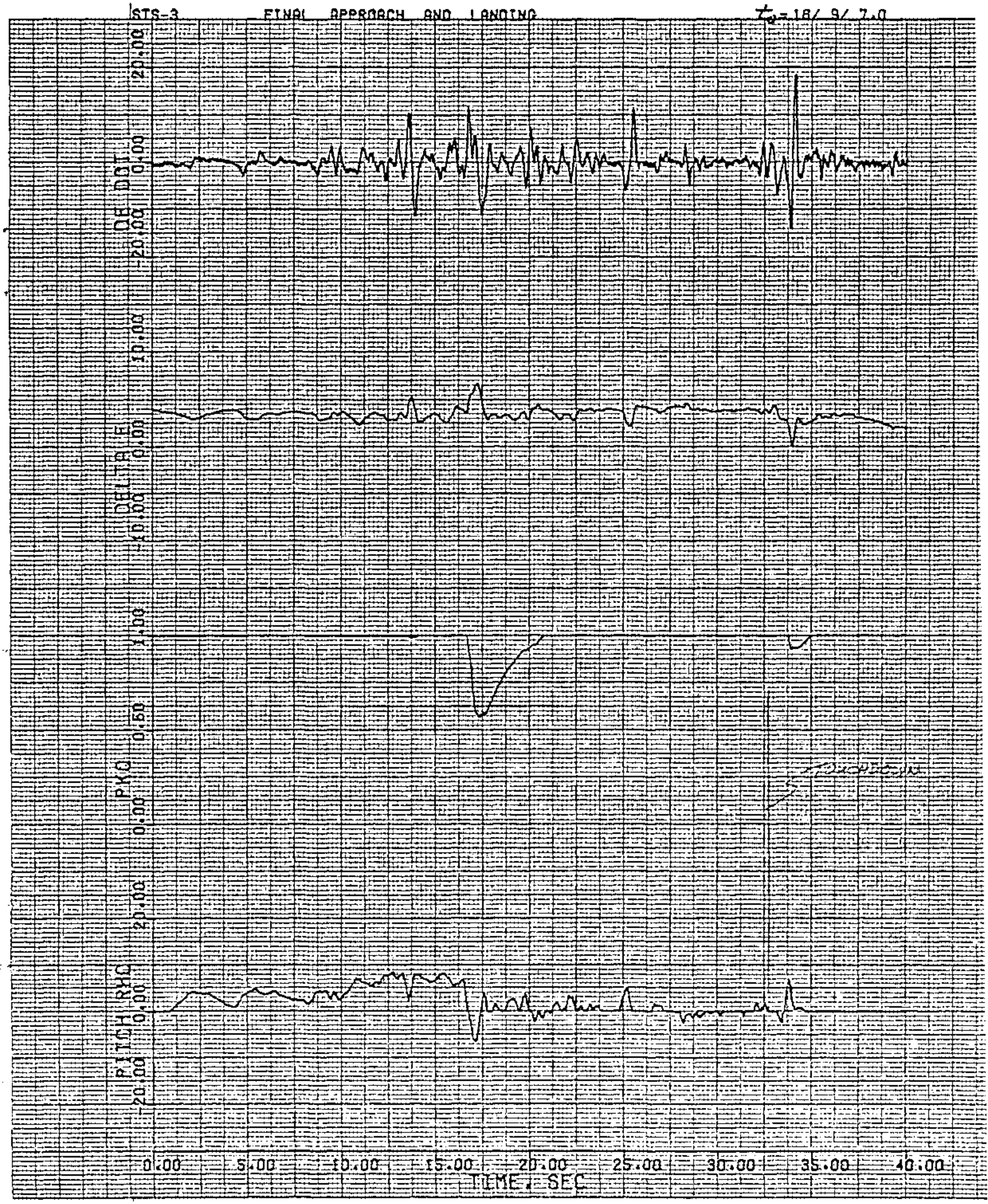

FIGURE 15b - (CONTINUED)

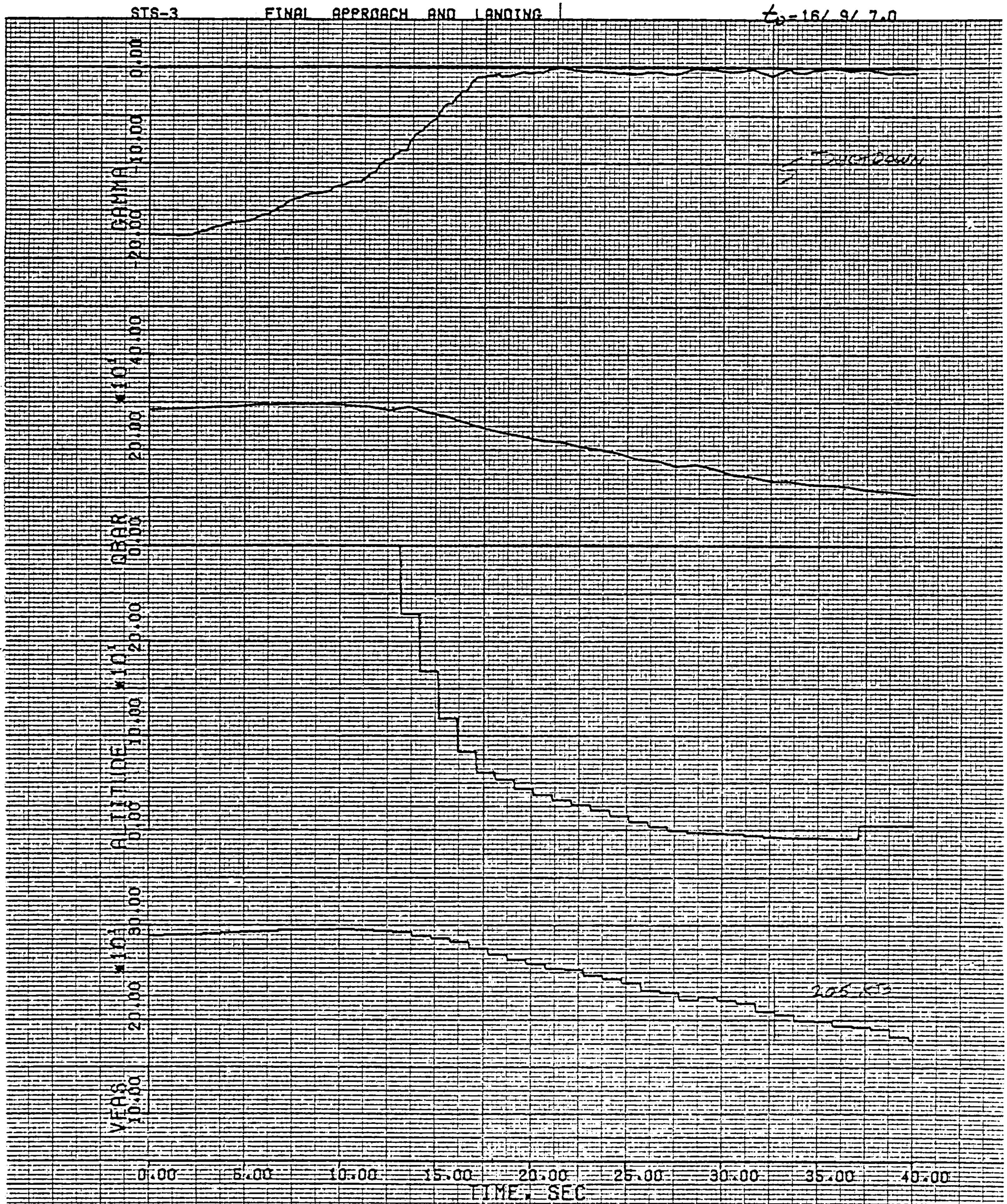

FIGURE 15c - (CONTINUED)

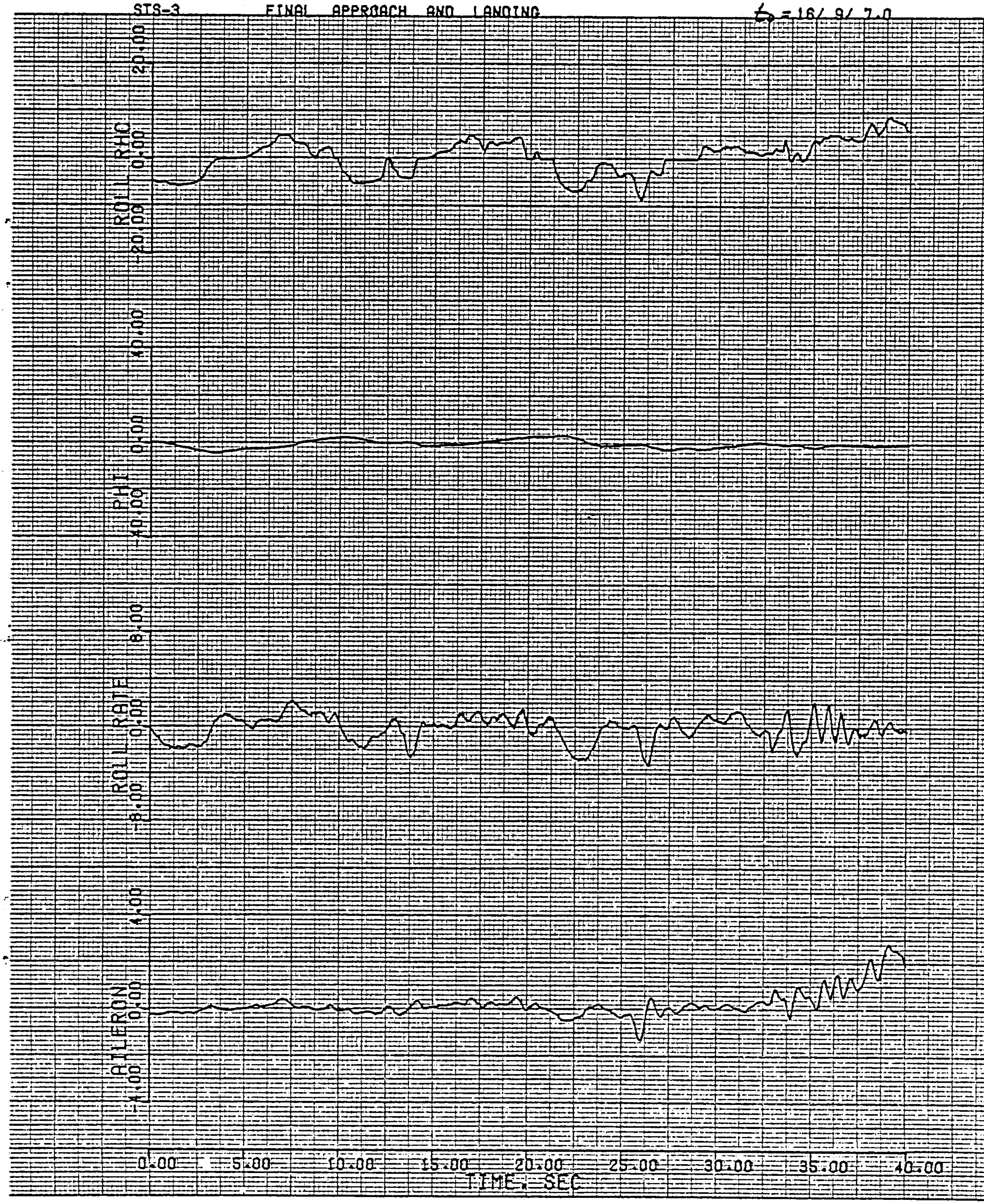

FIGURE 15d - (CONTINUED)

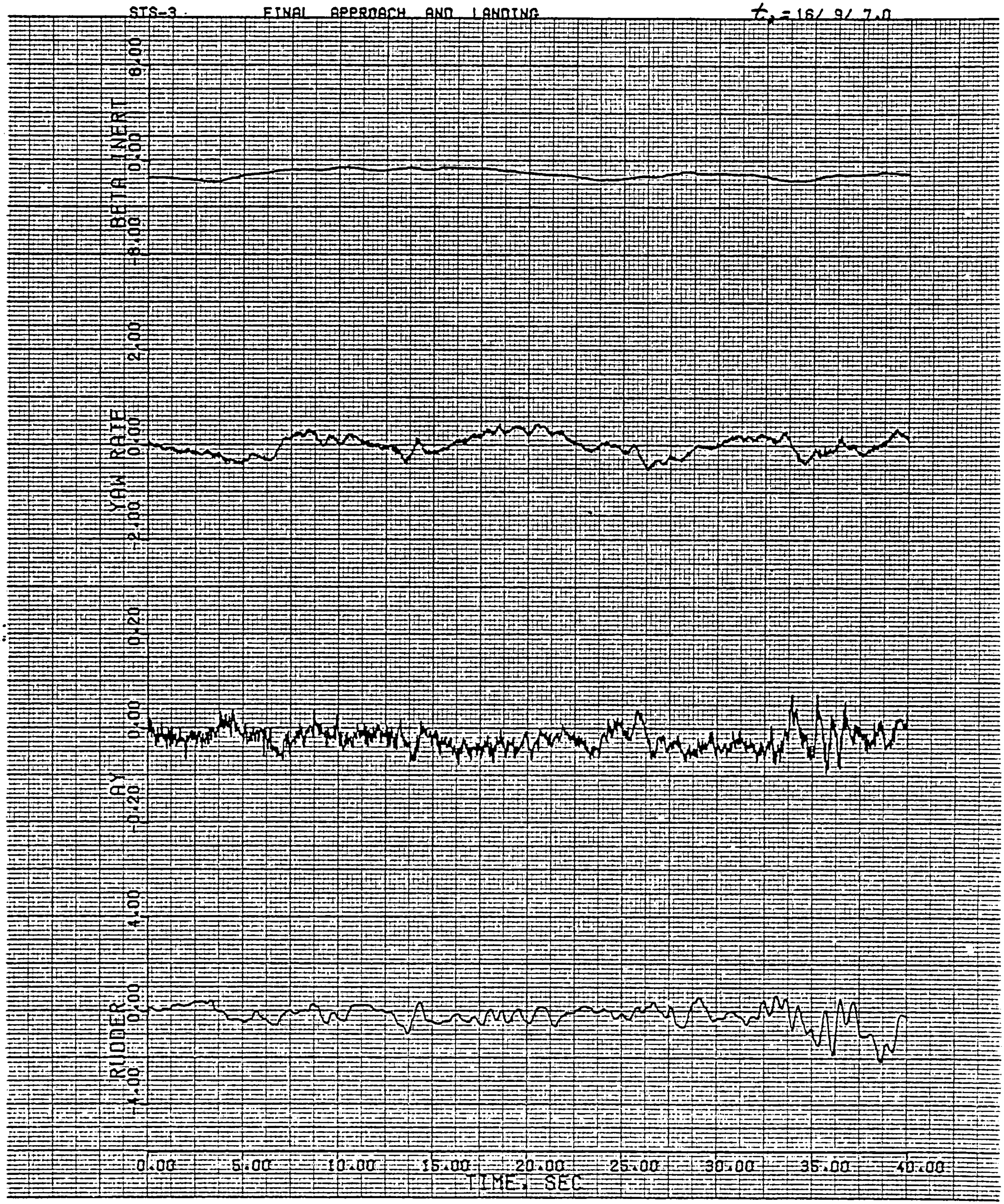

FIGURE 15e - (CONTINUED)

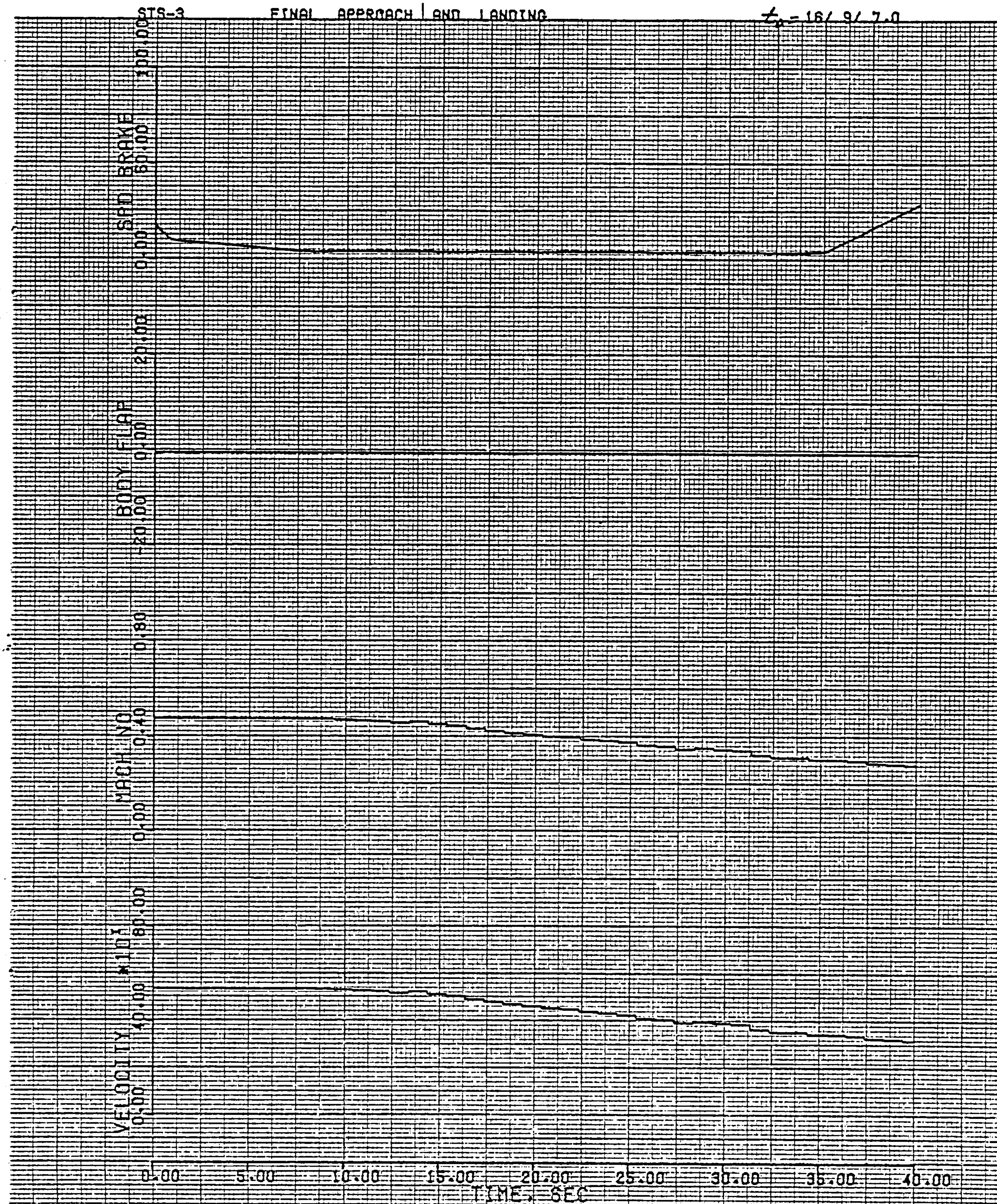

FIGURE 15f - (CONTINUED)

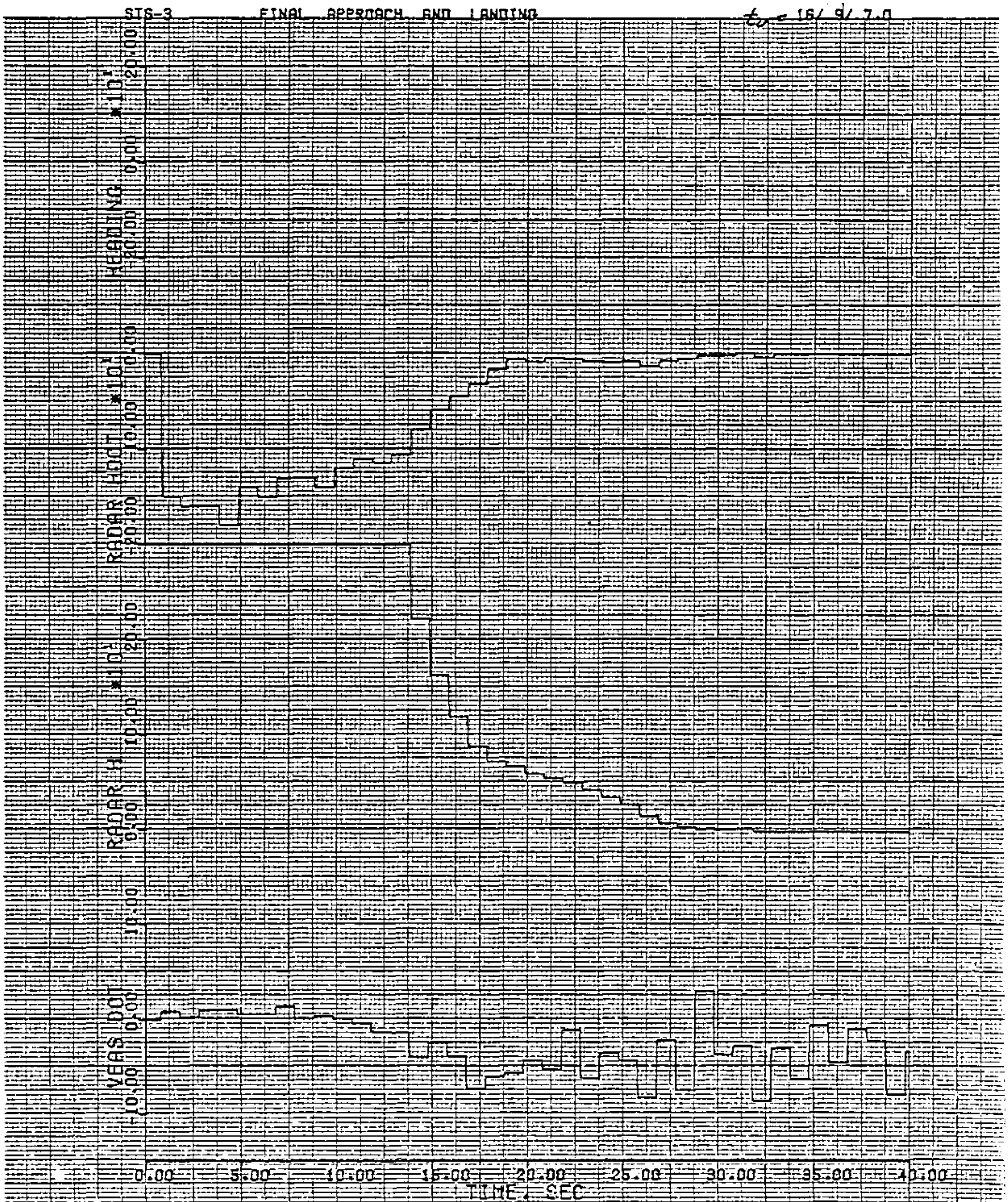

FIGURE 15g - (CONCLUDED)

REFERENCES

1. Maine, Richard E.; and Iliff, Kenneth W.: User's Manual for MMLE3, A General FORTRAN Program for Maximum Likelihood Parameter Estimation. NASA TP-1563, 1980.

2. Preliminary Analysis of STS-1 Entry flight Data, NASA TM-81363, 1981.

3. Preliminary Analysis of STS-2 Entry flight Data, NASA TM-81371, 1981.

4. Preliminary Analysis of STS-3 entry Flight Data, NASA TM-81373, 1982.

1. Report No.	2. Government Accession No.	3. Recipient's Catalog No.
NASA TM-81375		

4. Title and Subtitle	5. Report Date
PRELIMINARY ANALYSIS OF STS-4 ENTRY FLIGHT DATA	September 1982
	6. Performing Organization Code RTOP 989-10-00
7. Author(s)	8. Performing Organization Report No.
	10. Work Unit No.
9. Performing Organization Name and Address NASA Ames Research Center Dryden Flight Research Facility P.O. Box 273 Edwards, CA 93523	11. Contract or Grant No.
	13. Type of Report and Period Covered Technical Memorandum
12. Sponsoring Agency Name and Address National Aeronautics and Space Administration Washington, D.C. 20546	14. Sponsoring Agency Code

15. Supplementary Notes

16. Abstract

Dryden has completed a preliminary analysis of the data obtained during entry of the STS-4 Flight. Planned maneuvers were flown during this flight to increase the quality of stability and control analysis, similar to the techniques used during STS-3. This approach will unquestionably decrease the number of flights needed to fully document the Orbiter's flying qualities.

We have about exhausted the usefulness of the marginal quality small incidental motions for derivative estimation. Further efforts will require good quality maneuvers to improve the results along the nominal entry corridor and to expand the entry envelope. The derivatives obtained from STS-4 agreed fairly well with the derivatives obtained on previous flights. The dependence of aileron effectiveness on elevon position above a Mach number of 10 seen on STS-3 was conclusively verified on STS-4.

CSS Mode was engaged to fly the heading alignment circle. After engagement, several cycles of a low amplitude pilot induced oscillation (1-degree/second) at about 0.3 hertz can be seen. The potential PIO shown here should not present a significant problem. This flight condition does not require continuous, high-gain tracking of the guidance commands. No PIO suppressor activity was seen between preflare and touchdown. This approach demonstrates the advantage of the shallow final glideslope approach. In this type of approach, the pilot is not required to make accurate altitude judgements since an acceptable landing can be made without performing the final flare.

17. Key Words (Suggested by Author(s))	18. Distribution Statement
Orbiter Stability and control Performance Heating Derivative extraction	Unclassified - Unlimited Subject category 18

19. Security Classif. (of this report)	20. Security Classif. (of this page)	21. No. of Pages	22. Price*
Unclassified	Unclassified	92	A05